Jül-4272

Institute of Neurosciences and Biophysics (INB)
Cellular Signal Processing (INB-1)

Fluorescence Spectroscopy of Recoverin Function and Conformation

Iris von der Hocht

Mitglied der Helmholtz-Gemeinschaft

JÜLICH
FORSCHUNGSZENTRUM

Fluorescence Spectroscopy of Recoverin Function and Conformation

Iris von der Hocht

Berichte des Forschungszentrums Jülich; 4272
ISSN 0944-2952
Institute of Neurosciences and Biophysics (INB)
Cellular Signal Processing (INB-1) Jül-4272
D 38 (Diss., Köln, Univ., 2008)

Zu beziehen durch: Forschungszentrum Jülich GmbH · Zentralbibliothek, Verlag
D-52425 Jülich · Bundesrepublik Deutschland
☎ 02461 61-5220 · Telefax: 02461 61-6103 · E-Mail: zb-publikation@fz-juelich.de

Abstract

Recoverin is a neuronal calcium sensor protein (NCS-protein) from the vertebrate photoreceptor which is involved in light adaptation. Recoverin changes its conformation upon sequential binding of two calcium ions. This conformational change induces the extrusion of a covalently attached myristoyl residue from a hydrophobic binding pocket which enables Recoverin to interact with lipid membranes (calcium-myristoyl switch).

In this thesis, I report on my investigation of Recoverin's calcium myristoyl switch, using a recently developed modification of fluorescence correlation spectroscopy (FCS) that is called dual-focus FCS (2fFCS). This method allows for measuring absolute diffusion coefficients with an accuracy of better than a few percent. Recoverin, and the Recoverin mutants E85Q and E121Q which bind only one or no Ca^{2+}, respectively, were labeled with the fluorescent dye Alexa647. Differences in the hydrodynamic radius due to conformational changes of Recoverin and its mutants upon calcium binding were monitored by measuring the diffusion coefficient of these molecules as a function of free calcium concentration.

The calcium dependent interaction of Recoverin with lipid membranes was measured in solutions of small unilamellar vesicles (SUVs) of different lipid composition. Again, diffusion measurements were used to determine the fraction of free and lipid-bound Recoverin using the strongly different diffusion coefficients of both fractions. To account for the fluorescence brightness difference of the dye label when in solution and close to a lipid membrane, a new three-photon correlation analysis was developed and tested.

Kurzzusammenfassung

Recoverin ist ein neuronales Kalzium Sensor Protein (NCS-Protein) aus dem Photorezeptor der Wirbeltiere, das an der Lichtadaptation beteiligt ist. Recoverin ändert seine Konformation durch die sequenzielle Bindung von zwei Kalzium-Ionen. Diese Konformationsänderung induziert die Freisetzung eines kovalent gebundenen Myristoylrestes aus einer hydrophoben Tasche des Proteins und erlaubt Recoverin, an Lipidmembranen zu binden (Kalzium-Myristoyl-Switch).

In dieser Arbeit beschreibe ich die Untersuchung des Kalzium-Myristoyl-Switches von Recoverin mit einer vor kurzem entwickelten Modifikation der Fluoreszenz Korrelations Spektroskopie (FCS), der Zwei-Fokus FCS (2fFCS). Mit dieser Methode können absolute Diffusionskoeffizienten mit höchster Genauigkeit gemessen werden. Recoverin und die beiden Recoverin-Mutanten E85Q und E121Q, die nur ein bzw. kein Kalzium-Ion binden können, wurden mit dem Fluoreszenzfarbstoff Alexa647 markiert. Änderungen des hydrodynamischen Radius von Recoverin, die durch kalziuminduzierte Konformationsänderungen verursacht werden, können durch die Messung des Diffusionskoeffizienten als Funktion der Kalziumkonzentration beobachtet werden.

Die kalziumabhängige Wechselwirkung von Recoverin und Lipidmembranen wurde mit Suspensionen kleiner, unilamellarer Vesikel (SUV) unterschiedlicher Zusammensetzung untersucht. Auch hier wurde das Diffusionsverhalten gemessen. Die sehr unterschiedlichen Diffusionskoeffizienten der beiden Fraktionen wurden benutzt, um den Anteil von freiem und lipidgebundenem Recoverin zu bestimmen. Eine neue Drei-Photonen Korrelationsanalyse, mit der die unterschiedlichen Fluoreszenzhelligkeiten der Farbstoffmarkierung in Lösung und nahe der Membran berücksichtigt werden können, wurde entwickelt und getestet.

Content

1 Introduction

1.1 Phototransduction

Vision is the most sophisticated sense of humans. 80% of all information about our environment is attained by our eyes. Especially the perception of colors is well developed. The image of our environment is projected by the optical system (cornea and lens) of our eye onto the retina. There are two different types of photoreceptor cells in the retina, rods and cones. Rod cells are specialized for the detection of dim light, whereas cone cells work in bright light and are responsible for color vision.

The cylindrical rod cells have a synaptic terminus forming a synapse with another neuron in the retina, an inner segment containing the usual set of cellular equipment of organelles and the nucleus, and an outer segment. The outer segment developed evolutionally from a cilium and is the specialized part of the cell. The rod's outer segment (ROS) contains a stack of disk membranes which are tightly packed with Rhodopsin (R), the visual pigment. The large number of Rhodopsin molecules is necessary to achieve highest light absorption probability. The ROS contains all components that are necessary for the absorption of light, the conversion to a biochemical signal, amplification, and generation of an electrical signal (a change of the potential over the plasma membrane) that can be further processed by nerve cells (for review see: Stryer, 1996; Müller and Kaupp, 1998; Pugh *et al.*, 1999; Burns and Baylor, 2001).

How is the optical signal converted into an electrical signal? The whole phototransduction cascade is schematically depicted in Fig. 1.1. Rhodopsin belongs to the family of seven-helix receptor proteins. It is composed of apoprotein, opsin, and the chromophor 11-cis-retinal. Absorption of a photon by 11-cis-retinal induces its isomerization to all-trans-retinal. This photochemical reaction has a high quantum yield of 0.7 inside Rhodpsin. The constitutional change of the chromophor leads to a conformational change of the protein moiety. Thus, the optical information is converted into biochemical information. The photoactivated Rhodopsin then enhances the exchange of GDP to GTP on a heterotrimeric G-protein, Transducin (T). Transducin splits up in $T_{\beta,\gamma}$ and T_{α}-GTP. T_{α}-GTP stimulates the hydrolytic activity of Phosphodiesterase (PDE) by relieving its inhibitory γ subunit. The activated PDE hydrolyses cGMP, the second messenger of the phototransduction cascade, to 5'-GMP. The decrease in cGMP concentration leads to a closure of cyclic nucleotide-gated cation channels (CNG-channels) in the plasma membrane stopping the influx of Ca^{2+} and Na^{+} to the cytoplasm and thus hyperpolarizing the photoreceptor from a membrane potential of -40 mV to -70 mV. The potential difference is relayed passively to the synaptic terminus of the cell where it leads to a reduced emission of glutamate.

In the dark state of the photoreceptor, there is a steady circulation of Ca^{2+} in and out of the cell, which consists of an influx through the CNG-channels and

an efflux through a Na^+ /Ca^{2+}, K^+ exchanger (NCKX) that exchanges intracellular K^+ and Ca^{2+} with extracellular Na^+. The closure of the CNG-channels stops the influx of Ca^{2+}, but the efflux continues. Consequently, the free Ca^{2+} concentration is decreased from ~500 nM in the dark to ~50 nM. This part of the photoresponse is called the *rising phase*.

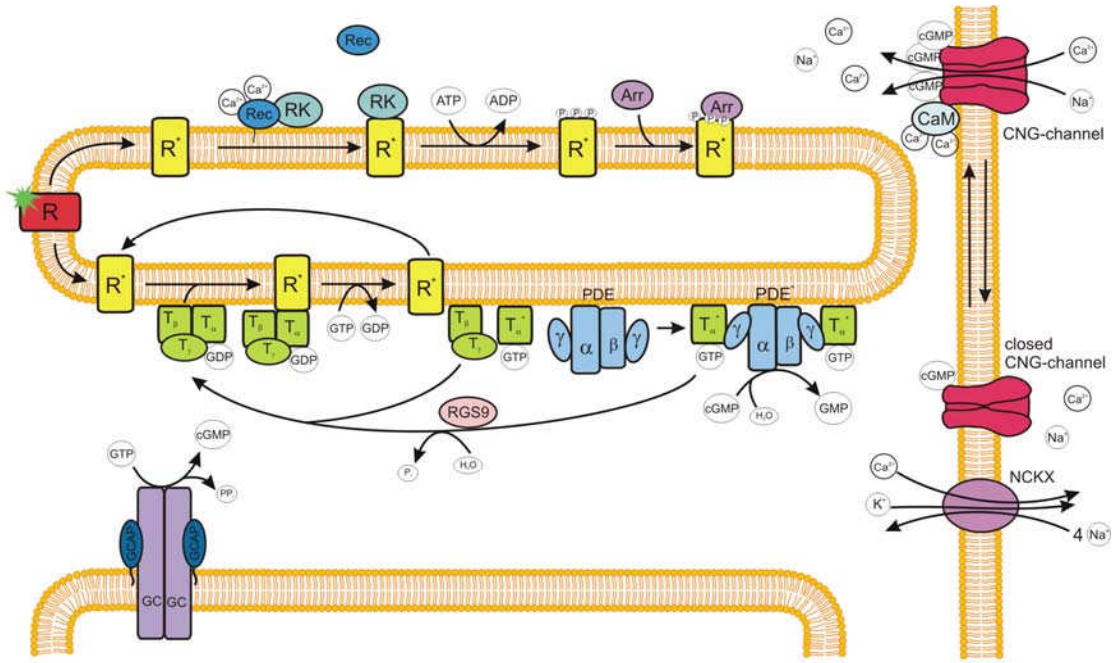

Fig. 1.1 Schematic representation of the rod phototransduction cascade. The asterisks indicate the active forms of proteins. Absorption of a photon by 11-cis-retinal, the chromophor of Rhodopsin (R, red), causes its photoisomerization to all-trans-retinal and a conformational change of R. R* (yellow) activates a heteromeric G-protein (Transducin, T, green) by enabling the exchange of GDP for GTP. T_α*-GTP stimulates the hydrolytic activity of Phosphodiesterase (PDE, blue) by relieving its inhibitory γ subunit. PDE* hydrolyses cGMP to GMP. The decrease of cGMP concentration leads to closure of cyclic nucleotide-gated cation channels (CNG-channels, magenta) in the plasma membrane stopping the influx of Ca^{2+} and Na^+ and thus hyperpolarizing the ROS to a membrane potential of -70 mV. There is a steady circulation of Ca^{2+} in the dark state of the photoreceptor in and out of the photoreceptor cell, which consists of an influx through the CNG-channels and an efflux through a Na^+ /Ca^{2+}, K^+ exchanger (NCKX) which exchanges intracellular K^+ and Ca^{2+} with extracellular Na^+. The closure of the CNG-channels stops the influx of Ca^{2+} and Na^+, but the efflux continues and consequently reduces the free Ca^{2+} concentration from ~500 nM in the dark to ~50 nM. Recovery of the photoreceptor's dark state is reached by deactivation of the active protein forms, restoring the cGMP concentration, and opening of the CNG-channels. R* is phosphorylated by Rhodopsin Kinase (RK, blue) which is, due to the low Ca^{2+} concentration, not longer inhibited by Recoverin (Rec, dark blue). Phosphorylated R* subsequently binds to Arrestin (Arr, violet), which suppresses further interaction of R with T. T_α*-GTP is deactivated through its intrinsic GTPase activity and allows PDEγ to reassociate with $PDE_{\alpha,\beta}$. RGS9 stimulates GTP hydrolysis by T. Guanylate Cyclase Activating Proteins (GCAP, dark blue) stimulate the synthesis of cGMP by Guanylate Cyclase (GC, violet). Thus the CNG-channels reopen to allow Ca^{2+} to flow into the cell. Calmodulin (CaM) modulates the affinity of the CNG-channels for cGMP. The calcium bound form of CaM binds to the channels and increases the affinity for cGMP.

Recovery of the photoreceptor's dark state is reached by deactivation of the active proteins of the cascade, restoring the cGMP concentration, and

reopening of the CNG-channels. Active Rhodopsin is phosphorylated by Rhodopsin Kinase (RK) which is, due to the low Ca^{2+} concentration, no longer inhibited by a calcium binding protein called Recoverin. Phosphorylated Rhodopsin subsequently binds to Arrestin (Arr), which suppresses further interaction of Rhodopsin with Transducin. T_α*-GTP is deactivated through its intrinsic GTPase activity and allows PDEγ to reassociate with $PDE_{\alpha,\beta}$. RGS9 stimulates GTP hydrolysis by Transducin. Guanylate Cyclase Activating Proteins 1 and 2 (GCAP) stimulate the synthesis of cGMP by Guanylate Cyclase (GC) at low calcium concentration. Thus, the CNG-channels reopen to allow Ca^{2+} to flow into the cell.

The two cycles of messengers (cGMP and Ca^{2+}) in the photoreceptor cell depend on each other and are connected via the GCAP/GC complex and the CNG-channels. cGMP is hydrolysed (by PDE) and synthesized (by GC) again during one photoresponse cycle, and the concentration of Ca^{2+} decreases due to CNG-channel closing and increases again after binding of cGMP and reopening of the channels.

Rod cells are optimized for vision in dim light. A single photon absorbed by a dark-adapted rod outer segment closes hundreds of CNG-channels resulting in hyperpolarisation of the plasma membrane. This is possible due to the high amplification during the phototransduction cascade: one activated Rhodopsin is able to activate up to 3000 Transducin molecules, and one PDE molecule hydrolyses up to 2000 cGMP molecules per second. The energy necessary for this amplification is provided by the metabolism of the cell. However, this means that the tightly packed Rhodopsin molecules in the disk membranes have to be very stable against thermal activation. The spontaneous isomerization of 11-cis-retinal would resemble the response to a single adsorbed photon. One can verify this in complete darkness: The grey blurred flashes one senses are provoked by spontaneous, thermal isomerizations of Rhodopsin.

Rod cells show an incredible large dynamic range in photodetection (from single photons to thousands of photons per second). The amazing ability of the visual system to adjust its performance to the ambient level of illumination is called light adaptation. This process enables vision during a starry night as well as at a sunny day on a glacier. Ca^{2+}, the other messenger of the photoreceptor cell besides cGMP, helps in adaptation, additionally to its role in the recovery of the dark state. At least three different calcium binding proteins (GCAP, Calmodulin, and Recoverin) sense the changes in calcium concentration in the rod cell and mediate this information to their target enzymes.

One important mechanism underlying adaptation is the tuning of the lifetime of photoactivated Rhodopsin due to the reversible inhibition dependent on the calcium concentration of Rhodpsin Kinase by Recoverin.

1.2 A protein named Recoverin

The question whether cGMP or Ca^{2+} is the transmitter in visual transduction was conclusively answered with the finding that cGMP is the transmitter of the transduction cascade after light excitation whereas Ca^{2+} is also involved in the restoration of the dark state and the adaptation to different light intensities (for review: Stryer 1986; Pugh and Cobbs 1986). In 1988, Koch and Stryer showed that the Guanylate Cyclase (GC) which synthesizes cGMP in the photoreceptor cell is controlled by an unidentified soluble calcium binding protein.

In 1991, two studies (Dizhoor *et al.*1991; Lambrecht and Koch 1991) were published describing the purification, characterization and sequencing of a calcium binding protein which activated the GC. This protein was named Recoverin because it activated the re-synthesis of cGMP by GC which leads to the recovery of the photoreceptor's dark state after light excitation. Three other research groups also published studies about the purification and sequencing of a 26 kD protein, most probably Recoverin from retinal rods but did not investigate the function of this protein (Dizhur *et al*. 1991; Kutuzov *et al*. 1991; McGinnis *et al*. 1992).

Recoverin is found in the retina in both photoreceptor types (rods and cones; Dizhur *et al*. 1991, Dizhoor *et al*. 1991, McGinnis 1992). The property of Recoverin to bind calcium was investigated by a $^{45}Ca^{2+}$-binding assay, and a shift in tryptophan fluorescence dependent on the Ca^{2+}-concentration (Lambrecht and Koch 1991, Dizhoor *et al*. 1991). Recoverin also displayed the calcium dependent mobility shift typical for calcium binding proteins in native gel electrophoresis but not in SDS-PAGE (Lambrecht and Koch 1992). The amino acid sequence of Recoverin also revealed that it has at least three EF-hand calcium binding motives (Dizhoor *et al*. 1991), one possibly disabled by a cysteine residue (Kutuzov *et al*. 1991). The deduced amino acid sequence shared 59% homology with visinin, a chicken retinal cone cell specific protein (Yamagata *et al*. 1990). The sequence of Recoverin was not directly accessible with Edman-Degradation because of the blocked N-terminus of the protein (Dizhoor *et al*. 1991; Lambrecht and Koch 1991; Kutuzov *et al*. 1991). Later, Dizhoor *et al*. could show that the N-terminus of Recoverin is indeed modified by myristoleate and related small fatty acids (Dizhoor *et al*. 1992). Zozulya and Stryer (1992) investigated the function of the posttranslational modification of Recoverin and came up with the calcium-myristoyl switch model: they suggested that the myristoyl residue is buried inside the protein in the calcium-free state, and extruded into solution upon binding of calcium, allowing Recoverin to associate with a lipid bilayer membrane. They could show that myristoylated Recoverin binds to ROS membranes as well as to DOPC liposomes at high calcium concentration. This indicates that the myristoyl residue interacts with the lipid bilayer and not, as was also suggested, with a protein in the ROS membrane (Dizhoor *et al*. 1992).

This finding raised the question how Recoverin can activate the GC (a membrane protein) at low calcium concentration when it leaves the membrane at low calcium concentration (Zozulya and Stryer 1992; Dizhoor *et al*. 1993). In contrast to other calcium binding effector molecules such as calmodulin Recoverin was also supposed to activate its target molecule in the calcium-free state. Gray-Keller *et al*. (1993) measured the effect of Recoverin and other homologous Ca^{2+}-binding proteins on the photoresponse using electrophysiological methods. They found a prolongation of the rising phase of the photoresponse without an effect on the recovery phase. This result suggested that Recoverin does not activate GC in a calcium dependent way but affects the termination of the phototransduction cascade. As a result, the conclusion that Recoverin is the calcium sensitive activator of GC was withdrawn (Hurley *et al*. 1993).

Later, two Guanylate Cyclase Activating Proteins (GCAP 1 and 2) present in the bovine retina were identified, sequenced and characterized (Gorczyca *et al*. 1994, Palczewski *et al*. 1994, Dizhoor *et al*. 1995, Frins *et al*. 1996). The original mistake in the assignment of the function of Recoverin may be explained by the presence of endogenous GCAPs in the Recoverin preparation used in the preceding works (Senin *et al*. 2002a). Recoverin is present in the ROS of the photoreceptor cells at quite high concentrations around 30 μM (Lambrecht and Koch, 1992; Klenchin *et al*. 1995), in contrast to approximately 3 μM of GCAP 1 and 2 (Hwang *et al*. 2003).

Thus, the search for the function of Recoverin in phototransduction started once again. The electrophysiological experiments of Gray-Keller *et al*. (1993) gave a hint that Recoverin might be involved in the termination of the phototransduction cascade. Also the first experiments with S-modulin, the frog homolog of Recoverin (Kawamura *et al*. 1993), indicated that S-modulin prolongs Phosphodiesterase (PDE) activation (Kawamura and Murakami 1991). Later Kawamura (1993) could show that the lifetime of active PDE is prolonged by inhibition of Rhodopsin phosphorylation. Rhodopsin is phosphorylated on the C-terminal tail (Hargrave *et al.*, 1980; Thompson and Findlay, 1984) by Rhodopsin Kinase (RK), a G protein-coupled receptor kinase, also assigned as GRK1. Rhodopsin Kinase phosphorylates only the activated form of the receptor (Metarhodopsin II), which leads to its inactivation (Kühn and Dreyer, 1972; Wilden and Kühn, 1982). It remained unclear whether S-modulin inhibits Rhodopsin Kinase itself or prevents interaction between the Kinase and activated Rhodopsin.

Gorodovikova and Philippov (1993) found a complex of Recoverin and most probably Rhodopsin Kinase in an isotonic ROS extract eluting from a sizing column at high calcium concentration. The direct interaction of Rhodopsin Kinase and Recoverin was proved later (Chen *et al*. 1995). Gorodovikova *et al*. (1994a and 1994b) showed that Recoverin regulates Rhodopsin phosphorylation dependent on the calcium concentration. Rhodopsin phosphorylation determines

the lifetime of active PDE. So, Recoverin inhibits Rhodopsin phosphorylation by Rhodopsin Kinase at high calcium concentration in bovine ROS as S-modulin does in frog rods.

The inhibition of Rhodopsin Kinase does not depend on the myristoyl residue of Recoverin: Kawamura *et al*. (1994) could show that non-myristoylated Recoverin also inhibited Rhodopsin phosphorylation in a calcium-dependent way. Binding of Recoverin to membranes is not necessary for inhibition of RK but the inhibition of Rhodopsin Kinase is done more efficiently by myristoylated Recoverin because both proteins are then bound to the disk membrane (Inglese *et al.*, 1992; Sanada *et al.*, 1996), thus increasing the effective concentration and leading to a higher Rhodopsin Kinase/Recoverin interaction rate (Senin *et al.*, 1995; Sanada *et al.*, 1995; Sanada *et al.*, 1996). Eventually, the interaction of Recoverin with RK is inhibited by autophosphorylation of Rhodopsin Kinase (Satpaev *et al.*, 1998).

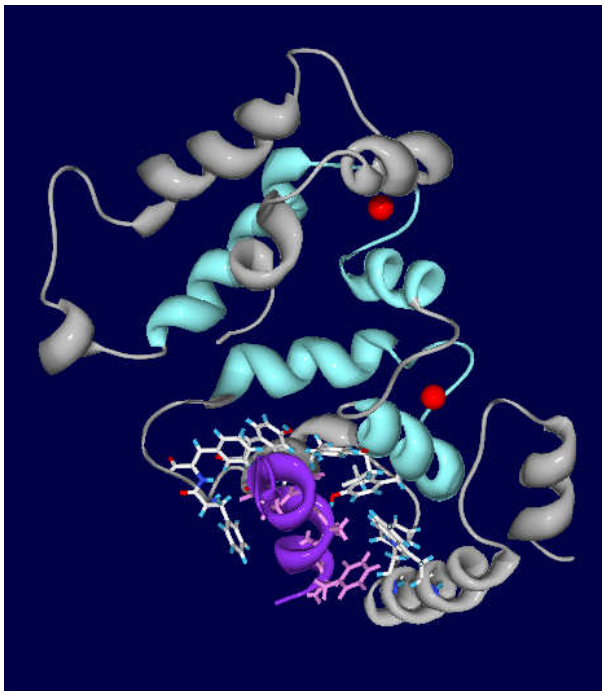

Fig. 1.2 Molecular structure of calcium bound Recoverin interacting with an N-terminal 25 amino acids long fragment of Rhodopsin Kinase (Ames *et al.* 2006). Residues of interacting hydrophobic amino acids are shown as ball-stick models.

From these studies, one may conclude that Recoverin prolongs the lifetime of photoexcited Rhodopsin by inhibiting Rhodopsin Kinase at high calcium levels which maximizes the sensitivity of the rod cell and contributes to adaptation to low light intensities. The shortened lifetime of activated Rhodopsin at low calcium levels may promote visual recovery and adaptation to high background light intensities.

After establishing the inhibition of Rhodopsin Kinase by Recoverin and the direct interaction of both proteins, the remaining question was the location of the interaction sites in Recoverin and Rhodopsin Kinase. The Recoverin binding domain of Rhodopsin Kinase is localized within the 25 N-terminal residues (Levay *et al.*, 1998). This domain also includes an autophosphorylation site (Ser21) which, when phosphorylated, possibly inhibits the interaction of Recoverin with RK (Satpaev *et al.*, 1998). The N-terminal region of Rhodopsin Kinase, residues 17-34, also interacts with activated Rhodopsin (Palczewski *et al.*, 1993) which implies that Recoverin inhibits Rhodopsin phosphorylation by

competing with Rhodopsin for binding to Rhodopsin Kinase. Later, it was shown that Recoverin interacts with an N-terminal amphipathic helix of Rhodopsin Kinase that is necessary for recognition of Rhodopsin as a Kinase substrate (Higgins *et al*., 2006).

Komolov *et al*. (2005) could show that the Rhodopsin Kinase-interaction-site of Recoverin is located in the N-terminal domain and that binding of Ca^{2+} to EF-Hand 2 is necessary to expose the hydrophobic and aliphatic residues that interact with Rhodopsin Kinase. An NMR-structure of calcium-bound Recoverin binding a Rhodopsin Kinase peptide of the N-terminal 25 amino acid residues was recently published by Ames *et al*. (2006) (see Fig. 1.2). This structure confirms, that upon unclamping of the myristoyl residue, a hydrophobic surface in the N-terminal domain of Recoverin is exposed that serves as a target binding site of Rhodopsin Kinase. In the calcium-free state of Recoverin the myristoyl group sequesters the N-terminal hydrophobic groove and covers the Rhodopsin Kinase binding site.

One could think that all these studies do not leave any doubt about the physiological function of Recoverin but as a matter of fact there is a controversy whether the inhibition of Rhodopsin Kinase by Recoverin is indeed its *in vivo* function. Almost all experiments described above are *in vitro* experiments and find a calcium affinity of Recoverin which is much lower than the calcium concentration that is present in the photoreceptor. The argument that extrapolation of the *in vitro* results to physiological conditions at e.g. much higher lipid concentration places the calcium affinity of Recoverin into the physiological range of calcium concentrations does not convince everyone. But there are some *in vivo* studies e.g. electrophysiological experiments on truncated ROS (Gray-Keller *et al.*, 1993; Erickson *et al*., 1998), or a knock out mouse lacking Recoverin (Makino *et al.*, 2004), that confirm the proposed function of Recoverin. A knock out mouse was also used in a recent study by Sampath *et al*. (2005) which gave evidence for an additional role of Recoverin in rods. It was shown that Recoverin enhances vision in dim light by influencing signal transfer from rods to rod bipolar cells. The underlying mechanism is not yet solved. Recoverin is not only present in the outer segment of the rod cell but throughout the whole photoreceptor cell. 12% of the rod's Recoverin content was found in the outer segment of dark-adapted mice, whereas light caused its reduction to only 1.8% (Strissel *et al.*, 2005). Thus, Recoverin moves toward the synaptic terminal of the rod cell upon illumination. This translocation might work in concert with the reduction in Ca^{2+} concentration and resulting deinhibition of Rhodopsin Kinase but, but taken into account that the majority of Recoverin resides outside the outer segment of rod cells it seems likely that Recoverin plays an additional role in rod cells.

Recoverin is a member of the huge family of neuronal calcium sensor proteins (NCS proteins). These proteins are, as the name implies, mainly expressed in the nervous system and sense changes in intracellular Ca^{2+}

concentration. This protein family can be further divided in five subfamilies: the frequenins, the visinin like proteins (VILIPs), the recoverins, the guanylate cyclase-acitvating proteins (GCAPs), and the K^+-channel interacting proteins (KChIPs). NCS proteins are involved in a large variety of cellular processes like vision, olfaction, ion channel regulation, gene expression and apoptosis (Braunewell and Gundelfinger, 1999; Burgoyne et al., 2004).

All NCS proteins consist of one chain of approximately 200 amino acids. The sequence contains four EF-hand motives but only two or three of them are functional and bind calcium with high affinity. The sequence CPXG in the first EF-hand impairs with calcium binding. The four EF-hands form two domains which combine to a compact protein structure in contrast to the dumbbell shape of Calmodulin for example. Almost all NCS proteins have an N-terminal acylation consensus sequence and are post-translationally acylated at their amino-terminal glycine. Myristic acid is the prevalent fatty acid. The sole exceptions are three KChIP forms. Ca^{2+}-binding induces a conformational change which can also involve the extrusion of the myristoyl group (Ca^{2+}-myristoyl switch). But not all NCS proteins carrying a myristoyl residue do perform this Ca^{2+}-myristoyl switch, in GCAPs the myristoyl group for example is involved in fine-tuning of Ca^{2+} affinity. Bovine Recoverin is the best investigated NCS-Protein and serves as a model protein for the whole protein family.

1.3 Goals of this study

This study is about biophysics: the quantification of Recoverin's properties (binding of calcium ions and interaction with a lipid bilayer) with a new single-molecule sensitive measurement technique.

The native system, the disk membranes from the photoreceptor cell, is highly complex. A preparation of disk membrane fragments would be too inhomogeneous to measure it with 2fFCS. Too many factors like the concentration of ions especially Ca^{2+} or proteins that might also interact with Recoverin cannot be controlled and might influence the outcome of the experiment. The complexity of the biological system had to be reduced to make a precise quantitative description of the system possible. An adequate model membrane system had to be found.

I investigated the calcium-dependent Recoverin-membrane interaction with the focus on the influence of lipid type or membrane composition. The influence of membrane density (the lipid concentration) on the calcium affinity of Recoverin was especially important. Systematic measurements of the influence of lipid concentration on the calcium affinity of Recoverin are performed to explain the discrepancy of *in vitro* measured calcium affinities of Recoverin and the calcium levels present in photoreceptor cells.

I started with the search for an adequate model membrane system that allows investigation of the membrane binding. This system will allow control of all parameters like lipid composition of the membrane and it should be suitable for using it with 2fFCS. I began to use two different model membrane systems: supported bilayers (SPBs) and giant unilamellar vesicles (GUVs). The results of the experiments with these model membrane systems are described in chapters 2.1 and 2.2.

On the other hand Recoverin is a very well characterized protein. The calcium binding of Recoverin was investigated in various studies using many different methods. Therefore Recoverin is ideal for testing a new method like 2fFCS. In chapter 2.3 I describe the measurement of conformational changes of Recoverin due to calcium binding with 2fFCS. These results are confirmed by measurements of the tryptophan fluorescence of Recoverin which are described in chapter 2.4.

And finally in chapter 2.5 the interaction of Recoverin with small lipid vesicles, the membrane binding of Recoverin dependent on calcium- and lipid concentration is described.

2 Results and Discussion

2.1 A simple model membrane system - Supported Bilayers

Supported bilayers (SPBs) were the first model membrane system which I have chosen for the investigation of the interaction of Recoverin with a lipid bilayer. These model membranes are easy to prepare, they are very well characterized and widely used since their discovery in 1984 (Brian and McConnell, 1984).

2.1.1 What are Supported Bilayers?

SPBs are lipid layers on a solid support composed of two layers of oriented phospholipids so that their polar hydrophilic heads face outward and their hydrophobic fatty acid residues are directed inward avoiding contact with water. These bilayers freely float on the supporting surface. There is no chemical linkage between the support and the lipids. In between the bilayer and the support is a very thin film (1 nm) of water (for review see: Sackmann, 1996; Richter *et al.*, 2006).

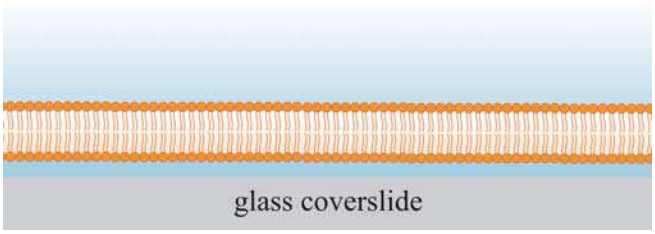

Fig. 2.1 Schematic drawing of a supported bilayer on a glass cover slide. The lipid bilayer is shown in orange.

SPBs can be prepared by the Langmuir-Blodgett technique, or by vesicle fusion. Preparation of defect-free fluid-phase SPBs by the Langmuir Blodgett technique is an extremely difficult task with poor reproducibility and control of the quality of the resulting bilayer (Bassereau and Pincet, 1997; Osborn and Yager, 1995).

Vesicle fusion means that small lipid vesicles adsorb on the solid support and then rupture and self-assemble to form a planar bilayer on this support. There are two scenarios of formation of a supported bilayer by vesicle fusion: In the first scenario the vesicles adsorb to the support and fuse spontaneously to form bilayer patches (Reviakine and Brisson, 2000). The second scenario assumes that vesicles remain intact when bound to a solid support and do not rupture to reorganize in a planar bilayer until a certain vesicular coverage of the surface is reached (Keller *et al.*, 2000). Rädler *et al.* (1995) observed a third mechanism of bilayer formation on solid supports: They deposited a blob of DOPC on a glass slide and hydrated it in water. This blob spread and slid over the surface to form a continuously bilayer. Obviously, the thin water layer between lipid and support allows for the sliding motion. The sliding motion of vesicles or bilayer patches is decreased or even prevented by divalent cations (Richter *et al.*, 2006). This might also be an explanation for the two found mechanisms of vesicle rupture: a mobile vesicle can

avoid contact with nearby vesicles. Thus, a high overall coverage has to be reached until vesicles fuse to form a continuous bilayer.

Suitable materials of support are e.g. glass, silicon, siliconoxide or mica. Many factors affecting the formation of SPBs have been identified, e.g. lipid composition, concentration of monovalent or divalent cations. One important driving force for vesicle fusion seams to be the high curvature of the lipid film in small vesicles. The molecular structure of phospholipids favors the formation of planar bilayers with zero curvature.

2.1.2 Imaging experiments

I prepared SPBs on a glass cover slide using vesicle fusion method. To check whether a continuous fluid bilayer on a glass cover slide was formed, fluorescence recovery after photobleaching (FRAP) measurements were performed. A 0.1% DHPE-Oregon Green labeling was used to fluorescently label

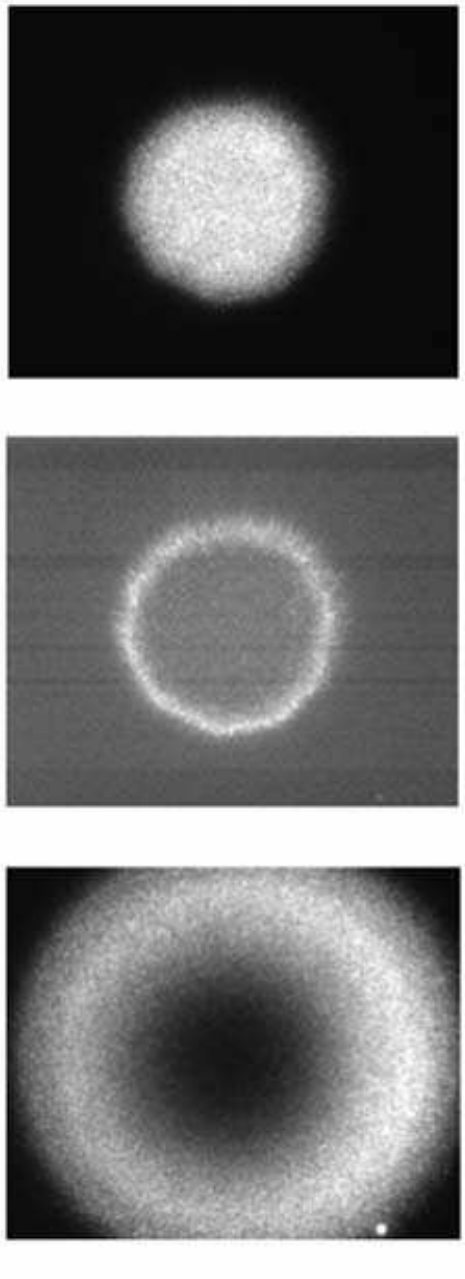

Fig. 2.2 Soy bean lecithin bilayer made by fusion of SUVs supported by a glass cover slide. 0.1% of the lipids are fluorescently labeled with Oregon Green®. The images at the left hand side show a FRAP experiment: the centre of the field of view is bleached within a circular area. The upper image shows the bilayer before bleaching and the image in the middle shows it after bleaching. After 15 s without excitation the aperture is opened. The recovery of the fluorescence in the bleached area is shown in the lower image. The grainy appearance of the bilayer is due to uneven excitation caused by coherent laser light guided through a multimode fiber. The lower diagram shows the intensity profile versus pixel number along a horizontal line in the middle of the lower image of fluorescence recovery. The straight line shows the profile directly after bleaching. The flattening of the gradient due to diffusion of lipid molecules in the bleached area is clearly visible. The bilayer prepared by vesicle fusion on the glass cover slide is continuous and fluid.

the resulting bilayer. Fig. 2.2 shows a typical FRAP experiment on a SPB made from soy bean lecithin. The bilayer was continuous over hundreds of micrometer. The lipids were mobile and a recovery of more than 90% was achieved after photobleaching.

Cover slides used for the preparation of SPBs had to be cleaned with freshly prepared Piranha-etch (for further information see “Materials and Methods” section). After treatment with Piranha-etch and extensive rinsing with de-ionized water, cover slides could be kept under water. Cleaning the glass slide with Piranha-etch had to be done not more than two hours before forming the membrane, otherwise, the chemical properties of the glass surface such as protonation or oxidation resulting from the Piranha-etch treatment changed in a way that prevented vesicle fusion. The glass cover slides usually showed no background fluorescence after cleaning with Piranha-etch. But some batches of cover slides could not be cleaned by that treatment. These cover slides showed residual fluorescence most probably due to contamination from the manufacturing process. They were not used for experiments.

Small unilamellar vesicles (SUVs) for the preparation of supported bilayers were prepared by sonification. An important condition was the correct temperature: It had to be above the main phase transition temperature of the lipids. The size of the vesicles was 80 nm - 100 nm as measured with dynamic light scattering.

I did not encounter any limitations concerning buffer composition or composition of the lipid mixture. The only prerequisite was a temperature above the main phase transition temperature of the lipid. Vesicles with the lipids in the gel phase adsorbed to the glass surface but did not fuse to build a bilayer on it. Vesicle fusion worked in pure water but as well as in buffer solutions with 100 mM to 150 mM KCl and 10 mM to 30 mM Hepes. Divalent cations such as calcium or magnesium also did not prevent vesicle fusion. Fusion to a continuous fluid bilayer worked for pure phospholipids like DOPC or mixtures like soy bean lecithin. Also, mixtures with up to 10% cholesterol or negatively charged phospholipids (the artificial ROS lipid mixture) formed a bilayer on the glass. Pure DOPE did not form a bilayer because the hydrophilic ethanolamine headgroup of this lipid is too small. This phospholipid prefers to build layers with negative curvature like inverse micelles. Vesicles that were stored for some days at 4° C adsorbed to the glass cover slide but did not fuse to form a continuous fluid-supported bilayer.

After ensuring that continuous fluid bilayers can be reproducibly prepared on glass cover slides, I started my investigation of the interaction of Recoverin with phospholipid bilayers. Buffer solutions of fluorescently labeled Recoverin (Recoverin-alexa647) and with varying calcium concentrations were prepared and added to SPBs. Then, binding of Recoverin to the surface was followed with a single molecule sensitive imaging camera. Single molecule binding events to the surface were detected, but the bound molecules occurred to be immobile. Also,

FRAP experiments with Recoverin concentrations allowing for a complete coverage of the bilayer surface revealed that Recoverin-Alexa647 was binding to the bilayer covered surface but did not move. This interaction with the SPBs was independent on calcium concentration. It was also detectable with 10 mM EGTA in the used buffer solution.

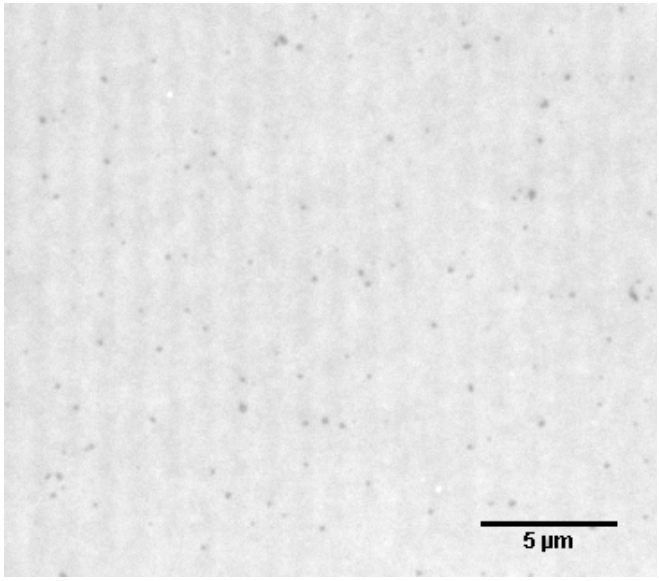

Fig. 2.3 Supported bilayer on a glass cover slide made from soy bean lecithin. The bilayer was labeled with 0.1% DHPE-Oregon Green®. One can clearly see defects (dark spots) in the bilayer. Vertical stripes are interference effects from illumination.

Recoverin like all proteins, has an affinity to stick to glass surfaces. Thus, each defect in the bilayer might allow Recoverin to adsorb to the glass surface. The defects in the membrane where Recoverin could adsorb to the glass surface can be seen in Fig. 2.3 showing the defects in a SPB made from soy bean labeled with 0.1% DHPE-Oregon Green. These defects were immobile and their formation could not be prevented or repaired by longer incubation with the vesicle solution to allow for additional vesicles to close the defects. Cleaning the glass cover slides twice with piranha solution or a combination of cleaning with detergence (Hellmanex II, Hellma GmbH & Co. KG, Müllheim, Germany) followed by cleaning in a KOH-bath and Piranha-etch had no effect. The bilayer had been never defect-free.

After realizing that I could not avoid the formation of defects in the bilayers, I tried to block the open glass surface against Recoverin adsorption by binding of an unlabelled protein such as bovine serum albumin (BSA). As it occurred, the addition of 100 µg/ml BSA to the buffer solution was insufficient Recoverin still adsorbed to the glass surface within seconds.

After incubation of the SPB with a BSA solution (1 mg/ml) for one hour, the SPB was destroyed. There was remaining no fluorescence of labeled lipids on the surface. BSA binds fatty acids, it carries hydrophobic substances through the blood. Thus, it seems possible that BSA bound to the fatty acid tails of the phospholipids and solved the bilayer. However, I obtained a homogeneous coverage of the glass surface with Recoverin-Alexa647 during FRAP experiments. Thus, a more probable explanation is that the protein has a higher affinity to the glass than the lipids. Then, even small defects in the bilayer below the optical resolution limit of the microscope will allow for binding of the protein

to the glass cover slide. By binding irreversibly, the lipid bilayer is successively displaced by the protein.

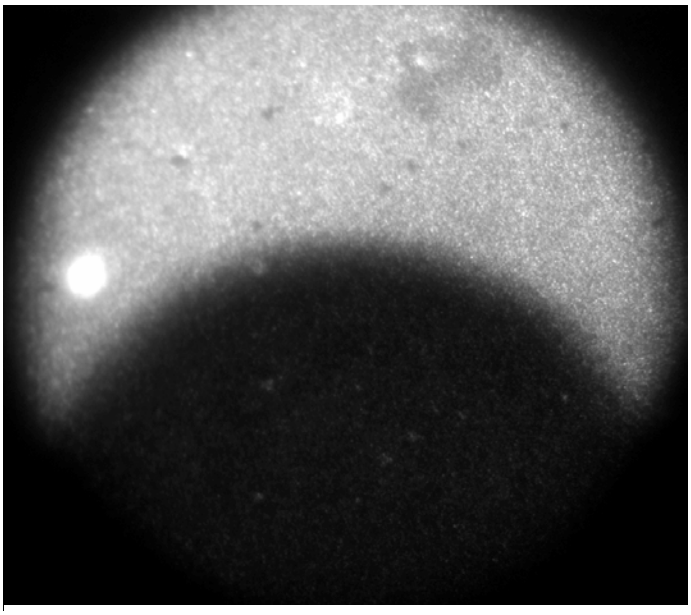

Fig. 2.4 DOPC vesicles labeled with 0.1% DHPE-Oregon Green adsorbed to a PEG coated glass cover slide. The vesicles bound densely to the surface but did not fuse to form a SPB. There was no fluorescence recovery in the bleached area (lower part of the field of view) after bleaching.

Another approach to prevent Recoverin adsorption to the glass cover slide was to block the glass against protein binding before building a bilayer: a polymer cushioned lipid bilayer. I cleaned the glass cover slides with Piranha-etch, silanized it with glycidyloxipropyltrimethoxysilane (GOPTS, ABCR, Karsruhe, Germany) and bound diamino-PEG (RAPP Polymere, Tübingen, Germany) to it (Piehler *et al*. 2000). There was almost no protein adsorption to a cover slide treated this way. On this polymer cushion, I deposited a solution of SUVs and incubated for several minutes to allow the vesicles to bind to the surface and to fuse for building a SPB. Unfortunately, the vesicles adsorbed densely to the polymer-covered glass slide but did not fuse to form a continuous and fluid SPB (see Fig. 2.4).

Although the problems encountered with SPBs prevented their further use in the study of Recoverin/lipid interactions, I studied lipid diffusion in a SPB by single molecule imaging. I wondered whether lipids in such a SPB are diffusing freely or whether there is some interaction with the glass support. For single molecule imaging I had to use a more photostable dye than Oregon Green®. I labeled DOPE with Atto655, or TMR, and prepared DOPC vesicles with a labeling ratio of 1:400,000 to form a SPB on a Piranha-etch cleaned glass cover slide.

As demonstrated in Fig. 2.5, some lipid molecules did not freely diffuse but were immobile. The fraction of immobile molecules was low but they showed up prominently in the images because they appeared brighter than mobile molecules. The fluorescent signal of immobile molecules was confined to very few pixels during the illumination time of each image and not spread over several pixels due to movement of the molecule during the illumination time. The spots where immobile molecules could be observed had a similar density and

distribution as the defects in the membrane shown in Fig. 2.3. It is probable that locations of the glass cover slide not covered by the SPB (for whatever reason) cause also the sticking of lipid molecules at the rim of the SPB. I observed also strong fluorescence blinking of the molecules in the SPB, which was possibly enhanced by the interaction with the surface.

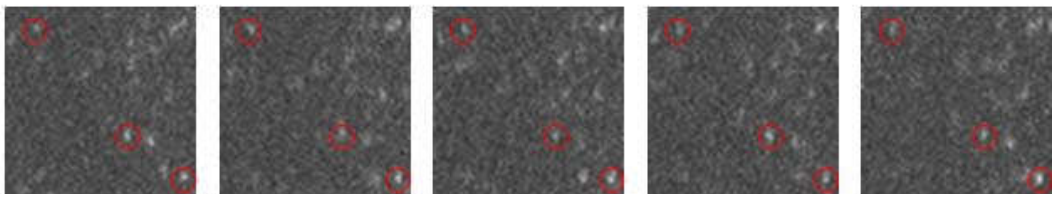

Fig. 2.5 Serial of five consecutive images showing the diffusion of single DOPE-TMR molecules in a DOPC SPB on a glass cover slide. The red circles highlight immobile molecules which are brighter than diffusing molecules because there signal is concentrated on less pixels than the signal of moving molecules during the illumination time. The illumination time was 30 ms with a gap of 1.94 ms in between for frame transfer. The edge length of the images is 4.6 µm.

2.1.3 2fFCS experiments

I took advantage of the newly developed 2fFCS method and investigated the diffusion of lipid molecules within a SPB not only with imaging but also with 2fFCS. In two-dimensional diffusion measurements, the diffusion time and thus the estimated diffusion coefficient as measured by standard, single-focus FCS sensitively depends on the diameter of the laser focus within the membrane's plane. However, a strongly focused laser beam is strongly divergent, i.e. its focus diameter changes quickly with position along the beam. It is therefore necessary to have exact knowledge about the position of the laser beam waist relative to the membrane. 2fFCS is insensitive to the exact position of the laser beam waist relative to the membrane because the determining parameter for calculating the diffusion coefficient is the distance between the foci and not their size. In contrast to the z-scan technique developed in Martin Hof's group in Prague (Benda *et al.*, 2003), 2fFCS should be able to resolve the correct diffusion coefficient by a single measurement instead of having to perform a whole z-scan through the membrane. For a z-scan several ACF measurements for different positions of the laser beam with respect to the SPB are performed. From these ACFs one estimates the diffusion time τ. The diffusion time is the time the ACF has dropped to 50% of its initial value. The obtained τ for each z-position of the laser are plotted versus the z-position of the laser focus getting, due to the strong divergence of the laser beam, a parabolic graph. This graph is fitted using beam waist and diffusion coefficient as fit parameters, yielding absolute values for both independently.

For the diffusion measurements, SPBs made from DOPC in pure water on glass cover slides were prepared. The SPBs were labeled with DOPE-Atto655 molecules in a ratio of 1:400,000. The diffusion of lipid molecules in these SPBs

was measured with 2fFCS. To compare the method with the z-scan technique a whole z-scan through the bilayer was also performed.

The values of the diffusion coefficients as determined with 2fFCS at various z-positions varied by more than 15% in a non systematic way. This large variation can be understood by inspecting the individual fits of the auto- and cross-correlation curves, as shown for example in Fig. 2.6A. The fit quality is rather poor, in particular at large lag times, and the measured correlations are not well described by the supposed model of freely diffusing dyes in two dimensions. This can be attributed to adsorption and desorbtion of the labelled lipid molecules to the supporting glass cover slide, which I already observed by direct imaging with single molecule sensitivity (see chapter 2.1.2). Thus, the analysis of the data was repeated employing more complex model which accounted also for

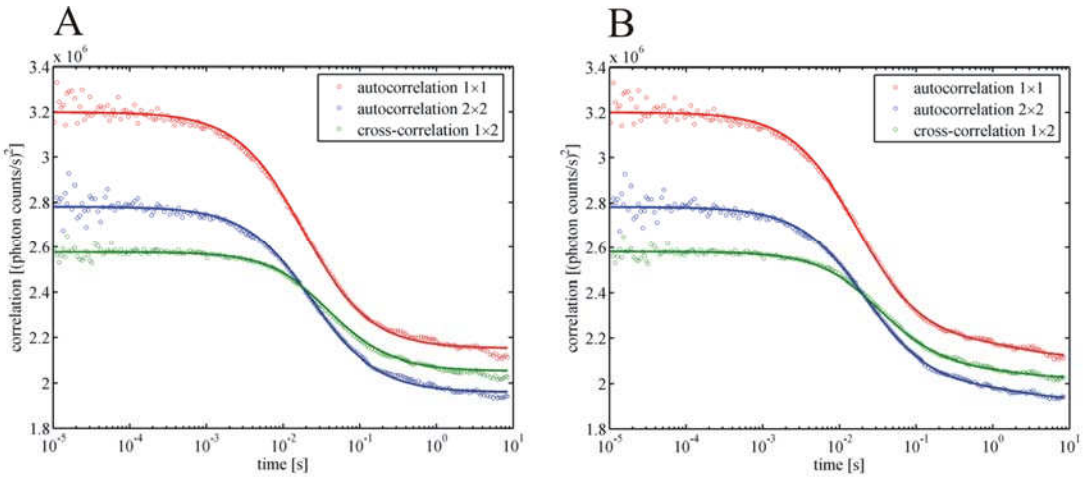

Fig. 2.6 A: Global least-squares fit of the two auto- and one cross-correlation curves using the free-diffusion model. B: The same as A but using the model including adsorption and desorption kinetics.

adsorption and desorption of lipid molecules. The free fit parameters of the model were: beam waist, the diffusion coefficient, and the adsorption and desorption rate constants k_{on} and k_{off} of lipid molecules. For a detailed description see Dertinger *et al*. (2006). The fit result of the new model to the same data as shown in Fig. 2.6A is presented in Fig. 2.6B, showing a clear improvement of fit quality.

Still, there was a considerable variation in all obtained values of the diffusion coefficient. An explanation of this strong variation can be found when realizing the slowness of the observed adsorption/desorption kinetics: On average, a molecule adsorbs to the surface ca. every hundred milliseconds, and the desorption kinetics is even slower by more than one order of magnitude. Thus, during the time of one measurement (15 min) only a statistically small number of adsorption and desorption events takes place. Thus, curves measured at different times vary considerably and give strongly varying results. Another peculiarity is that the obtained desorption rates are so small that the assumed desorption process is probably rather photobleaching than real desorption followed by diffusion out of focus. Extending the measurement time is not a practicable option: To obtain a

reasonable statistical accuracy, measurement times of several hours would be needed, assuming that no change in the sample takes place. To alleviate the situation to some extent, a global fit of all z-scan sets of curves was performed, with one set of parameters (beam waist, diffusion coefficient, k_{on} and k_{off}) for each z-scan. All fit results are listed in Table 2.1.

Table 2.1 Results of the global fit of all z-scan sets with the extended model taking adsorption and desorption kinetics of the lipid molecules into account

	$1/k_{on}$ [s]	$1/k_{off}$ [s]	$K_{eq} = k_{off}/k_{on}$	D [µm²/s]
focus 1	0.071	2.3	0.031	3.28
focus 2	0.090	3.4	0.026	3.22
2-focus	0.086	2.7	0.031	3.30

As shown by the values listed in Table 2.1, roughly 97% of all molecules are bound to the surface on average at any time. This has a profound influence on measurement performance and the values of the extracted diffusion coefficients.

Benda *et al*. (2003) found a similar diffusion coefficient of 4.0 ± 0.5 µm²/s for DOPC on a borosilicate glass cover slide and 4.2 ± 0.4 µm²/s for DOPC on mica by using the z-scan technique. This group used also phospholipids with labeled hydrophilic headgroups (Rhodamine Red-X DHPE from Molecular Probes, Leiden, The Netherlands). Przybylo *et al*. (2006) found a diffusion coefficient of 3.1 ± 0.3 µm²/s for DOPC on mica, also using the z-scan technique. There, a phospholipid with the fluorescent dye linked to the hydrophobic tail (C8-BODIPY 500/510 C5-HPC, Invitrogen) was used as the fluorescent probe. With a headgroup-labeled phospholipid as fluorescent probe (BODIPY FL DHPE, Invitrogen), a diffusion coefficient of 3.5 ± 0.3 µm²/s was found for DOPC on mica (Przybylo et al., 2006). The seen differences among different fluorescent probes were within the measurement error: Thus, the nature of the probe seems to have a rather minor impact on the measured diffusion coefficient.

In agreement with results from Przybylo et al. (2006) I found a more than two times bigger diffusion coefficient for phospholipids in free-standing bilayers of GUVs (see chapter 2.2.3). Thus, adsorption of the lipids to the solid support of SPBs (most possibly within defects in the bilayer) is not the only interaction of the phospholipids with the solid support. There is also a strong frictional coupling of the lipid bilayer with the solid support and in between the two bilayer leaflets, as also suggested in other studies (Merkel *et al.*, 1989; Zhang and Granick, 2005). It is implausible to assume that only the diffusion within the monolayer next to the solid support is influenced. Different diffusion behavior within the two monolayers would show up in FCS measurements as two distinctly diffusing fractions.

Summarizing all results of this chapter, it seems to be clear, that SPBs are not a suitable model system for investigating the interaction of Recoverin with lipid bilayers. It occurred to be impossible to prepare defect-free SPBs on glass cover slides. Moreover, the observed influence of the support on lipid diffusion makes this model membrane system not recommendable for further use. I decided to turn to another, more appropriate model membrane system with no interaction artifacts from supporting surfaces.

2.2 Getting away from the surface - Giant Unilamellar Vesicles

The experiments with supported bilayers revealed that these bilayers had defects which caused unspecific adsorption of Recoverin to the solid support. Moreover, diffusion measurement showed that there are strong interactions of the lipids with the solid support. Thus, the model system for investigating the interaction of Recoverin with lipid membranes should be one with free standing lipid bilayers having no interaction with any support.

2.2.1 How GUVs look like and why to use them

Small unilamellar vesicles (SUVs) have sized of a few nanometers, large unilamellar vesicles (LUVs) go up to 10 µm in diameter, and giant unilamellar vesicles (GUVs) have sizes between 10 µm and 100 µm in diameter. Thus, GUVs are liposomes that have the sizes comparable to eukaryotic cells and may be even bigger than cells. They provide free standing bilayers that do not have any coupling with a solid support like SPBs do. Due to their size, GUVs can be directly observed with a light microscope, and the bilayers of GUVs are quasi-planar on the length scale of a laser focus. Although it might be necessary to immobilize them for long term measurements, GUVs exhibit also almost no self diffusion because of their size.

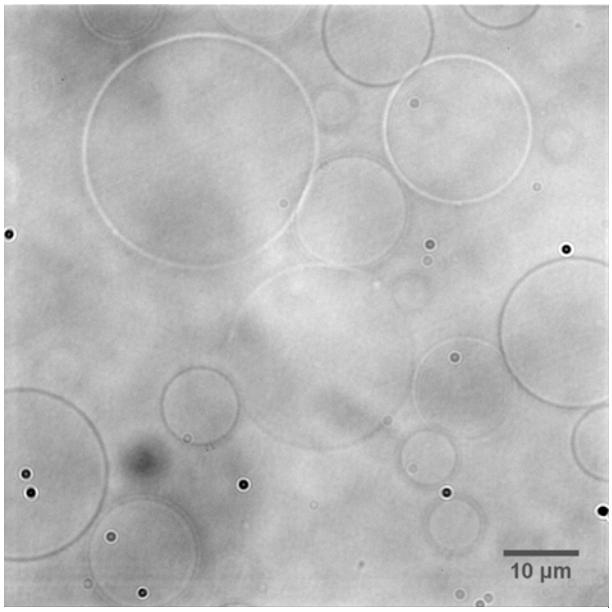

Fig. 2.7 Wide field image of giant unilamellar vesicles (GUVs) made from DOPC via electroformation. Black spots are dust particles on the camera optics.

GUVs are stable for several days, and their bilayer is closed and free of defects, and they are tight for ions and all neutral molecules of the size of glucose or larger. As a result, GUVs are sensitive to osmotic gradients. When preparing GUVs, one is free to control and to choose the lipid composition of the bilayer. There are no limitations in lipid composition. The only prerequisite, again, is to work in a suitable temperature range. Temperature has to be, as always, above the main phase transition temperature of the lipid to allow the formation of vesicles.

Thus, GUVs have the properties one would like to have for a model membrane system. They provide free standing, defect free bilayers with variable lipid composition. They are visible in the microscope, so the membrane is easy to find, and they are stable within measurement time.

2.2.2 Preparation of GUVs – Electroformation

How can GUVs be prepared? The challenge when working with GUVs is the demanding method of their preparation. The method that gives the highest yield of GUVs (from 10 to 100 µm) within a couple of hours is electroformation. This method was discovered by Angelova and Dimitrov in 1986 (Angelova and Dimitrov, 1986). It relies on the hydration of dry films of lipids under the influence of an oscillating electric field. This empirical method was optimized in the following years, and the resulting vesicles were extensively studied and characterized (Dimitrov and Angelova, 1987; Dimitrov and Angelova, 1987a; Dimitrov and Angelova, 1988; Angelova et al., 1992). Although there have been several attempts to find the underlying mechanism of vesicle formation by oscillating electric fields and to isolate all factors that influence the electroformation process. GUV preparation by electroformation is not yet fully understood (Dimitrov and Angelova, 1986; Angelova and Dimitrov, 1988; Dimitrov and Angelova, 1988; Angelova et al. 1992).

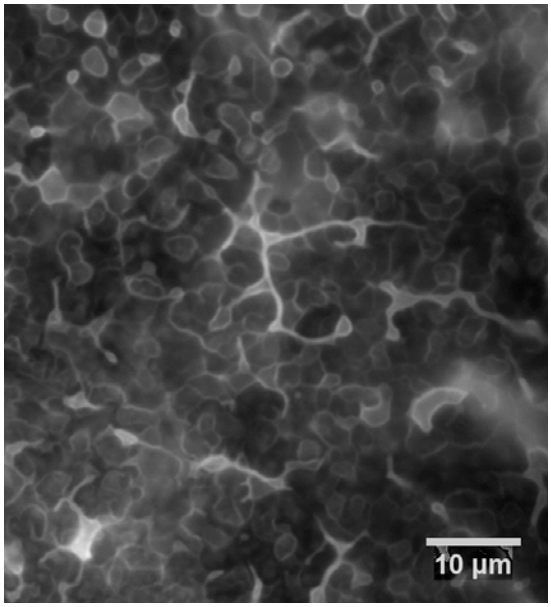

Fig. 2.8 Fluorescently labeled DOPC hydrated with 250 mM glucose solution on the ITO cover slide in the electroformation cell before the oscillating electric field is applied. The aqueous solution causes swelling of the dry lipid layers and pre-forms vesicles.

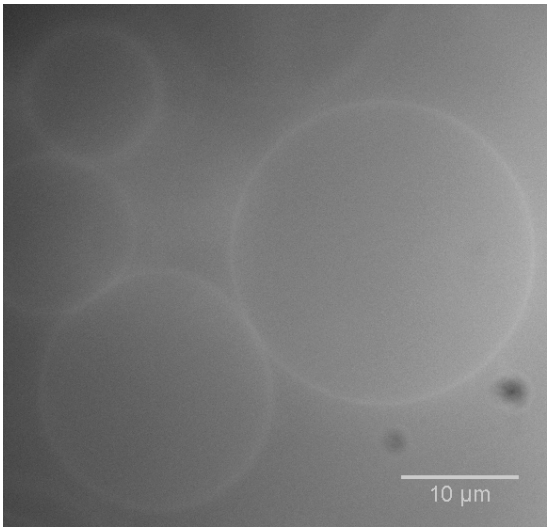

Fig. 2.9 Fluorescence image of GUVs made from DOPC in glucose solution via electroformation. Black spots are shadows of dust particles on the optics.

The technique of electroformation works as follows: A solution of lipids in an organic solvent (usually chloroform) is deposited on an electrode e.g. platinum wires or ITO coated glass slides. The organic solvent is evaporated and the thin lipid film (I used 5 µg/cm² lipid corresponding to 25 lipid bilayers) is hydrated with pure water or a non-ionic aqueous solution, e.g. glucose. The macroscopically smooth lipid film is microscopically rough-textured

and gets even rougher by hydration (see Fig. 2.8). After immersing the lipid film on the electrodes in solution, an oscillating electric field (usually 10 V/cm and 10 – 15 Hz) is applied. The lipid film swells and the lipid bilayers separate. Small hemispheric bubbles emerge which grow and swell under continuous action of the electric field. The bubbles remain linked to the lipid film and become more and more spherical. Finally, the joint regions fuse. This process results in large globular vesicles and small hemispheric bubbles on the electrode surface. The vesicles detach from the surface and are pushed away from it by new growing bubbles and vesicles. After two to four hours, there are several layers of GUVs in the electroformation cell. I did not meet any limitations concerning the lipid composition of pure and neutral phospholipids like DOPC or mixtures like soy bean lecithin. Even mixtures with up to 10% cholesterol or up to 15% negatively charged phospholipids like DOPS could be used for GUV electroformation.

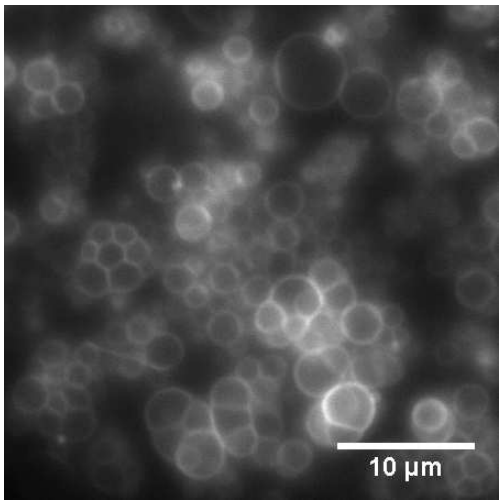

Fig. 2.10 Electroformation with ionic solutions: No giant vesicles but only a foam of small bubbles developed after applying an oscillating electric field.

A limitation of the technique is its inability to form vesicles in ionic solutions. Even small amounts of ions in solution compensate the electric field and thus prevent vesicle formation.

Montes *et al*. (2007) reported on a method that should allow the preparation of GUVs in ionic solutions. They use an electric field of 500 Hz instead of 10 - 15 Hz which is usually used. However, I did not manage to prepare GUVs in ionic solutions following their protocol. Unfortunately, this protocol was found similar to all protocols for electroformation, empirically and was specifically optimized for the electroformation cell as used by Montes *et al*. (Luis Bagatolli, personal communication, 2007). Because, the underlying mechanism of electroformation is not yet fully understood, there is no explanation why the protocol proposed by Montes *et al*. works in their case, and why increasing the frequency of the electric field to 500 Hz should help the formation of GUVs in ionic solutions.

A second method to prepare giant vesicles is by gentle hydration. In this method, a thin and dry lipid film prepared also from a chloroform solution, was hydrated with an aqueous solution over more than 12 hours. Any agitation of the sample was avoided. In this case, the presence of ions does not disturb the build-up of GUVs because no electric field is involved. With this method, vesicles of all sizes form spontaneously. The great disadvantage of this method is its low yield of unilamellar vesicles (see Fig. 2.11).

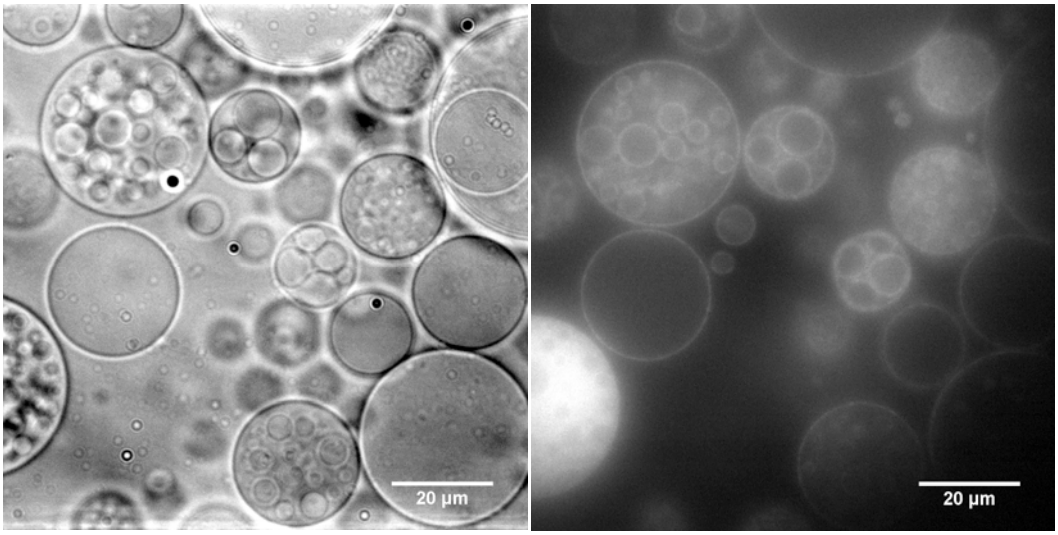

Fig. 2.11 Giant vesicles made by gentle hydration from soy bean lecithin fluorescently labeled with 0.1% DHPE Oregon Green. Vesicles are filled with sucrose solution and outside the vesicles is an isotonic glucose solution to make the vesicles settle down on the cover slide. On the left hand side is shown a wide field image with lamplight and on the right hand side is shown the fluorescence image of almost the same area. Only very few vesicles are unilamellar, most large vesicles have enclosed smaller ones.

Single molecule imaging of fluorescently labeled molecules (DOPE-TMR and DOPE-Atto655) diffusing within the lipid bilayer of a GUV showed no immobilized molecules. Molecular motion was significantly faster than that of lipid molecules in SPBs.

2.2.3 2fFCS experiments - lipid diffusion

Diffusion of fluorescently labeled phospholipids (DOPE-Atto655) in GUV membranes was characterized with 2fFCS. Observing lipid diffusion with single molecule imaging already indicated that there was no sticking of lipid molecules, and that the diffusion was faster than in SPBs. 2fFCS was used to quantify this observation more precisely.

Because the cells employed for GUV electroformation used optically transparent ITO electrodes, there was no problem to measure 2fFCS directly through the ITO-coated cover slides. After electroformation, the GUVs settled down after reaching equilibrium conditions and the stop of any convection, but it occurred to be advantageous to immobilize them, so that a GUV could not roll out of the laser focus. The protocol for immobilization of GUVs is given in the “Material and Methods” section.

I measured how water and different aqueous solutions inside and outside the vesicle influence lipid diffusion. For that purpose, I prepared vesicles in water,

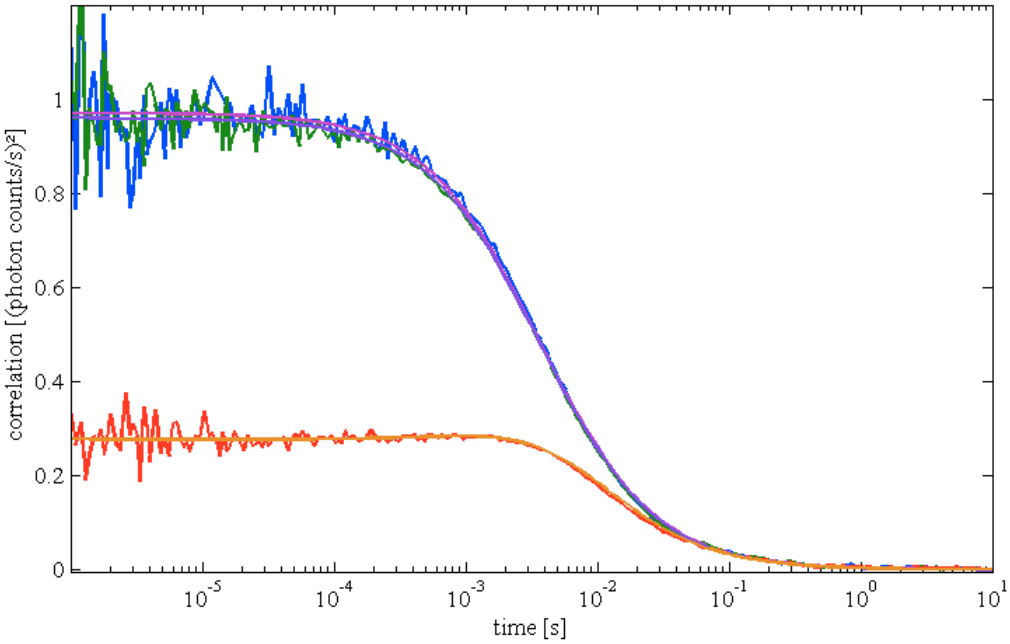

Fig. 2.12 2fFCS measurement of DOPE-Atto655 diffusion in a GUV bilayer made from DOPC. Inside the vesicle was glucose solution, outside was an isotonic salt buffer. Measured autocorrelation curves are shown in blue and green with fitted curves shown in purple and violet. The measured cross-correlation function is shown in red with a fitted curve shown in orange

glucose or sucrose solution and exchanged afterwards the liquid outside the vesicles for an isotonic salt buffer solution. It was impossible to have a salt buffer inside the vesicles because ions prevented vesicle build-up via electroformation.

Table 2.2 Diffusion coefficients measured by 2fFCS of DOPE-Atto655 in GUVs bilayers made from DOPC via electroformation dependent on the solution inside and outside the GUV.

inside vesicle	outside vesicle	diffusion coefficient
water	water	$(8.0 \pm 0.2) \cdot 10^{-8}$ cm²/s
247 mM glucose	247 mM glucose	$(7.5 \pm 0.4) \cdot 10^{-8}$ cm²/s
247 mM glucose	100 mM KCl; 30 mM Hepes pH 7.2; 10 mM K_2CaEGTA	$(9.0 \pm 0.4) \cdot 10^{-8}$ cm²/s
238 mM sucrose	238 mM sucrose	$(6.8 \pm 0.2) \cdot 10^{-8}$ cm²/s
238 mM sucrose	100 mM KCl; 30 mM Hepes pH 7.2; 10 mM K_2CaEGTA	$(7.3 \pm 0.4) \cdot 10^{-8}$ cm²/s

Fig. 2.12 presents a typical 2fFCS measurement. The fit quality is excellent, and there are no adsorption and desorption processes as was seen for the diffusion of lipids in SBPs. The used dye Atto655 shows no photophysics on the microsecond timescale (such as triplet state photophysics). Therefore the measured correlation curves could be fitted without any additional term for photophysics. The results of the measurements with all measured combinations of different solutions inside and outside the vesicle are shown in Table 2.2.

The phospholipid diffusion coefficient in GUV bilayers is more than two times larger than the diffusion in SPBs ($3.3 \cdot 10^{-8}$ cm²/s; see chapter 2.1.3). These results are in perfect agreement with the z-scan results of Przybylo *et al.* (2006): they found a diffusion coefficient of $(7.8 \pm 0.8) \cdot 10^{-8}$ cm²/s for diffusion in a GUV bilayer measured in glucose, and $(3.1 \pm 0.3) \cdot 10^{-8}$ cm²/s for diffusion in a SBP bilayer on mica also measured in glucose. The diffusion coefficient of $3.3 \cdot 10^{-8}$ cm²/s measured in water for a SPB on glass shows that the surrounding medium seems not to have such a strong influence on the diffusion in SBP bilayers as it has for GUVs. The coupling of the lipid bilayer with the solid support of SPBs is much stronger than the influence of the surrounding medium on the lipid diffusion (Przybylo *et al.*, 2006).

When comparing the diffusion coefficients listed in Table 2.2 one can observe that sugars, especially sucrose, slow down the diffusion compared to water, whereas a salt solution compensates this effect. A possible explanation is clustering of phospholipids due to H-bonds in between the lipid headgroups and the OH-groups of the sugar. Doeven *et al*. (2005) found a similar effect of sugar on the lateral mobility of DiO (fluorescent lipid analogue) in GUV membranes. The diffusion coefficient of $7.7 \pm 0.8 \cdot 10^{-8}$ cm²/s in water was lowered to $4.1 \pm 0.7 \cdot 10^{-8}$ cm²/s in 1.5 M glucose and to $2.5 \pm 0.6 \cdot 10^{-8}$ cm²/s in 1.5 M sucrose.

2.2.4 Interaction of Recoverin with GUVs

After characterizing the lipid diffusion in GUV bilayers, I investigated the interaction of Recoverin-Alexa647 with GUVs in dependence on the free calcium concentration. I was interested in the average residence time of Recoverin at the bilayer in particular whether this residence time would be dependent on the calcium concentration. The diffusion of Recoverin molecules in solution would be much to fast to be resolved with the single molecule sensitive camera, adding only a homogeneous fluorescence background to an image. However, when binding to the membrane, Recoverin mobility should slow down enough so that individual diffusing molecules should be recognizable in an image series. Thus, the time resolution and sensitivity of the camera should help to discriminate Recoverin in solution from that bound to the membrane. However, it would be impossible to distinguish Recoverin molecules leaving the membrane from fluorophors that photobleached. Thus, the residence time would be measured, would give a lower limit of the residence time of Recoverin at the membrane. Furthermore, these

measurements would help to estimate the number of Recoverin molecules bound to the GUV membrane in dependence on the calcium concentration. Therefore, all the experimental conditions, especially the Recoverin concentration in solution should be kept constant.

When I added Recoverin-Alexa647 in calcium buffer at high calcium concentration to a preparation of GUVs, I could nicely observe that Recoverin was not able to enter the vesicles: the interior of the vesicles remained dark, whereas the solution outside was bright because of the homogeneous background fluorescence from Recoverin molecules in solution. The fluorescence intensity occurred to be slightly larger close to the GUV membrane indicating that Recoverin was indeed bound to the membrane (see Fig. 2.13). Unfortunately, I

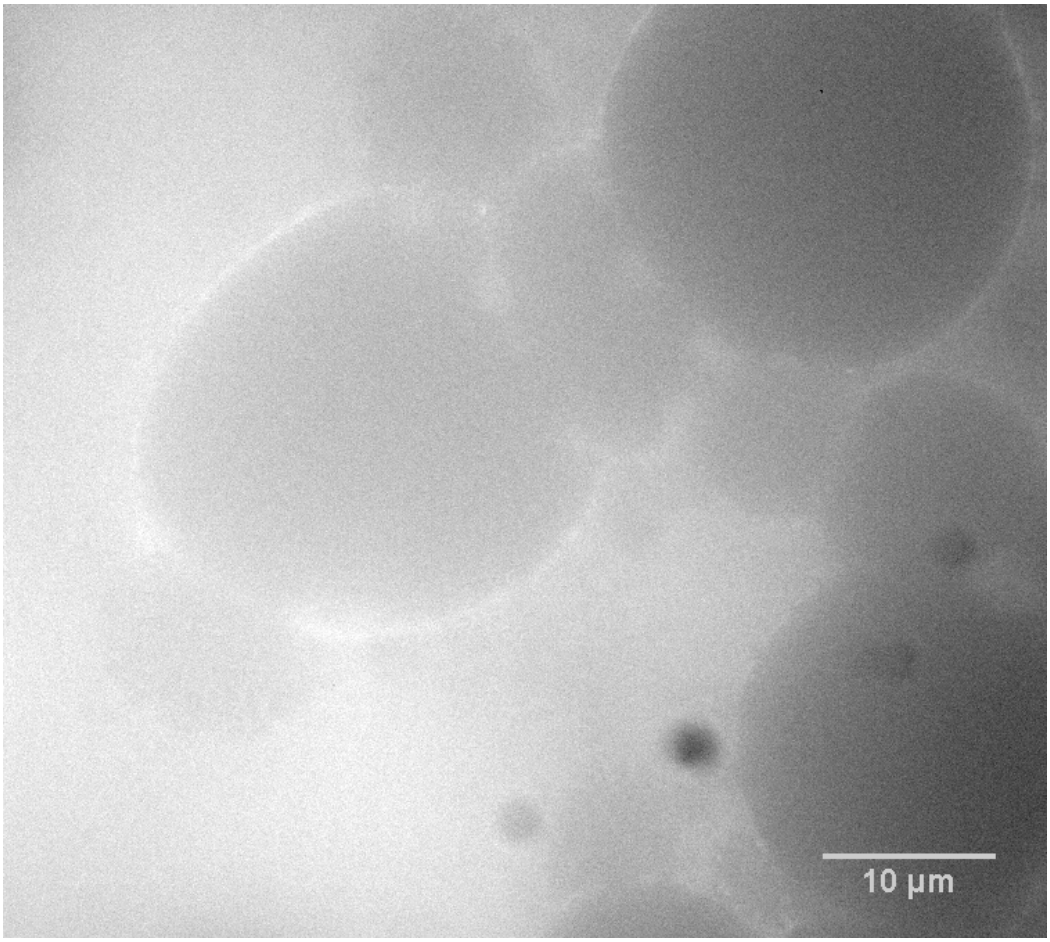

Fig. 2.13 Interaction of Recoverin-Alexa647 and GUVs at high calcium concentration. Recoverin cannot enter the vesicles therefore they appear dark inside. Fluorescent light is detected from everywhere along the optical axis. Fluorescence which does not come from the focal plane also adds to the background. Recoverin binds to the GUV bilayer which can be judged from the brighter fluorescence signal at the boundary of the dark interior of the GUVs.

could not identify individual molecules in the images, because the fluorescence background from solution was much too large. In other words, the affinity of Recoverin for the lipid bilayer was too small, so that the ratio of bound and free Recoverin was too small to observe individual bound molecules on the high

background of freely diffusing molecules. Potential solutions to this problem are using model membrane systems with a higher density of lipid bilayers, or the reduction of background light by an illumination mode that excites fluorescence only in the focal plane of the objective, such as Selective Plane Illumination Microscopy (SPIM), a microscopy technique employed by the group of E. Stelzer (EMBL Heidelberg).

The next step was to use 2fFCS for measuring the amount of Recoverin bound to the GUV's bilayer and freely diffusing in solution. For doing that, the laser foci were placed on the GUV membrane, so that the detection volume was cut by the membrane. Outside the vesicle was Recoverin diffusing in solution and bound to the membrane, and there was no fluorescence inside the vesicle (see Fig. 2.14). It was expected to measure two differently diffusing species: rapidly diffusing Recoverin in solution and slowly diffusing Recoverin bound to the bilayer. When the detection volume is situated close to a boundary restricting the diffusive motion of the molecules, i.e. if some part of the detection volume is cut off by the boundary, the temporal decay of the fluorescence autocorrelation is changed, which means the *apparent* mobility of the molecules is changed. Using a complex data evaluation, it was tried to estimate which part of the foci was cut off by the GUV. How the ACF is influenced by the cut-off of the detection volume can be qualitatively seen in Fig. 2.15 for a measurement on freely diffusing Atto655 outside the vesicle.

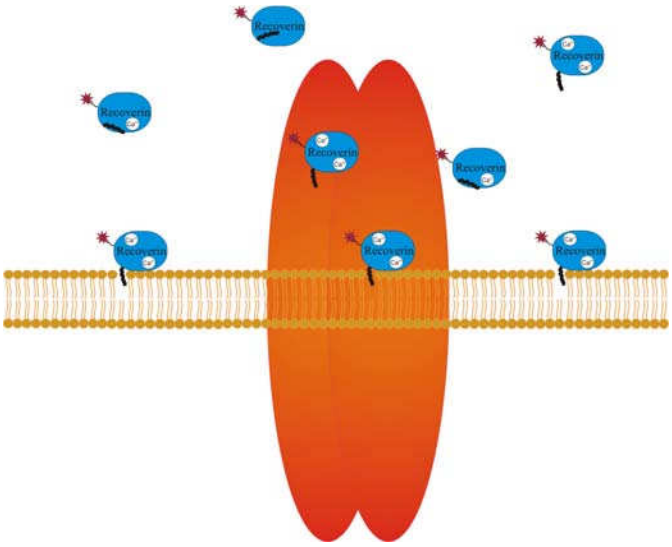

Fig. 2.14 Schematic of the 2fFCS experiment for the measurement of the amount of Recoverin bound to the GUV membrane.

The diffusion time gets longer thus the diffusion coefficient seams to be lower with increasing cut off of the focus. This is contra intuitive in the first moment because one should think that the focus becomes smaller with increasing cut off and therefore the diffusion time in the focus should get shorter. But when cutting the centre part of the focus with high detection probability the border area of the focus with low detection probability becomes more important. So the probability to detect a photon becomes lower but the area where to detect a photon with low probability increases and therefore the diffusion time gets longer with increasing cut off of the focus.

The following fitting parameters entered the data analysis: two parameters describing laser focusing and confocal detection, the position of the foci along the

optical axis with respect to the bilayer, and the diffusion coefficients of Recoverin in solution and in the bilayer.

As it occurred, Recoverin diffusion in solution and in the bilayer as measured for different cut offs of the foci could not be fitted consistently with such a model. The main reason is probably non-negligible vertical membrane undulations as also reported by other groups (Fradin *et al.*, 2003). The already very complex model and the high number of involved fit parameters prevented any further refinement, because increasing model complexity and number of fit parameters would no longer yield any reasonably reliable and stable fit results.

To better estimate the influence of the cut-off of diffusion measurements with FCS, I carried out a series of measurements for increasing cut-offs of the detection volume. I prepared and immobilized GUVs, and added afterwards a

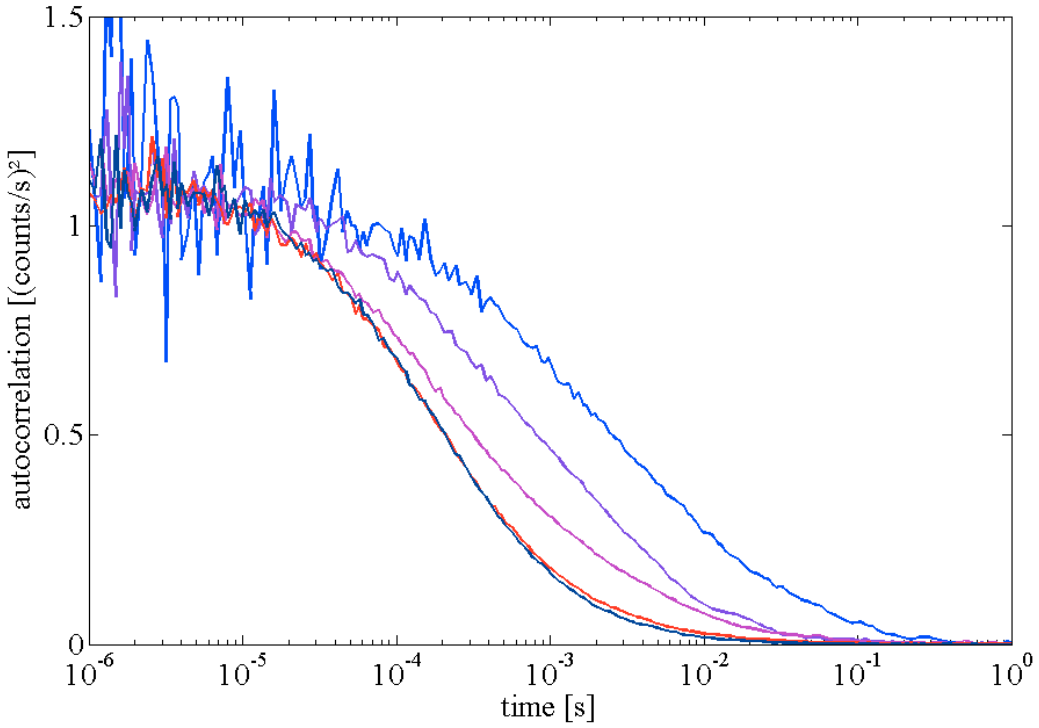

Fig. 2.15 ACFs for increasingly larger cut-offs of the detection volume. The ACF of Atto655 diffusing in solution is shown in dark blue. The ACFs of nearly no, 1.5 µm, 2.5 µm and 3.5 µm cut-off are shown in red, purple, violet and blue. It is clearly seen that the temporal decay of the ACF, and correspondingly the diffusion time, is significantly shifted towards larger time values with increasing cut-off of the detection volume.

nanomolar solution of Atto655. Atto655 does not bind to the GUV bilayer and cannot enter the vesicle. In the beginning, the laser focus was positioned above the top side of the GUV membrane, and then several ACFs were measured for decreasingly lower vertical position of the laser focus. Thus, a series of ACFs for increasingly larger cut-off of the detection volume was obtained. The measured ACFs are shown in Fig. 2.15. Due to the difficulty of exactly locating the position of the laser focus with respect to the GUV membrane, the result bears only qualitative character. Moreover, as already mentioned above, the shape of the

measured ACFs suggests non-negligible vertical undulations of the GUV's lipid layer (Fradin *et al.*, 2003). However, it is clearly seen that the temporal decay of the ACF, and as a result, the diffusion time, is significantly shifted towards larger values with increasing cut-off of the detection volume.

2.3 Measuring conformational changes with 2fFCS

It is challenging to measure conformational changes of proteins by only monitoring their diffusion behavior. In this chapter, I present 2fFCS measurements of the diffusion coefficient of Recoverin and Recoverin mutants as a function of free calcium concentration. As will be seen, it is indeed possible to resolve Ca^{2+}-dependent conformational changes of these proteins, due to the high measurement accuracy achievable with 2fFCS. Recoverin is an extensively characterized protein and is therefore ideal for checking the reliability of 2fFCS and its applicability to resolve small conformational changes in proteins.

2.3.1 What changes when the functional EF-hands of Recoverin bind calcium ions?

In general, diffusion coefficients are dependent on size and shape of the diffusing molecules. Size and shape of Recoverin are changing when it binds two calcium ions, which triggers the extrusion of a myristic acid residue that is covalently bound to the N-terminus of the protein. The conformational changes of the protein are accompanied by changes in its hydration layer and the flexibility of certain parts of its molecular structure.

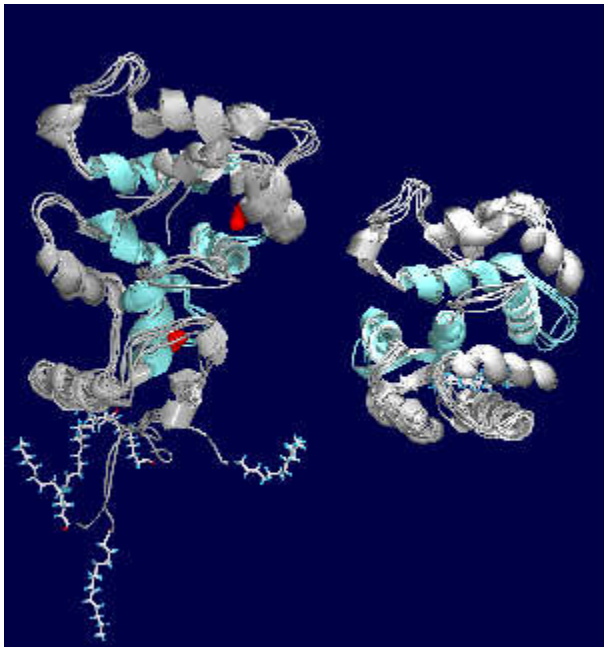

Fig. 2.16 Solution structures of Ca^{2+} saturated (left) and Ca^{2+} free (right) Recoverin. Ca^{2+} ions are shown in red, functional EF-hands are shown in turquoise. Due to rotation of the C-terminal domain with respect to the N-terminal domain upon Ca^{2+}-binding, Ca^{2+} bound Recoverin is elongated and more flexible compared to Ca^{2+} free Recoverin. Especially the C-terminus and the N-terminal region with the myristoyl residue are disordered. The N-terminal myristoyl residue is sequestered in a deep hydrophobic pocket of the compact and more rigid Ca^{2+} free protein.

Recoverin is a compact protein consisting of two domains separated by a narrow cleft (Flaherty *et al.*, 1993). Each domain contains two helix-loop-helix EF-hand motives: EF-1 and EF-2 in the N-terminal domain, and EF-3 and EF-4 in the C-terminal domain. The linker between the domains is U-shaped, and the four EF-hands form a compact array at one face of the protein (Flaherty *et al.*, 1993). In the calcium-free state, the myristoyl group is located in a deep hydrophobic pocket located in the N-terminal domain formed by five α-helices (Tanaka *et al.*, 1995). EF-hands 1, 2 and 3 contribute hydrophobic residues that interact with the myristoyl residue (Ames *et al.*, 1997).

Only two of the four EF-hands of Recoverin, namely EF-2 and EF-3, have the common amino acid sequence of the binding loop and show a high affinity for Ca^{2+}. EF-1 and EF-4 are disabled due to mutations. The myristoyl group of calcium-bound Recoverin is extruded into solution and forms, together with the eight disordered N-terminal residues, a flexible arm (Ames *et al.*, 1997). The conformations of the C-terminal domains of the Ca^{2+}-bound and Ca^{2+}-free forms are quite similar, apart from changes in EF-3. In contrast, the N-terminal domain undergoes a remarkable rearrangement caused by rotation of the backbone at G42. The N-terminal domain is also rotated by 45° relative to the C-terminal domain due to a conformational change near G96 in the interdomain linker (Ames *et al.*, 1997). Therefore, the Ca^{2+}-bound form of Recoverin is elongated and less compact as compared with the Ca^{2+}-free form.

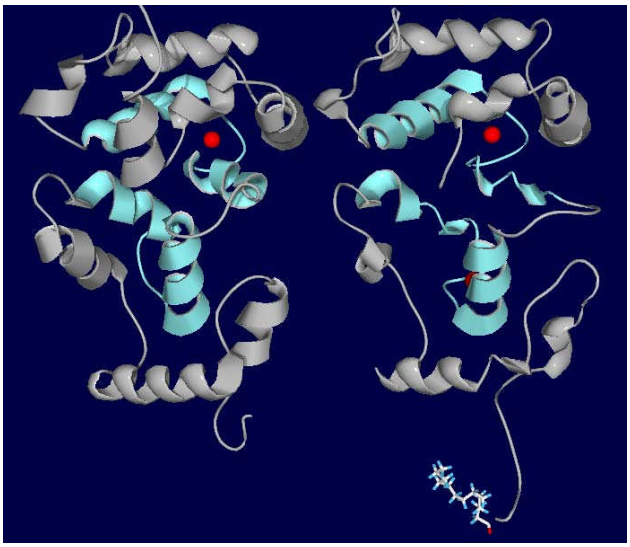

Fig. 2.17 Comparison of the molecular structures of non-myristoylated Recoverin with one Ca^{2+} ion bound and Ca^{2+} saturated wild type Recoverin. The N-terminal domain of non-myristoylated Recoverin is relaxed and adopts a conformation similar to Ca^{2+} saturated wild type Recoverin although there is no Ca^{2+} bound to EF-2.

A missing myristoyl residue has almost no influence onto the conformation of the C-terminal domain of Recoverin, but changes completely the N-terminal domain conformation (Tanaka *et al.*, 1995). The N-terminal domain is relaxed by the missing stabilization of the myristoyl residue. The overall topology of non-myristoylated Recoverin, with one Ca^{2+} bound to EF-3 is similar to that of Ca^{2+}-bound and myristoylated Recoverin (Ames *et al.*, 1997; Weiergräber *et al.*, 2003). So far, crystallization of the Ca^{2+}-free form of non-myristoylated Recoverin was not successful, which may be explained by a too high flexibility of the structure that is no longer stabilized by Ca^{2+} and myristoylation.

Flaherty *et al.* (1993) realized that EF-3 has a higher affinity for Ca^{2+} than EF-2, and Ames *et al.* (1994) suggested that the binding of Ca^{2+} to EF-3 induces EF-2 to adopt a conformation that favors binding of a second Ca^{2+} by Recoverin. This would suggest a sequential binding of the two calcium ions, whereas Ca^{2+}-binding by EF-2 is impossible until Ca^{2+} is bound by EF-3. This was verified by studies on S-modulin (the frog homolog of Recoverin) mutants (Matsuda *et al.*, 1998), and later by studies on Recoverin mutants (Permyakov *et al.*, 2000; Senin *et al.*, 2002). The highly conserved bidentate ligand glutamic acid was exchanged

by glutamine at position 12 in the loop of EF-2 and EF-3 (Alekseev *et al.*, 1998). The mutant E85Q (disabled EF-2) binds one calcium ion in EF-3, whereas the mutant E121Q (disabled EF-3) does not bind Ca^{2+} at all (Senin *et al.*, 2002). The structure of the mutants does not differ from the wild type structure as was checked by CD-spectroscopy (Permyakov *et al.*, 2000) and two dimensional ^{1}H-^{15}N-NMR (Ames *et al.*, 1994; Ames *et al.*, 2002). The Recoverin mutants E85Q and E121Q have been also used in my work for 2fFCS measurements to resolve effects of binding no, one or both Ca^{2+} ions on the diffusion coefficient.

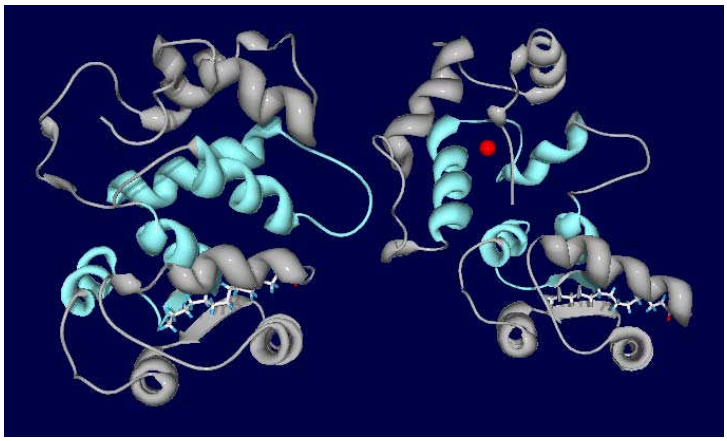

Fig. 2.18 Molecular structures of Ca^{2+} free wild type Recoverin and E85Q Recoverin mutant with one Ca^{2+} ion bound to EF-3. Ca^{2+} is shown in red, EF-2 and EF-3 are shown in turquoise. The carboxyl end of the myristoyl residue of the E85Q mutant is extruded to the solvent due to the missing interaction with EF-3 and movement of the N-terminal helix.

The structure of the myristoylated E85Q mutant with one Ca^{2+} ion bound was solved by NMR spectroscopy (Ames *et al.*, 2002). The structure of this intermediate state represents a hybrid of the structures of calcium-free and calcium-bound Recoverin. Ca^{2+}-binding to EF-3 lead to a rotation of the C-terminal domain of 45° about glycine at position 96. This alters the interaction of EF-2 and EF-3 and thus effects also the conformation of the N-terminal domain. The conformational change causes an increased affinity for Ca^{2+} in EF-2 and leads to exposure of the carboxyl end of the myristoyl residue to water.

2.3.2 From diffusion coefficients to binding constants

In what follows, I will present the results of 2fFCS measurements of the diffusion coefficient of wild type Recoverin and its different mutants as a function of the free Ca^{2+} concentration. The measured diffusion coefficients can be translated into Ca^{2+}-dependent Stokes radii via the Stokes-Einstein equation:

$$D = \frac{k_B T}{6\pi\eta r_S} \qquad \textbf{Eq. 2.1}$$

where D is the diffusion coefficient of a sphere with radius r_s at temperature T in a solvent with viscosity η, and k_B is the Boltzmann constant.

Recombinant myristoylated wild type Recoverin and the mutantsE85Q and E121Q as well as non-myristoylated Recoverin were specifically labeled at their native cysteine (position 38 of the amino acid sequence) with the maleimid-functionalized red fluorescent dye Alexa647. The diffusion was measured in calcium buffered solutions with different free Ca^{2+} concentrations at

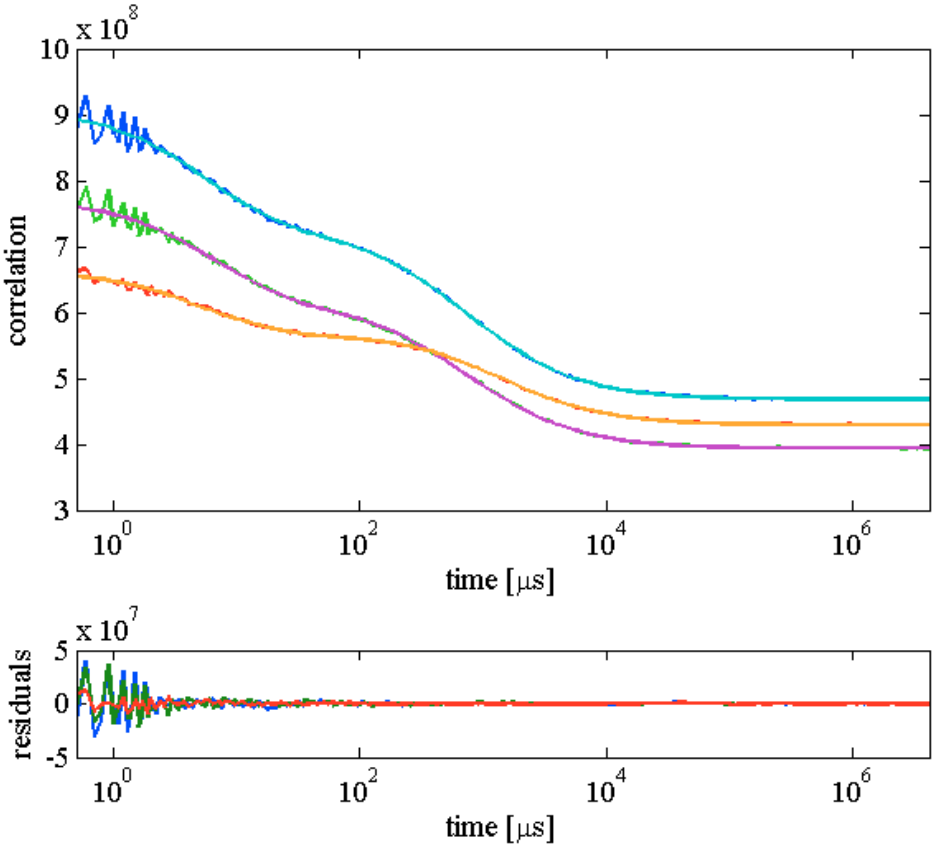

Fig. 2.19 2fFCS measurement of wtRecoverin-Alexa647 in 110nM free Ca^{2+} containing buffer. Measurement time was 30 min at 25° C and an excitation power of 12 µW for each laser. The autocorrelations are shown in blue and green, the cross-correlation is shown in red, the three lines of the global fit are shown in cyan, violet and orange. The offset between the two autocorrelations is caused by slightly different laser excitation power. Two additional decay parameter for each curve were used to fit the photophysics of the dye.

25° C. Total excitation power was 12 µW per laser. Measurements for each calcium concentration where repeated many times at several days to determine a standard deviation of the determined diffusion coefficients. Least square fitting of the two autocorrelation and one cross-correlation curves was done with a global fit which simultaneously reproduced the shape as well as amplitudes of both autocorrelation and the cross-correlation functions. Fit parameters were the relative amplitudes of the correlation functions, the diffusion coefficient, the laser beam waist, and a confocal pinhole parameter that defined the depth of view of fluorescence detection. The fitting model and the parameters are described in more detail in the dissertation of Thomas Dertinger (University of Cologne, 2007).

At least one additional decay parameter was necessary for fitting the photophysical decay of the correlation function in the µs regime of Alexa647. Due to the cis/trans photo-isomerization of Alexa647, the fit quality was improved when two decay times were used. A typical fit result for wtRecoverin-Alexa647 in Ca^{2+}-buffer is shown in Fig. 2.19. Data of each measurement were fitted several times to check the stability of the fit. Standard deviation of the diffusion coefficients was less than 0.5%.

The whole set of determined diffusion coefficients measured in 18 calcium buffers was used to calculate the corresponding Stokes radii using Eq. 2.1 as a function of the free Ca^{2+} concentration. The data were fitted with a binding model derived from the Hill equation to determine the Ca^{2+} dissociation constant and a Hill coefficient (Eq. 2.2):

$$r_S = \frac{A_1 - A_2}{1 + \left([Ca^{2+}]/K_D\right)^H} + A_2 \qquad \textbf{Eq. 2.2}$$

where r_S is the Stokes radius of Recoverin at a certain free Ca^{2+} concentration $[Ca^{2+}]$; A_1 and A_2 are the Stokes radii of the proteins at very low and very high free Ca^{2+}, K_D is the calcium dissociation constant, where the calcium binding is half-maximal, and H is the Hill coefficient which is a measure for the cooperativity of the binding.

2.3.3 Calcium binding of wild type Recoverin

At low calcium concentrations, wtRecoverin-Alexa647 binds no Ca^{2+} and has the compact apo-conformation, whereas it binds two calcium ions at high calcium concentrations and adopts the more elongated and more flexible calcium-bound conformation. Although the protein becomes less compact, the Stokes radius decreases from 25.3 Å to 24.1 Å after calcium binding (Fig. 2.20). The decrease in Stokes radius is half-maximal at a free calcium concentration of 4 [1.3 - 12] µM.

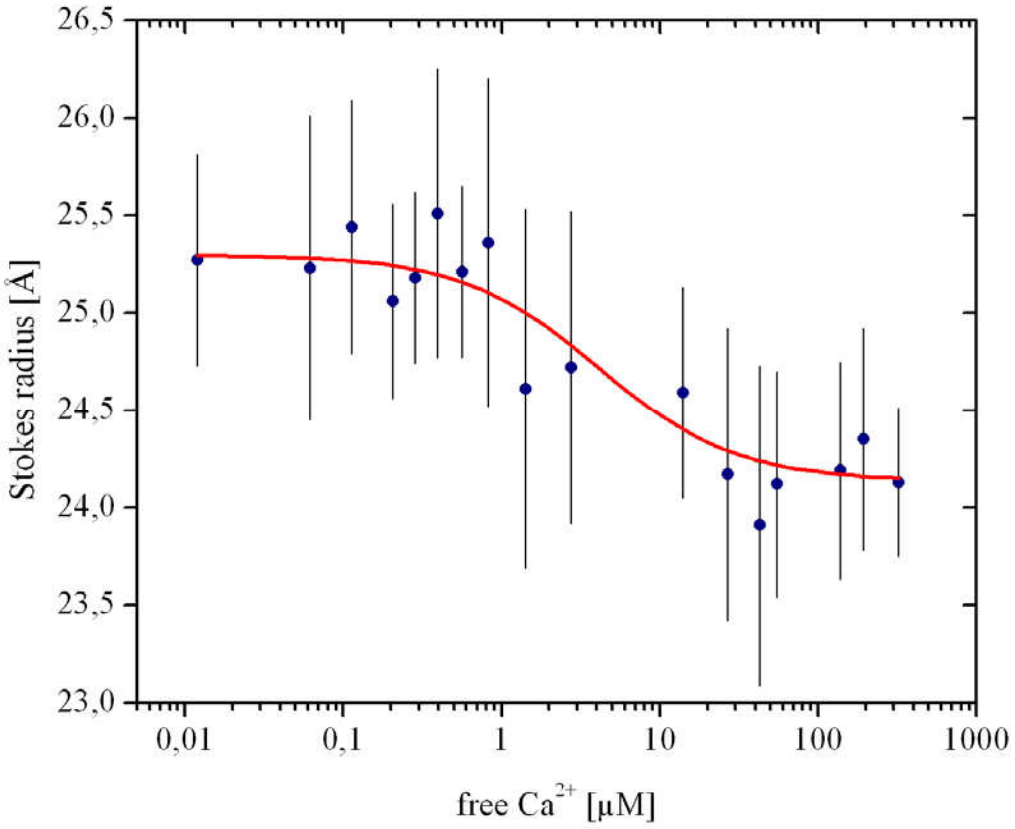

Fig. 2.20 The Stokes radius of wtRecoverin-Alexa647 as a function of free Ca^{2+} concentration. Standard deviations, shown as vertical error bars, were calculated from all measurements at a certain free Ca^{2+} concentration ($n \geq 8$). The red line shows the best fit corresponding to Eq. 2.2. Measurement temperature was 25° C. At low free Ca^{2+} concentrations the protein shows a Stokes radius of 25.3 ± 0.3 Å which decreases upon Ca^{2+}-binding at higher free Ca^{2+} concentration to 24.1 ± 0.3 Å. The estimated Ca^{2+} dissociation constant is K_D = 4 [1.3 – 12] µM. There is no cooperativity in the binding process, the Hill coefficient is 1.

2.3.4 Recoverin E85Q – Binding only one calcium ion

The Recoverin mutant E85Q with disabled EF-hand 2 binds only one Ca^{2+} ion to EF-hand 3. The diffusion coefficient of this mutant was measured to check the influence of the first Ca^{2+} binding event on the conformation independent on the second Ca^{2+} binding.

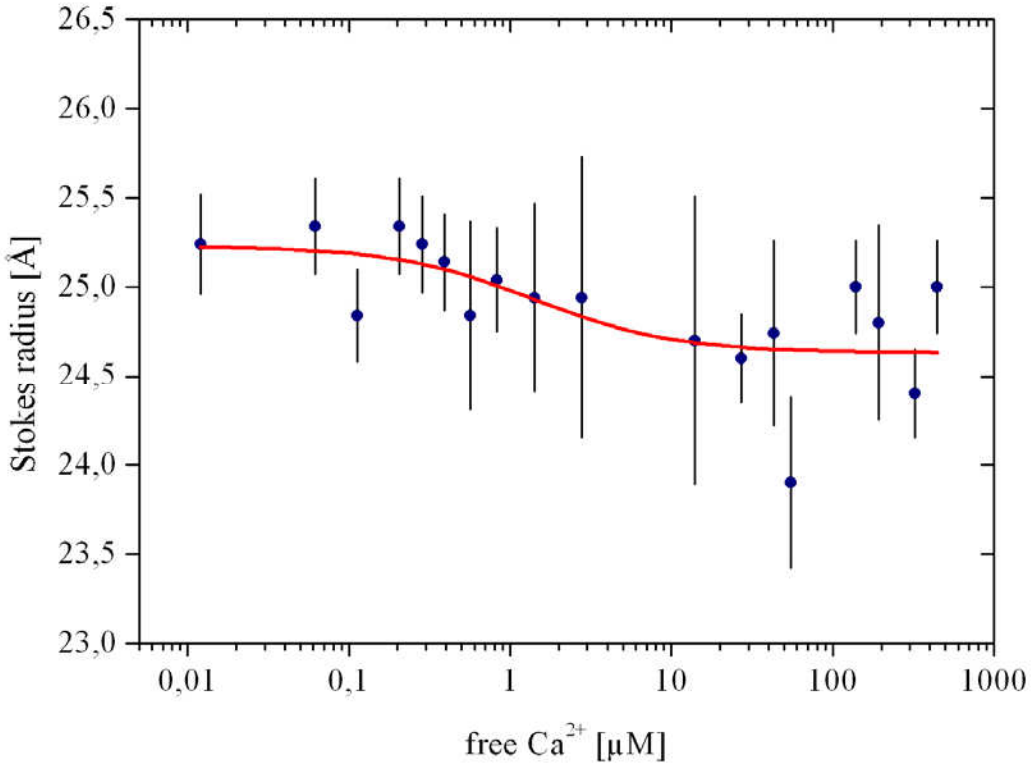

Fig. 2.21 The Stokes radius of Recoverin-Alexa647 E85Q as a function of free Ca^{2+} concentration. Standard deviations, shown as vertical error bars, were calculated from all measurements at a certain free Ca^{2+} concentration ($n \geq 10$). The red line shows the best fit corresponding to Eq. 2.2. Measurement temperature was 25° C. At low free Ca^{2+} concentration the protein shows a Stokes radius of 25.2 ± 0.2 Å which decreases upon Ca^{2+}-binding to 24.6 ± 0.2 Å. The estimated Ca^{2+} dissociation constant is K_D = 1.4 [0.58 - 3.4] µM which is lower than for the wild type protein. There is also no cooperative binding, the Hill coefficient is 1.

The Stokes radius as a function of the free Ca^{2+} concentration of Recoverin-Alexa647 E85Q is shown in Fig. 2.21. In the calcium free-state, the mutant E85Q has the same conformation as the wild type protein and also shows the same Stokes radius, namely 25.2 ± 0.2 Å. The Stokes radius decreases upon Ca^{2+} binding to 24.6 ± 0.2 Å. This decrease is by 0.5 Å smaller than for the wild type protein. Thus, binding of only one Ca^{2+} ion causes also a change in the Stokes radius, but the decrease is smaller than the difference in Stokes radius after binding of two Ca^{2+} ions. The estimated Ca^{2+} dissociation constant is K_D = 1.4 [0.58 - 3.4] µM which is lower than for the wild type protein. There is also no cooperative binding, the Hill coefficient is 1.

2.3.5 Recoverin E121Q – Binding no calcium

The Recoverin mutant E121Q with EF-hand 3 disabled does not bind calcium at all. EF-2 is not disabled but cannot bind Ca^{2+} as long as there is no Ca^{2+} bound to EF-3. No calcium binding means no change in conformation. Thus, this mutant can be considered to be a control sample.

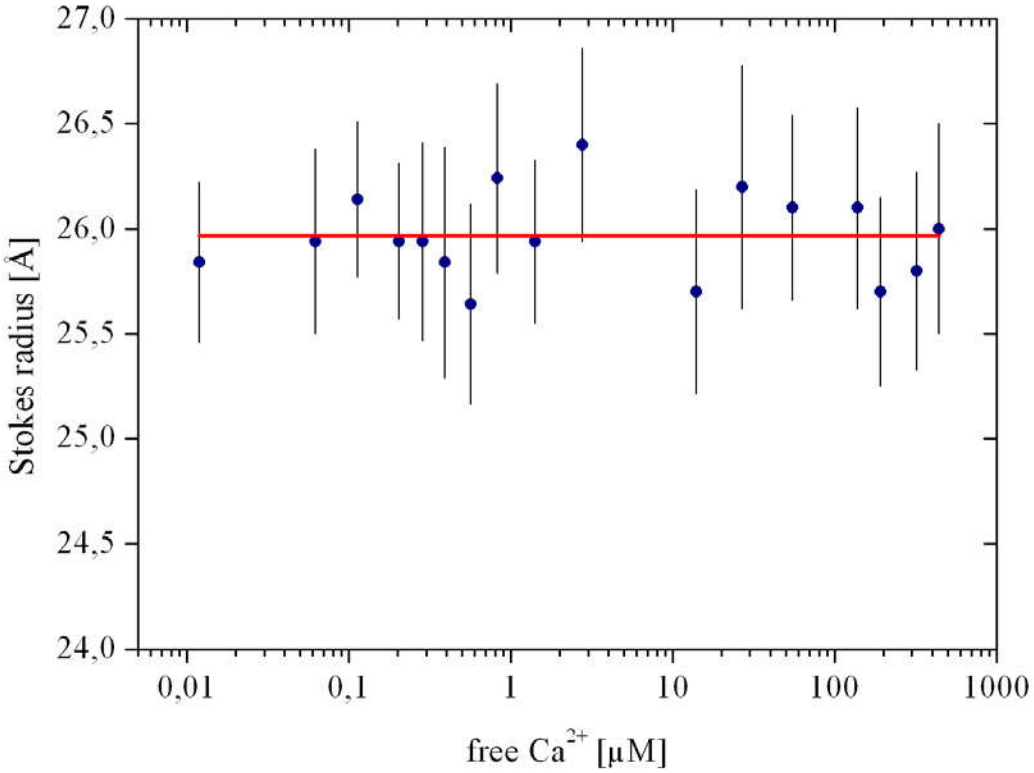

Fig. 2.22 The Stokes radius of Recoverin-Alexa647 E121Q as a function of the free Ca^{2+} concentration. Standard deviations, shown as vertical error bars, were calculated from all measurements at a certain free Ca^{2+} concentration ($n \geq 10$). Measurement temperature was 25° C. The Stokes radius does not depend on the Ca^{2+} concentration. There is no calcium binding and therefore no change in the conformation of Recoverin-Alexa647 E121Q. The Stokes radius is 26 ± 0.1 Å which is larger than the Stokes radius of the calcium-free conformation of the wild type protein even though the conformation of the calcium-free forms of these proteins should be identical.

Fig. 2.22 shows the Stokes radii of the mutant E121Q as a function of free Ca^{2+}. As expected, the Stokes radius does not change with calcium concentration, because there is no calcium binding and therefore no change in conformation of the protein. The estimated Stokes radius of 26 ± 0.1 Å is by 0.7 Å larger than the Stokes radius of calcium-free wtRecoverin-Alexa647 although the conformation of calcium-free wild type protein and of this mutant should be the same.

2.3.6 2fFCS measurements of non-myristoylated Recoverin

Besides the conformational changes due to Ca^{2+} binding, the extrusion of the myristoyl residue should also change the diffusion behaviour of Recoverin. Thus, for getting the whole picture, I investigated the non-myristoylated form of Recoverin. The missing myristoyl residue significantly disturbs the structure of Recoverin. Non-myristoylated Recoverin tents to aggregate, which troubled several 2fFCS-measurements. Calcium binding seems to stabilize the protein, because aggregation was less noticeable at high Ca^{2+} concentrations.

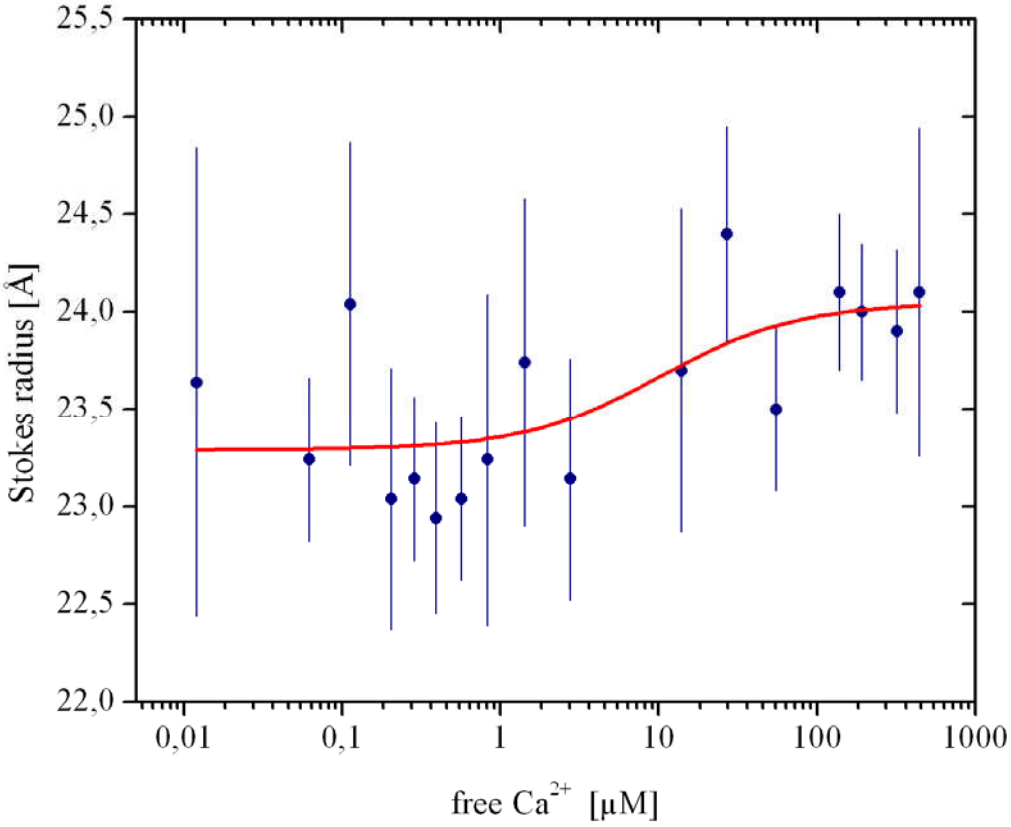

Fig. 2.23 The Stokes radius of non-myristoylated Recoverin-Alexa647 dependent on the free Ca^{2+} concentration. Unlike the Stokes radii of wtRecoverin and the mutant E85Q the Stokes radius of non-myristoylatd Recoverin becomes larger with increasing calcium concentration. The Stokes radius increases from 23.3 ± 0.2 Å to 24.0 ± 0.2 Å. The conformational change was half-maximal at 10 [3.7 – 27] µM free Ca^{2+}.

The Stokes radius of non-myristoylated Recoverin-Alexa647 as a function of the free calcium concentration is shown in Fig. 2.23. In contrast to the Stokes radius of wtRecoverin and E85Q, the radius of non-myristoylated Recoverin-Alexa647 *increases* from 23.3 ± 0.2 Å to 24.0 ± 0.2 Å. The conformation of non-myristoylated calcium-bound Recoverin is similar to the conformation of calcium-saturated wtRecoverin which is reflected by the same

Stokes radius at high Ca^{2+} concentration as measured by 2fFCS. The conformational change was half-maximal at 10 [3.7 – 27] µM free Ca^{2+}.

2.3.7 Changes in the triplet state of Alexa647

Besides yielding a diffusion coefficient, 2fFCS measurements give also values for the triplet state lifetime of a dye. The triplet state lifetime of Alexa647 attached to Recoverin increases with increasing calcium concentration, because the conformational changes of the protein change the local environment of the attached dye.

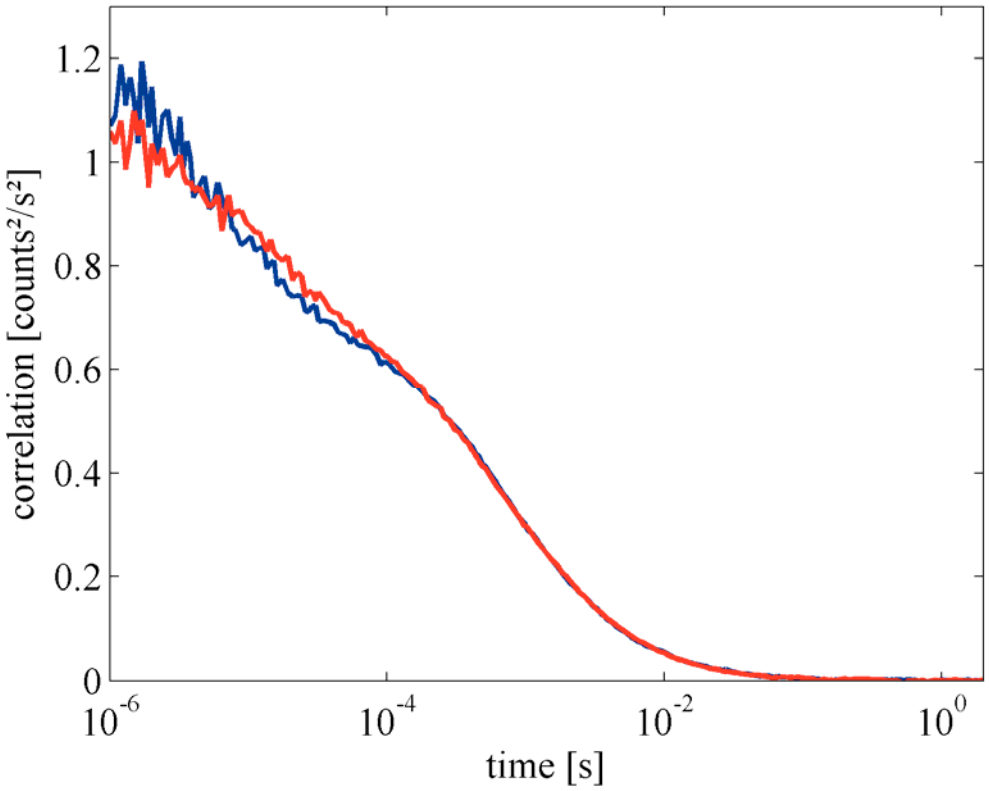

Fig. 2.24 Difference in the triplet state lifetime. Autocorrelations of 2fFCS measurements of wtRecoverin-Alexa647 at 60 nM free Ca^{2+} (blue) and 320µM free Ca^{2+} (red) are shown.

Fig. 2.24 shows two autocorrelation functions as measured by 2fFCS at high (320 µM, red curve) and at low (65 nM, blue curve) free Ca^{2+} concentrations. The difference in the triplet state dynamics is clearly visible. I fitted all measurements with one exponent for the triplet state kinetics. The resulting triplet state lifetime as a function of free Ca^{2+} concentration for the wild type protein is shown in Fig. 2.25. At low Ca^{2+} concentration, Alexa647 shows a triplet state lifetime of 8.3 ± 0.2 µs which increases to 13.2 ± 0.2 µs at high Ca^{2+} concentration. The half-maximal shift of the triplet state lifetime is reached at 4.4 [3.6 – 5.3] µM free Ca^{2+}. A K_D value of 4.4 µM corresponds well to the K_D value of 4 µM found by fitting the decrease of the Stokes radius.

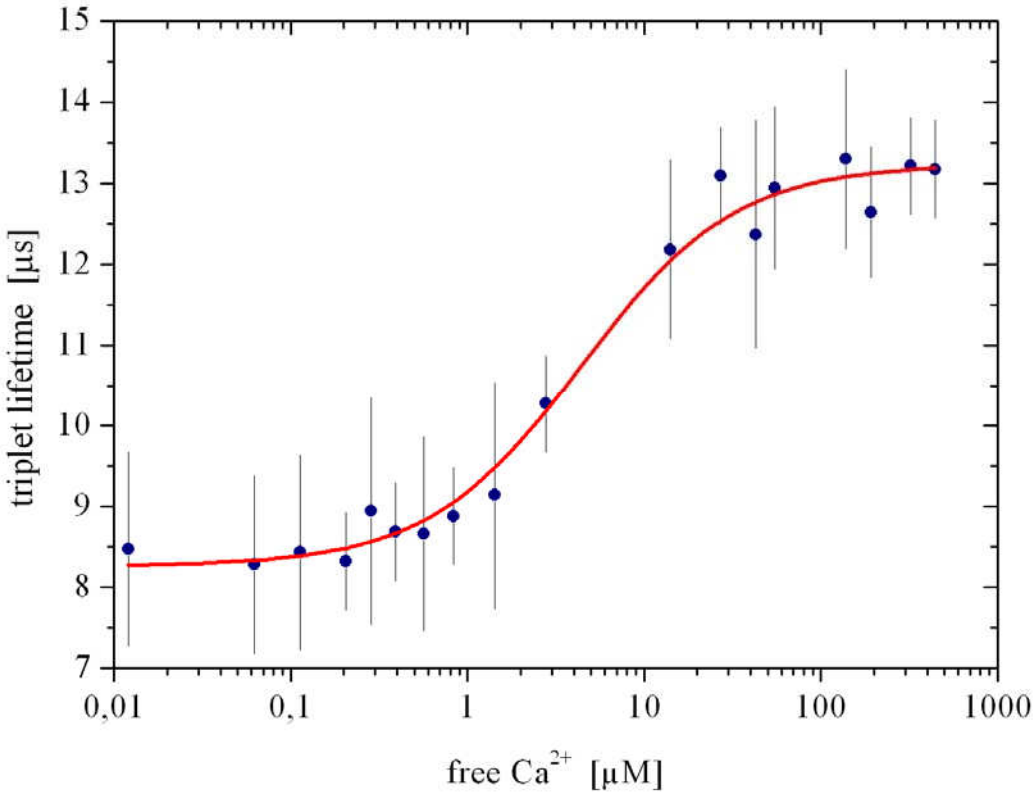

Fig. 2.25 The triplet state lifetime of wtRecoverin-Alexa647 as a function of the free Ca^{2+} concentration. Standard deviations, shown as vertical error bars, were calculated from all measurements at a certain free Ca^{2+} concentration ($n \geq 8$). The red line shows the best fit corresponding to Eq. 2.2. Measurement temperature was 25° C. At low Ca^{2+} concentration Alexa647 shows a triplet state lifetime of 8.3 ± 0.2 µs which increases to 13.2 ± 0.2 µs at high Ca^{2+} concentration. The half-maximal shift of the triplet state lifetime is reached at 4.4 [3.6 – 5.3] µM free Ca^{2+}.

The triplet state lifetime of the mutant E85Q changes also in dependence on free Ca^{2+} concentration. Fig. 2.26 shows the triplet state lifetime as a function of free Ca^{2+} concentration. Recoverin-Alexa647 E85Q shows a triplet state lifetime of 10.8 ± 0.2 µs at low Ca^{2+} concentration which increases to 16.3 ± 0.2 µs at high Ca^{2+} concentration. The half-maximal shift of the triplet state lifetime is reached at 4.1 [3.4 - 5.0] µM free Ca^{2+}. A K_D value of 4.1 [3.4 - 5.0] µM corresponds to a K_D value of 1.4 [0.58 - 3.4] µM found by evaluating the decrease of the Stokes radius of the mutant E85Q.

Recoverin-Alexa647 E121Q and non-myristoylated Recoverin-Alexa647 do not show any change of the triplet state lifetime that would be dependent on free Ca^{2+} concentration. Recoverin-Alexa647 E121Q exhibits the short triplet state lifetime of the Ca^{2+} free conformation of wtRecoverin-Alexa647 or Recoverin-Alexa647 E85Q. Thus, both, the Stokes radius as well as the triplet state lifetime of Recoverin-Alexa647 E121Q, indicate that there is no Ca^{2+} binding and thus no conformational change in this protein. In contrast, non-myristoylated Recoverin-Alexa647 exhibits a long triplet state lifetime of the calcium bound forms of both wtRecoverin-Alexa647 and Recoverin-Alexa647 E85Q.

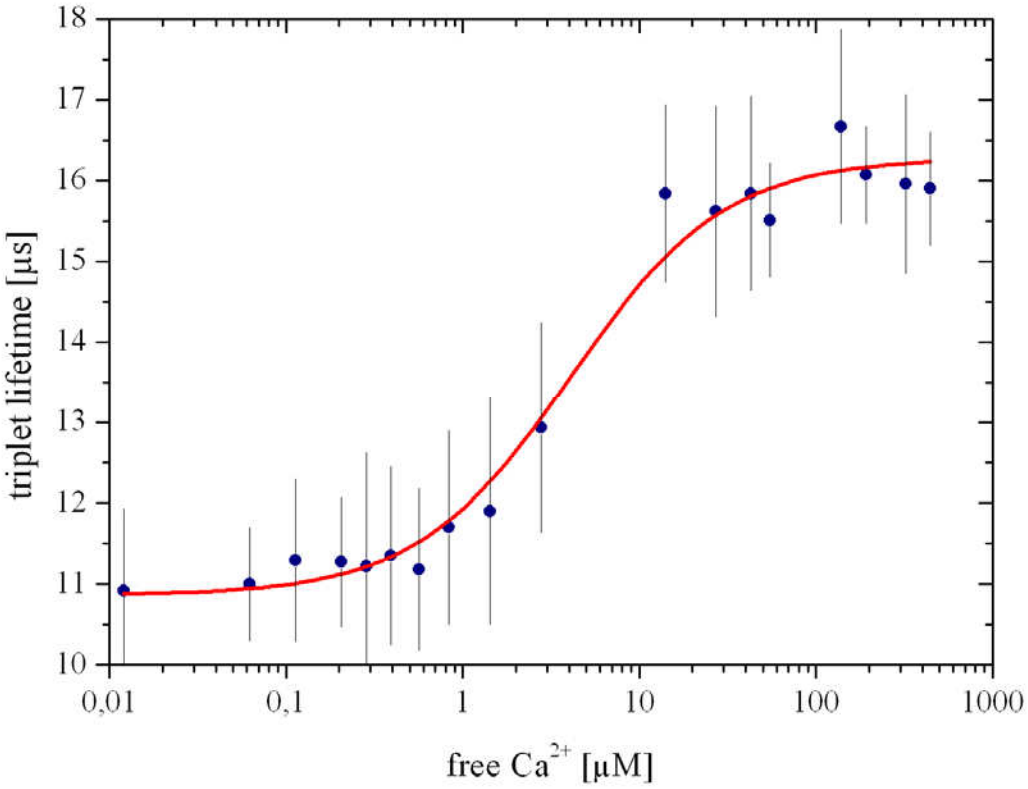

Fig. 2.26 The triplet state lifetime of Recoverin-Alexa647 E85Q dependent on the free Ca^{2+} concentration. Standard deviations, shown as vertical error bars, were calculated from all measurements at a certain free Ca^{2+} concentration ($n \geq 10$). The red line shows the best fit corresponding to Eq. 2.2. Measurement temperature was 25° C. At low Ca^{2+} concentration Alexa647 shows a triplet state lifetime of 10.8 ± 0.2 µs which increases to 16.3 ± 0.2 µs at high Ca^{2+} concentration. The half-maximal shift of the triplet state lifetime is reached at 4.1 [3.4 - 5.0] µM free Ca^{2+}.

2.3.8 Discussion of 2fFCS experiments with wtRecoverin and its mutants

The measurement results presented above clearly show that it is possible to resolve small conformational changes of proteins by measuring their diffusion coefficients with 2fFCS. The fixed distance between the two foci in 2fFCS makes this method highly accurate, reliable, and reproducible. Repeating measurements after weeks resulted in the same values for the diffusion coefficients. Global fitting of all three correlation curves, which takes into account the shape of the curves as well as their relative amplitudes, was very stable, although two additional parameters were necessary to fit the complex photophysics of Alexa647. 2fFCS allows for determining the diffusion coefficient with an accuracy of better than 2%. The calcium dependent changes in the diffusion coefficient of Recoverin were 4-5% for the wild type protein, so that the accuracy of this method was good enough to resolve them, especially if one takes into account that the accuracy gets even better when evaluating whole sets of measurements at different free calcium concentrations.

The determination of the diffusion coefficient of labeled proteins was slightly less accurate than for pure dyes. One reason was probably the presence of small amounts of free dye in the samples, or protein aggregation. However, protein solutions are in general not as homogeneous as solutions of smaller molecules like fluorescent dyes. Proteins obey certain flexibility and do usually not have only one rigid conformation. This is also one of the main reasons which makes single molecule spectroscopy of proteins so interesting. Thus, flexibility and variability of protein conformation might cause the larger deviations of protein size as measured with 2fFCS.

A crucial point of the 2fFCS measurements was the temperature control of the sample. Due to the strong dependence of the viscosity of water on temperature, even small changes of sample temperature cause large changes in the diffusion coefficient. For obtaining stable measurement conditions, the whole lab was heated to 25° C to thermostate the measurement setup. Cooling of the sample due to evaporation and convection inside the sample solution was minimized by sealing the sample container. The sample holder as well as the objective was temperature-controlled by a custom made water cycling system. Sample temperature was measured with a small thermocouple sensor inside the immersion water. The sample was equilibrated for at least 15 min on the microscope prior of starting the first measurement. All these precautions allowed me to keep the temperature stable and to obtain reliable data.

A second crucial topic was the preparation and calibration of the used calcium buffers. The prepared calcium buffers were calibrated against a calibration kit with the same composition. Free calcium concentration was determined and checked with two different methods: using the calcium sensitive dye bis-Fura and a calcium sensitive electrode. The results of both methods

yielded identical results, making sure that the determined values of free calcium concentration in all buffers are indeed accurate.

After having measured the diffusion and thus hydrodynamic size of Recoverin and ist mutants as a function of calcium, I am now ready to ask the question: Do the determined values correspond to the structural information one has from other studies? Unfortunately, there are no values available for the Stokes radius of Recoverin from other studies, but one may inspect the relative changes of the Stokes radius and can compare the Stokes radii of the wild type protein and the different mutants of Recoverin. There is much structural information available, and one knows which structures and conformations of Recoverin and its mutants are similar and which are different. Fig. 2.27 displays all four series of measurements that had been preformed for Recoverin and its mutants with 2fFCS.

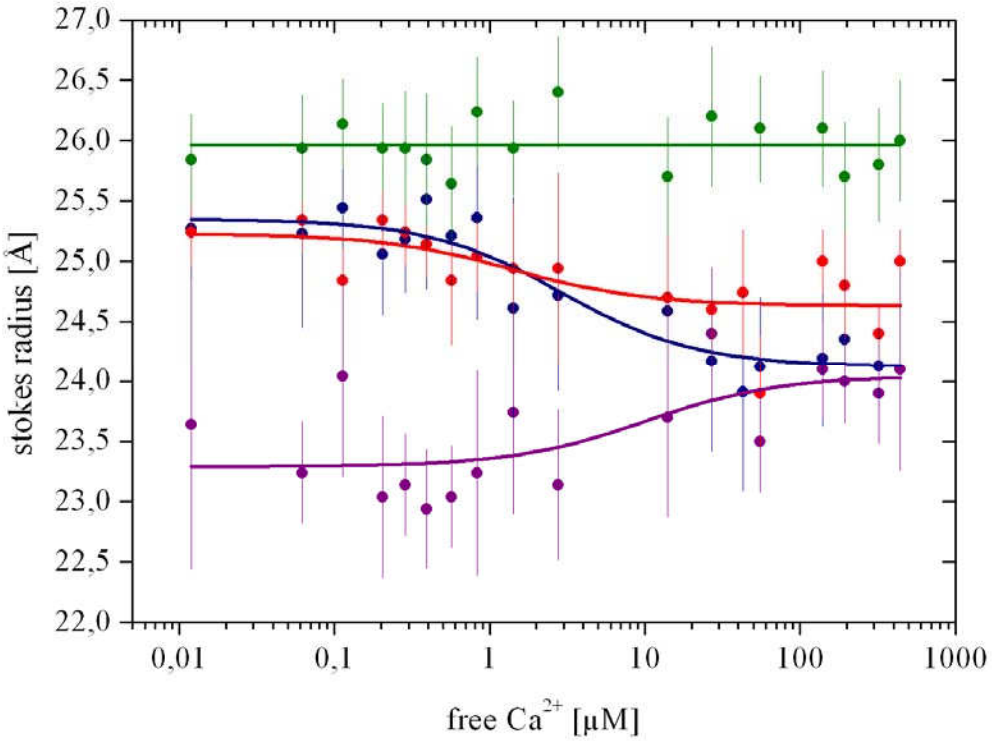

Fig. 2.27 Stokes radii dependent on the free Ca^{2+} concentration. Colorcode: wtRecoverin-Alexa647 (blue), Recoverin-Alexa647 E85Q (red), Recoverin-Alexa647 E121Q (green) and non-myristoylated Recoverin-Alexa647 (purple).

Let us start with the wild type protein. The Stokes radius decreases with high Ca^{2+} concentration although a comparison of the calcium-free and the calcium-bound structures indicates that the calcium-free structure is more compact than the calcium-bound one (Fig. 2.16). However, the calcium-bound structure is more flexible than the calcium free structure. In particular, the N-terminus with the myristoyl residue is flexible in the calcium-bound conformation, in contrast to being clamped in the calcium-free form. I could not find an explicit theory, but it seems a reasonable assumption that more flexible molecules should be able do diffuse faster than rigid molecules.

The structure of the calcium-free forms of the mutants E85Q and E121Q should be the same as the structure of the calcium-free wild type protein. The mutation in EF-2 and EF-3 do not alter the structure of the mutants as revealed by CD and NMR spectroscopy (Permyakov *et a*l., 2000; Ames *et al*., 1994 and 2000)

The Stokes radius of the calcium-free mutant E85Q is the same as that of calcium-free wild type protein, but the Stokes radius of Recoverin E121Q is by 0.7 Å larger than that of the wild type protein. Gensch *et al*. (2007) found that the reactivity of the cysteine at position 38 in Recoverin E121Q to thiol reactive substances such as 5,5'-dithio-bis-(2-nitrobenzoic acid) (DTNB) or Alexa647-maleimide is lower than in wild type Recoverin or Recoverin E85Q. This indicates that the mutant E121Q has a different conformation than the wild type or the mutant E85Q and explains the larger Stokes radius of this protein. Recoverin E121Q does not bind calcium and should thus not show a change in conformation. And indeed, that is the case: the Stokes radius of Recoverin E121Q does not depend on calcium concentration.

The mutant E85Q can bind only one calcium ion, and the conformational change stops halfway, which also becomes clear when considering the structure of calcium-saturated Recoverin E85Q (Fig. 2.18) which is a hybrid of the calcium-free and the calcium-saturated structure of the wild type. With increasing Ca^{2+} concentration, the Stokes radius of Recoverin E85Q decreases similar to the Stokes radius of wild type Recoverin. But the decrease is not as large as for the wild type.

The structure of non-myristoylated Recoverin with one bound Ca^{2+} is similar to the structure of the calcium-saturated wild type protein (Fig. 2.17), and indeed, the measured Stokes radii of these protein conformations are identical. The Stokes radius of calcium-free non-myristoylated Recoverin-Alexa647 is smaller than its value of the calcium-bound protein. There is no structure of non-myristoylated calcium-free Recoverin available. However, the structure of the N-terminal domain should be similar to the relaxed conformation in the calcium-bound state of Recoverin with extruded myristoyl residue. The whole protein should be flexible due to the missing stabilization by the myristoyl residue and the bound calcium ions. This can also explain the small Stokes radius of calcium-free non-myristoylated Recoverin: this form of the protein is the most flexible form and can, therefore, diffuse faster resulting in a smaller Stokes radius. The high flexibility of non-myristoylated calcium-free Recoverin is also indicated by the difficulties to crystallize this conformation (Weiergräber *et al*. 2003).

Thus, similar Stokes radii were found for similar structures which fit nicely to the information known from other studies. How about the calcium binding constants found with 2fFCS?

Table 2.3 Calcium binding constants estimated from the change in the Stokes radius of the protein and in the triplet state lifetime of the dye Alexa647 as measured by 2fFCS for wtRecoverin-Alexa647 and for the Recoverin mutants E85Q, E121Q, and non-myristoylated Recoverin.

	K_D from Stokes radius	K_D from triplet state lifetime
wtRecoverin-Alexa647	4 [1.3 – 12] µM	4.4 [3.6 – 5.3] µM
Recoverin-Alexa647 E85Q	1.4 [0.58 – 3.4] µM	4.1 [3.4 – 5.0] µM
Recoverin-Alexa647 E121Q	no change in Stokes radius	no change in triplet state
non-myristoylated Recoverin-Alexa647	10 [3.7 – 27] µM	no change in triplet state

The calcium binding constants estimated from the change in the Stokes radius and the increase in the triplet state lifetime of Alexa647 are shown in Table 2.3. No cooperativity was found for the calcium binding of Recoverin. For comparison, literature values as found with other methods are shown in Table 2.4.

All reported literature values, which are in good agreement, find that calcium binding of wtRecoverin and Recoverin E85Q takes place at higher free Ca^{2+} concentrations than found in the present study. Thus, the first question is: does 2fFCS measure the same process as all these other studies? The core assumption was that binding of calcium ions to EF-3 and EF-2 of Recoverin cause a conformational change in the protein which results in a change of its diffusion that can be detected with 2fFCS. The measurement of the Trp-fluorescence uses the same assumption, namely, that binding of Ca^{2+} causes a conformational change that results in a change of the Trp-emission properties. The $^{45}Ca^{2+}$-titration method directly monitors the binding of Ca^{2+} ions. The prominent feature of all these methods, except the measurement of the change in Trp-fluorescence by Ames *et al*. (1995) and the measurement of the shift in the emission maximum of Alexa647 by Gensch *et al.*, is that no calcium buffers were used, and the protein concentration was in the micromolar range. Thus, all these binding constants might be too large, because the sample solution becomes Ca^{2+}-depleted at too large Recoverin concentrations. The binding constant found for Recoverin-Alexa647 by Gensch *et al*. (2007) is indeed lower than those found by other studies. But the observed higher calcium affinity could also be caused by the influence of the fluorescent dye bound to the protein.

Table 2.4 Calcium binding constants and Hill coefficients for wtRecoverin, the mutant E85Q, and non-myristoylated Recoverin determined with various methods in other studies.

	K_D	Hill coeff.	method	reference
wtRecoverin	17 µM	1.75	Flow dialysis, $^{45}Ca^{2+}$-titration	Ames *et al.* 1995
	15 µM	1.80	Trp-fluorescence	Ames *et al.* 1995
	17.2 µM	1.4	$^{45}Ca^{2+}$-titration	Baldwin and Ames 1998
	17.9 µM	1.4	Trp-fluorescence	Baldwin and Ames 1998
	17.6 µM	1.9	$^{45}Ca^{2+}$-titration	Senin *et al.* 2002
wtRecoverin-Alexa647	10.9 µM	1.13	shift of emission maximum of Alexa647	Gensch *et al.* 2007
Recoverin E85Q	34.6 µM	1.0	$^{45}Ca^{2+}$-titration	Senin *et al.* 2002
	100 µM	1.0	$^{45}Ca^{2+}$-titration	Ames *et al.* 2002
non myr. wtRecoverin	0.11µM and 6.9µM		Flow dialysis, $^{45}Ca^{2+}$-titration	Ames *et al.* 1995
	0.11 µM and 8.0 µM		$^{45}Ca^{2+}$-titration	Baldwin and Ames 1998
non myr. Recoverin E85Q	0.15 µM	1.0	$^{45}Ca^{2+}$-titration	Ames *et al.* 2002
	0.26 µM		$^{45}Ca^{2+}$-titration	Weiergräber *et al.* 2003

Usually, the calcium affinity of non-myristoylated Recoverin is higher than that of myristoylated Recoverin because the energy necessary for exposing the hydrophobic myristoyl residue to water has not to be compensated by the binding energy of Ca^{2+} (Ames *et al.*, 1995; Baldwin and Ames, 1998). The myristoyl residue induces also cooperativity of binding (Ames *et al.* 1995). Non-myristoylated Recoverin exhibits a two step binding curve which cannot be resolved by 2fFCS. In contrast to the results of other studies, I found a lower or at least similar calcium affinity of non-myristoylated Recoverin as compared to that of the myristoylated protein. I find also a Hill coefficient of 1 for my measurements of myristoylated protein, compared to 1.4 – 1.9 found in other

studies and 1.13 found by Gensch *et al*. (2007) for wtRecoverin-Alexa647. Thus, the influence of the myristoyl residue on the calcium binding process seems to be lower for fluorescently labeled Recoverin. This might be caused by an interaction of the fluorescent dye and the myristoyl residue.

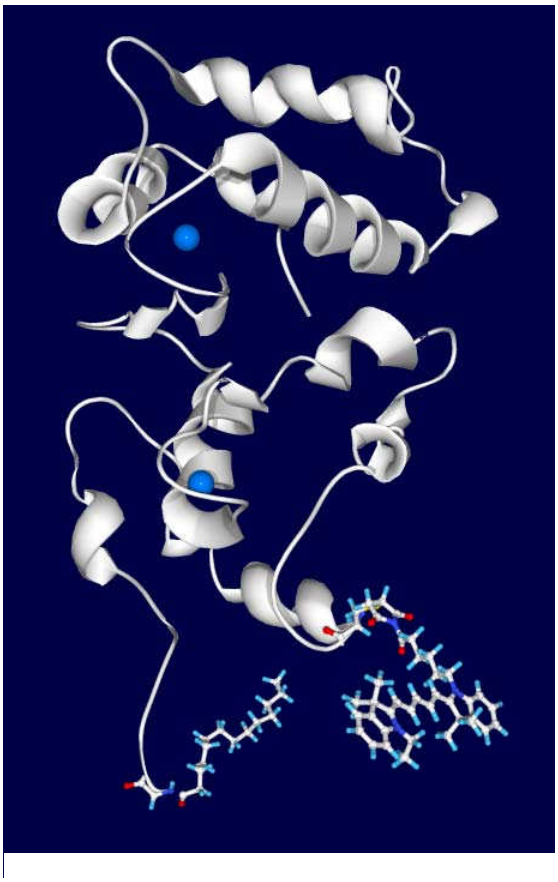

Fig. 2.28 Molecular structure of calcium bound Recoverin with Cy5maleimid linked to C38. The vicinity of myristoyl residue and fluorescent dye is obvious. Myristoyl residue and N-terminus are flexible up to the first helix. Alexa647 a cyanine dye like Cy5 has most probably a longer linker in between chromophor and maleimid than Cy5.

Alexa647 is covalently linked to the cysteine at position 38 in the amino acid sequence in the first EF-hand which is relatively close to the N-terminus with the myristoyl residue. Alexa647 has a long linker between the fluorophor and the maleimid to minimize the influence of the protein on the fluorescence properties of the dye. This linker is flexible, and the myristoyl residue together with the N-terminus of the protein is also flexible in the calcium bound state. It is reasonable to assume that the hydrophobic myristoyl residue can interact with the hydrophobic Alexa647. This interaction stabilizes the exposure of the myristoyl residue and therefore increases the calcium affinity of Recoverin-Alexa647 compared to that of unlabeled protein. This dye/myristoyl interaction is also proved by the observed changes in triplet state lifetime of Alexa647. The triplet state lifetime of Alexa647 depends on calcium concentration for wild type Recoverin and for the mutant E85Q, but not for the non-myristoylated wild type protein. Thus, there is an interaction of the hydrophobic fluorescent dye Alexa647 and the hydrophobic myristoyl residue that stabilizes the myristoyl exposure and therefore the calcium-bound conformation of the protein. This explains the low calcium-binding constants as found with 2fFCS.

A similar effect was observed by Baldwin and Ames (1998). They mutationally decreased the hydrophobicity of the myristoyl binding pocket and, in this way destabilized the calcium-free conformation of Recoverin finding an increased calcium affinity of the mutants. It is also known that the presence of lipid in solution increases the calcium affinity of Recoverin, because the

hydrophobic myristoyl residue can incorporate itself into the lipid membrane (Zozulya and Stryer 1992; Lange and Koch 1997).

The K_D values of 34.6 µM and 100 µM found for Recoverin E85Q by Senin *et al*. (2002) and Ames *et al*.(2002) are much higher than the K_D value of 1.4 µM as found in the present study for Recoverin-Alexa647 E85Q. Ames *et al*. (2002) suggested that much of the binding energy of the first calcium ion is used to drive a large conformational change within the protein. In the mutant E85Q, this conformational change is not supported by the binding energy of the second calcium ion. The non-myristoylated E85Q mutant has, in contrast, a very high calcium affinity and a K_D value of 150 nM (Ames *et al*. 2002) to 260 nM (Weiergräber *et al*. 2003). This shows that the exposure of the myristoyl residue is indeed an energy-consuming process. Furthermore, the low K_D value of Recoverin-Alexa647 E85Q as found with 2fFCS shows also the stabilizing effect of the dye on the calcium-bound conformation of Recoverin, due to the stabilization of the water exposed conformation of the myristoyl residue by the interaction with the hydrophobic dye.

To confirm the influence of Alexa647, linked to Cys38 of Recoverin, on the calcium affinity of the protein, I measured the calcium dependent change of tryptophane fluorescence of wild type Recoverin and wild type Recoverin-Alexa647 (see chapter 2.4). This method uses the intrinsic properties of the protein and does not need a fluorescent label.

Why did I link the fluorescent dye to C38? Firstly, C38 is the only native cysteine of Recoverin. Mutations that change the position of cysteine in the protein might dramatically influence protein functions and properties such as its calcium affinity. Secondly modifications of C38 had been already successfully employed in other studies. For example, Recoverin was immobilized via coupling of C38 to thiol reactive substances on a sensor chip for SPR experiments. These experiments showed that the basic functions such as inhibition of Rhodopsin Kinase, or the calcium myristoyl switch, were not affected by the immobilization procedure (Lange and Koch, 1997). Even the influence of Alexa647 linked to C38 of Recoverin was investigated (Gensch *et al*. 2007). There, the basic functions of Recoverin were also not affected, but the calcium affinity was found to be slightly increased.

2.4 Calcium induced shift in tryptophan fluorescence

2.4.1 Tryptophan fluorescence of Recoverin

Recoverin has three tryptophan residues – W31 in EF-1, W104 in EF-3 and W156 in EF-4. A conformational change of the Recoverin structure induced by Ca^{2+} binding changes the local environment of the tryptophan residues and alters their fluorescence properties (Dizhoor *et al.*, 1991). In contrast to the 2fFCS measurements, this method is a label-free method, because it uses the intrinsic fluorescence properties of the protein.

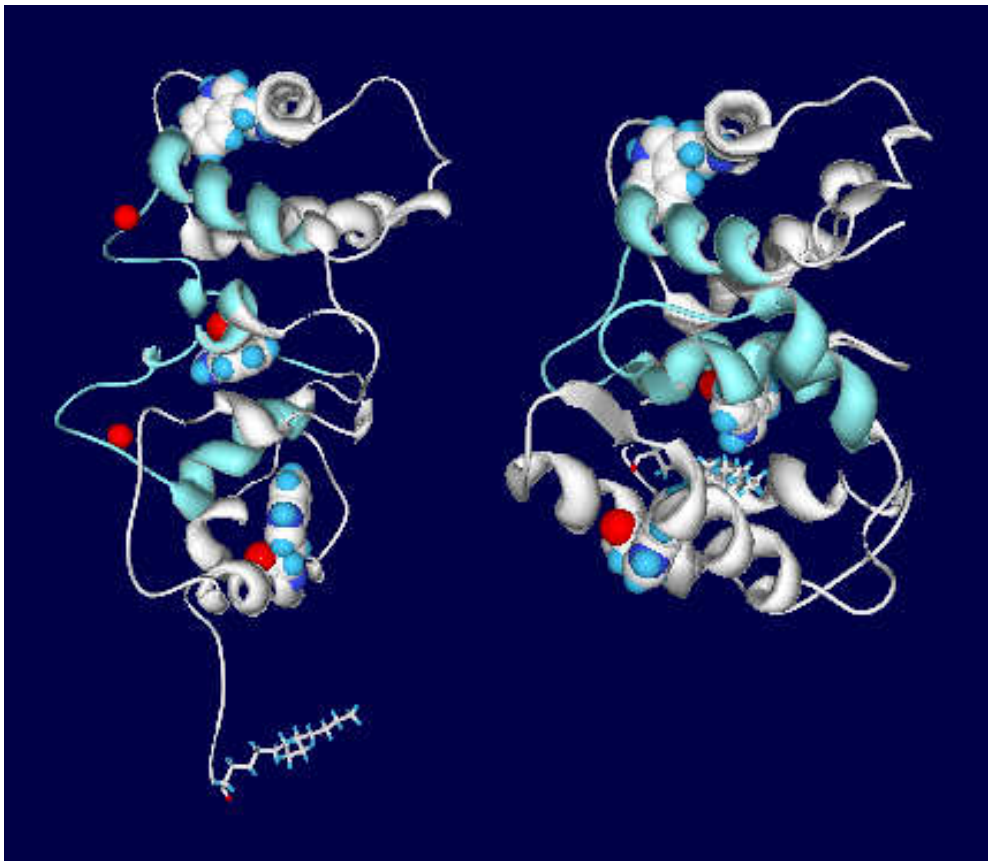

Fig. 2.29 Molecular structures of calcium bound (left) and calcium free (right) Recoverin. Tryptophan residues W31, W104 and W156 are shown as space filling models. The Environment of W156 does not change much but the environment of W31 and W104 which both interact with the myristoyl residue in the calcium free conformation is different after calcium binding.

Fig. 2.29 shows the position of Recoverin's three tryptophan residues in the molecule. The environment of W156 in EF-hand 4 is not very different before and after calcium binding, but the environment of W31 in EF-hand 1 and of W104 in EF-hand 3 changes due to conformational changes induced by calcium binding. W 31 and W104 both interact with the myristoyl residue in the Ca^{2+} free state of Recoverin. Thus, the environment of W31 and W104 becomes more polar due to the missing interaction with the hydrophobic myristoyl residue in the

calcium-bound state. This causes the fluorescence emission maximum of tryptophan to shift to the red end of the spectrum (Dizhoor *et al*., 1991).

2.4.2 Changes in tryptophan fluorescence of wild type Recoverin

The effect of Ca^{2+} binding on the fluorescence emission of wild type Recoverin was measured with a 2 µM solution of protein over the whole range of calcium buffers. The fluorescence emission maximum shifted towards the red with increasing free Ca^{2+} concentration, and the fluorescence intensity decreased. Fig. 2.30 shows four selected tryptophan fluorescence spectra at four different free Ca^{2+} concentrations as measured for wild type Recoverin.

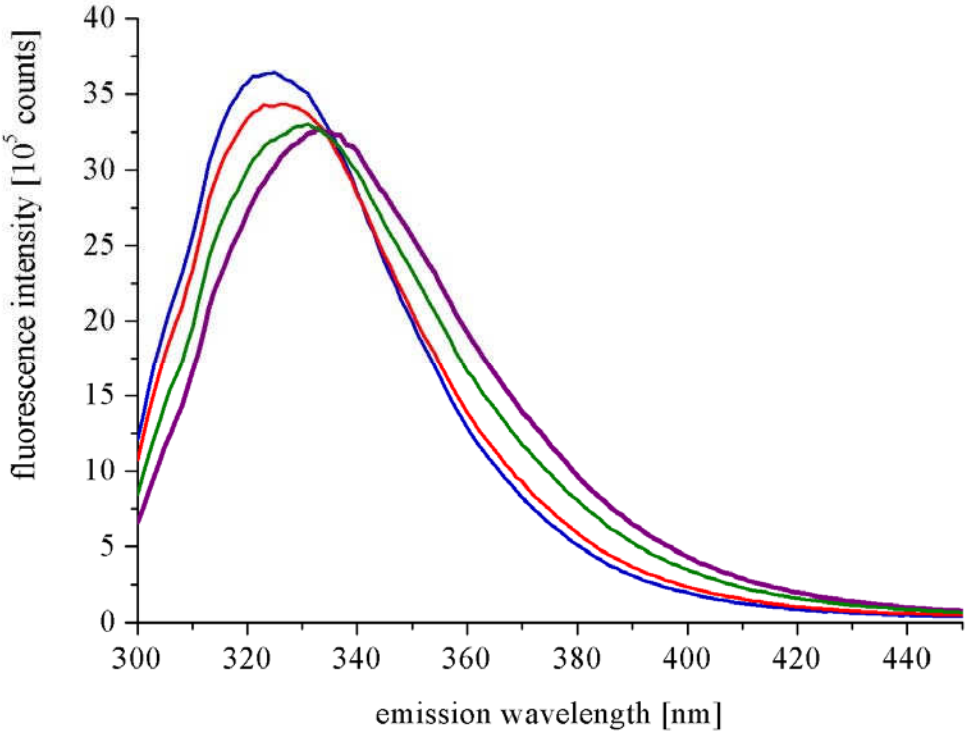

Fig. 2.30 Selected tryptophan fluorescence spectra of wild type Recoverin. 2 µM solutions of wild type Recoverin in calcium buffers of different free Ca^{2+} concentration were excited at 280 nm. Free Ca^{2+} concentrations were 65 nM (blue), 2.8 µM (red), 14 µM (green) and 440 µM (purple). The fluorescence emission maximum shifted to the red with increasing Ca^{2+} concentration and the fluorescence intensity decreased.

One can use the position of the emission maximum to estimate a Ca^{2+} binding constant. Fig. 2.31 shows the emission maximum as a function of free Ca^{2+} concentration. The red line is a fit of the data to a Hill binding model (Eq. 2.2) as already used before to fit the Stokes radius dependence on free calcium concentration. The emission maximum shifts from 324 nm at low Ca^{2+} concentration to 333 nm at high Ca^{2+} concentration.

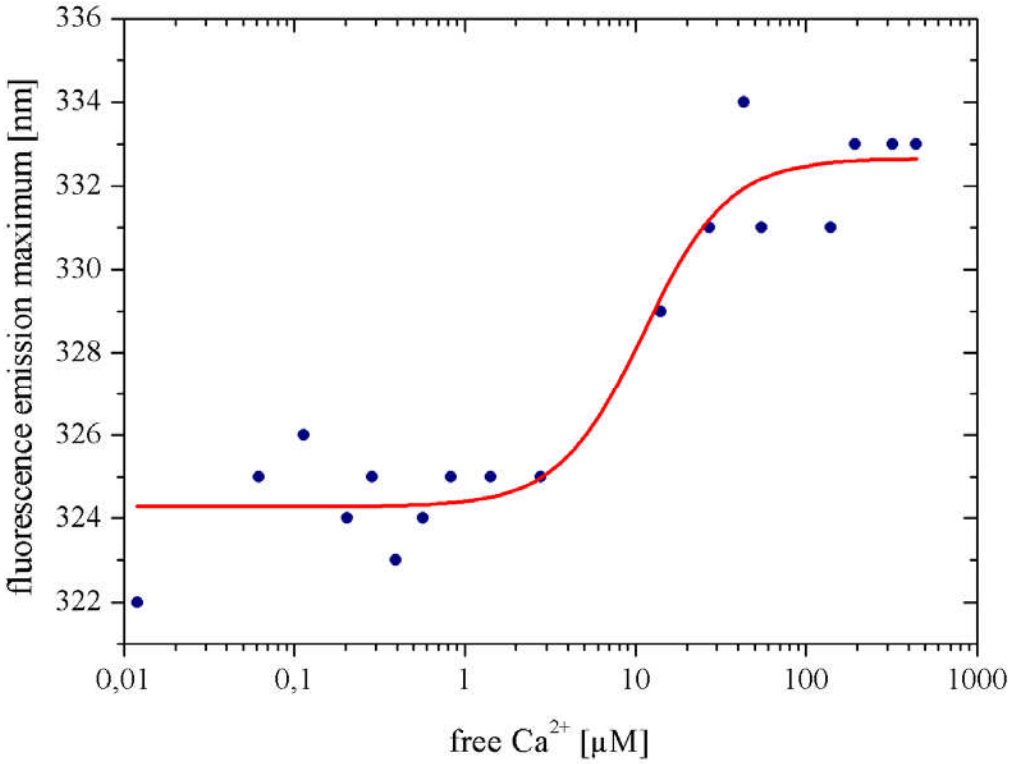

Fig. 2.31 Shift of the fluorescence emission maximum dependent on the free Ca^{2+} concentration. The red line shows the best fit of the data to a Hill model (Eq. 2.2). The estimated K_D value is 11 [8 – 15] µM and the Hill coefficient is 1.75 ± 0.9.

The shift of the fluorescence emission maximum was blurred by measurement noise, and the spectral resolution of the used spectrometer (1 nm) was too low for a precise determination of the Ca^{2+} dissociation constant. Therefore, the ratio of the fluorescence emission intensity at 348 nm and 310 nm was chosen to quantify the red shift of the spectrum in a more precise way.

The ratio of the fluorescence emission at 348 nm and 310 nm F(348)/F(310) as a function of free Ca^{2+} concentration is presented in Fig. 2.32. Data points are less scattered, and the Ca^{2+} binding constant can be estimated more accurately. The determined value of K_D is 12.3 [11.8 – 12.8] µM, and the Hill coefficient is 1.4 ± 0.1. This K_D value is much higher than the K_D value of 4 [1.3 – 12] µM as measured with 2fFCS. A Hill coefficient value larger than one verifies the cooperativity of calcium binding found in other studies, in contrast to the 2fFCS experiments where the Hill coefficient was equal to one, indicating non-cooperativity of binding.

.

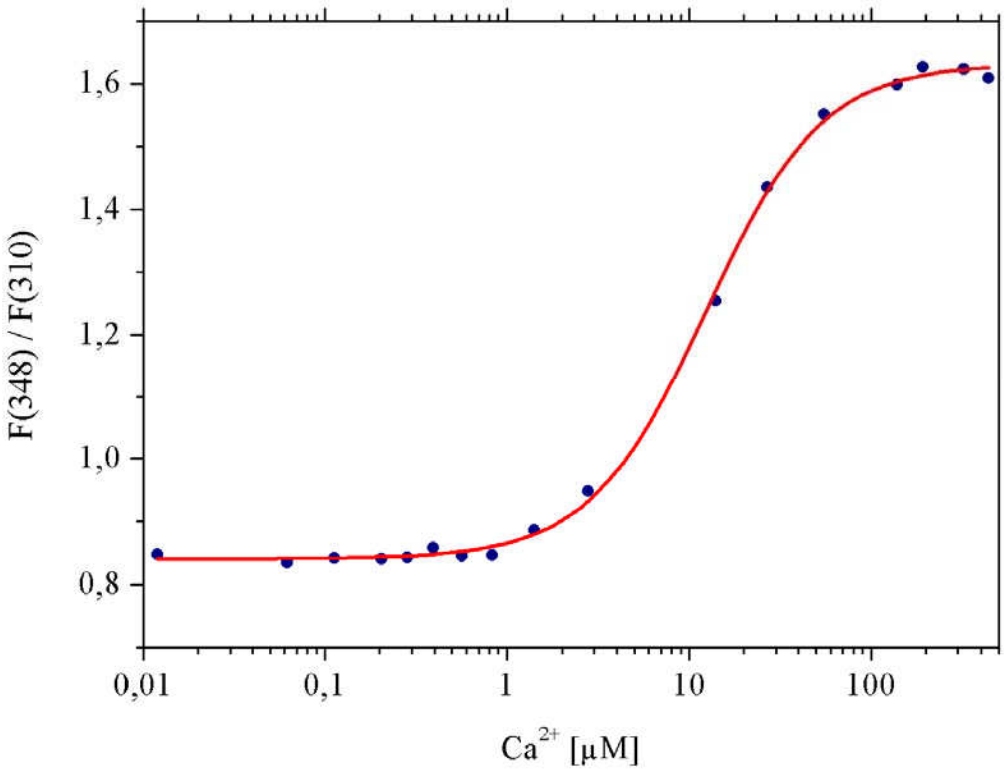

Fig. 2.32 Quotient of tryptophan fluorescence emission of wild type Recoverin at 348 nm and 310 nm dependent on free Ca^{2+} concentration. The red line shows the best fit according to Eq. 2.2. The estimated K_D is 12.3 [11.8 – 12.8] µM and the Hill coefficient is 1.4 ± 0.1.

2.4.3 Tryptophan fluorescence of wild type Recoverin-Alexa647

To confirm the influence of the Alexa647-label on the calcium affinity of the protein, I used the calcium dependence of the tryptophan fluorescence and compared it for the labeled and unlabeled wild type protein. There might be some light absorption by Alexa647 at 280 nm, but Alexa647 fluorescence is emitted only between 620 nm and 770 nm, which is far away from the measured tryptophan fluorescence emission wavelengths.

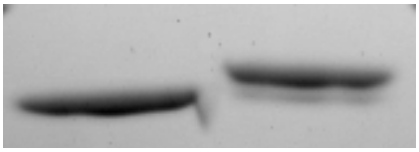

Fig. 2.33 Detail of a SDS acrylamide gel analyzed by electrophoresis. Unlabeled Recoverin (left) shows a higher mobility than Recoverin labeled with Alexa647 (right). A small amount of Recoverin remained unlabeled (second weak band right).

The presence of free Alexa647 does not influence the measurement, but the presence of unlabeled Recoverin would skew the results. Therefore, label ratio of Recoverin with Alexa647 was checked by SDS gel electrophoresis. The increase of molecular weight by Alexa647 is large enough to lower the electrophoretic mobility of the labeled protein. The sample of labeled Recoverin displayed a weak second band in

SDS polyacrylamide electrophoresis, corresponding to unlabeled Recoverin with higher electrophoretic mobility (Fig. 2.33).

The effect of Ca^{2+} binding on the fluorescence emission of wild type Recoverin-Alexa647 was measured using a 1 µM solution of protein over the whole range of calcium buffers. In contrast to unlabeled protein, tryptophan emission maximum did not shift to the red with increasing free Ca^{2+} concentration. The observed spectra broadened, and the fluorescence intensity decreased by more than 50%. Fig. 2.34 shows four selected tryptophan fluorescence emission spectra for the labeled protein at four different free Ca^{2+} concentrations.

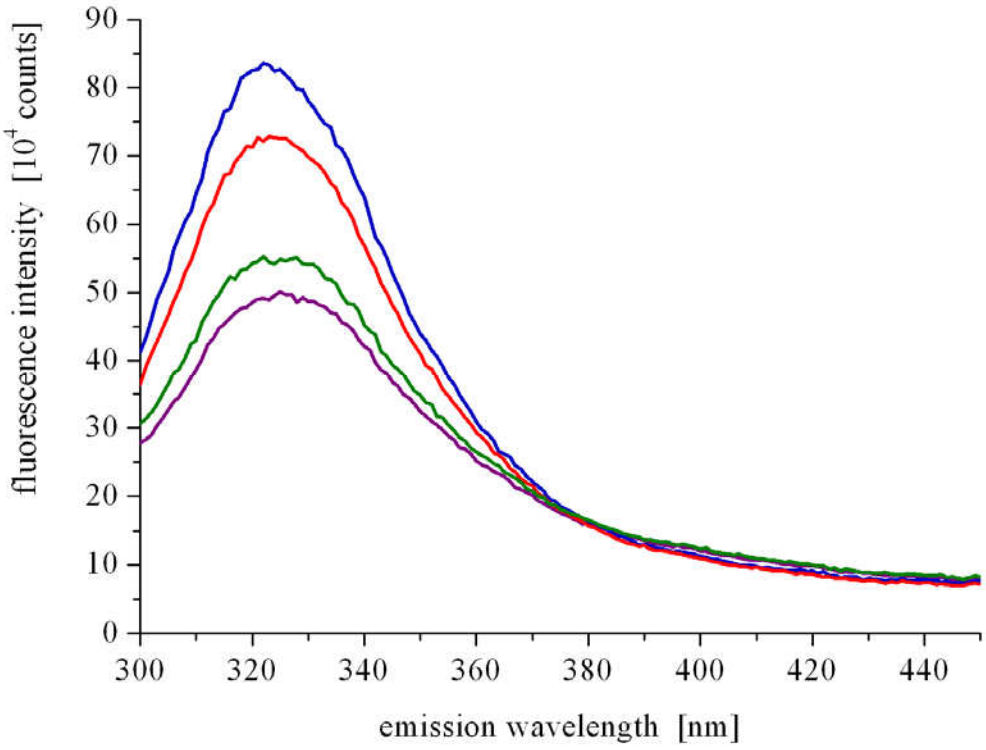

Fig. 2.34 Selected tryptophan fluorescence spectra of wild type Recoverin-Alexa647. 1µM solutions of labelled protein in calcium buffers of different free Ca^{2+} concentration were excited at 280 nm. Free Ca^{2+} concentrations were 65 nM (blue), 2.8 µM (red), 14 µM (green) and 440 µM (purple). The fluorescence emission maximum did not shift to the red with increasing Ca^{2+} concentration but the fluorescence intensity strongly decreased.

The ratio of the tryptophan fluorescence emission at 360 nm and 310 nm, displaying the largest change as a function of Ca^{2+} concentration, was chosen for quantifying the spectral shift of the emission. Fig. 2.35 shows this ratio as a function of the free Ca^{2+} concentration. The red line shows a fit according to Eq. 2.2. The estimated K_D is 4.2 [3.6 – 4.9] µM, and the Hill coefficient is 1.5 ± 0.3. This K_D of 4.2 µM is much smaller than the K_D of 12.3 µM as determined with the shift in tryptophan fluorescence of unlabeled Recoverin, but it is very similar to

the K_D of 4 µM as determined by the change in diffusion as measured with 2fFCS. This shows that the properties of Recoverin, in particular its calcium affinity, is influenced by the presence of the Alexa647 linker at position C38.

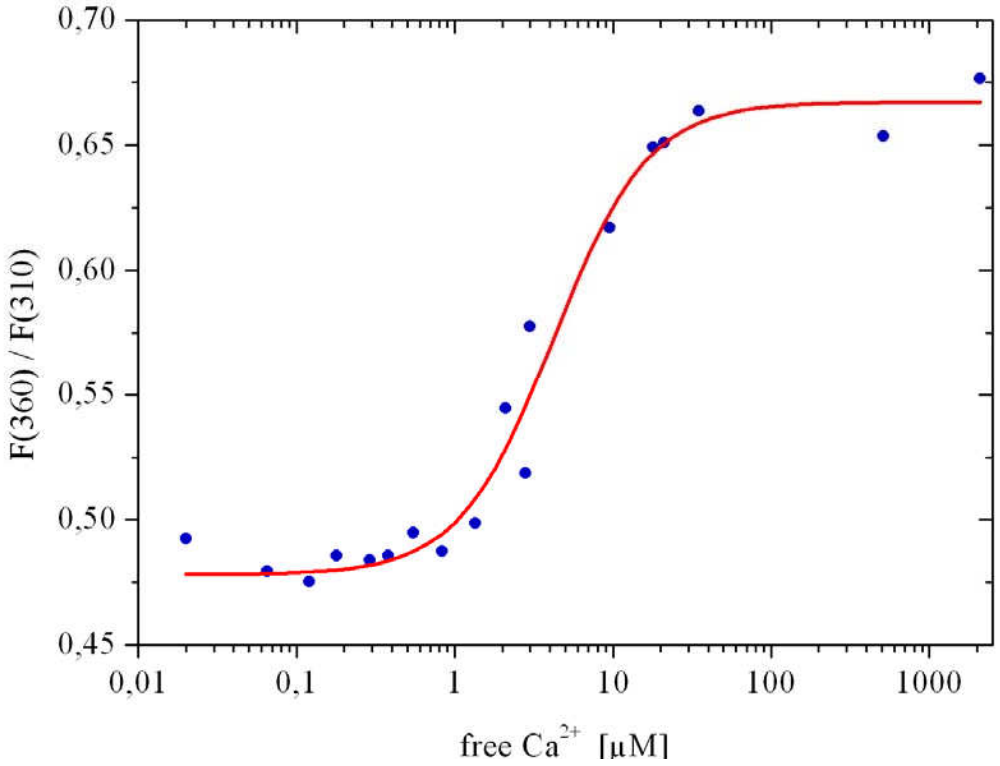

Fig. 2.35 Quotient of tryptophan fluorescence emission of wild type Recoverin-Alexa647 at 360 nm and 310 nm dependent on the free Ca^{2+} concentration. The red line shows the best fit according to Eq. 2.2. The estimated K_D is 4.2 [3.6 - 4.9] µM and the Hill coefficient is 1.5 ± 0.3.

Besides the calcium dependent spectral shift, there is also a pronounced calcium dependent decrease in fluorescence emission intensity, which can be used as well for estimating the value of K_D. Fig. 2.36 displays the fluorescence intensity maximum as a function of calcium concentration. The red line represents again a fit according to Eq. 2.2. The estimated K_D value is 3.0 [2.5 – 3.6] µM, and the Hill coefficient is 1.6 ± 0.4, which corresponds to the values found before when using the spectral fluorescence emission ratio at 360 nm and 310 nm.

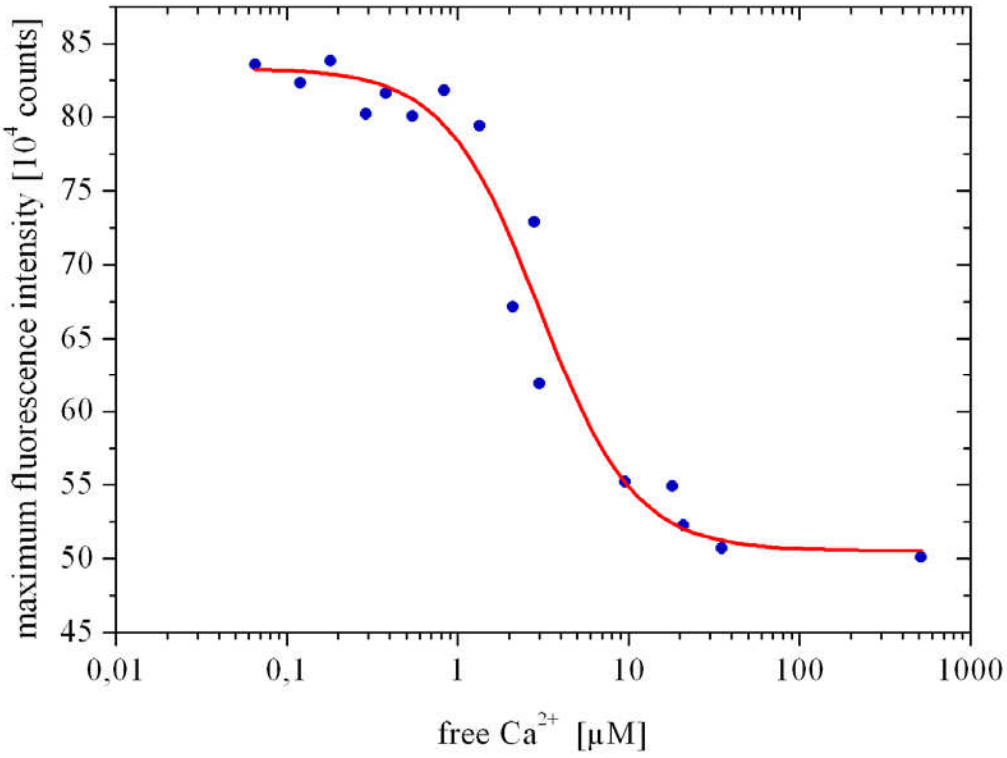

Fig. 2.36 Decrease in fluorescence intensity at the emission maximum dependent on the calcium concentration of wild type Recoverin-Alexa647. The red line shows the best fit according to Eq. 2.2. The estimated K_D is 3.0 [2.5 – 3.6] µM and the Hill coefficient is 1.6 ± 0.4.

2.4.4 Tryptophan fluorescence upon binding of one Ca^{2+} ion – Recoverin E85Q

The Effect of Ca^{2+} binding on the fluorescence emission of Recoverin E85Q was measured using a 2µM protein solution over the whole range of calcium buffers. The fluorescence emission maximum shifted from 324 nm to 333 nm with increasing free Ca^{2+} concentration, and the fluorescence intensity decreased similarly to wild type Recoverin. Fig. 2.37 displays four selected spectra of tryptophan fluorescence emission for Recoverin E85Q. The free Ca^{2+} concentrations are the same as for wild type Recoverin in Fig. 2.30.

Similar to the analysis of the emission shift for wild type protein, the ratio of the fluorescence emission intensities at 348 nm and 310 nm was used. Only one Ca^{2+} ion is bound to Recoverin E85Q, so there should be no cooperativity in calcium binding and therefore no cooperativity in the conformational changes as measured with tryptophan fluorescence emission. Fig. 2.38 shows the spectral emission ratio as a function of free calcium concentration. As already observed for wild type Recoverin, the ratio increases from 0.82 at low Ca^{2+} concentrations to 1.64 at high Ca^{2+} concentrations. The red line shows a fit according to Eq. 2.2. The estimated K_D is 10.6 [9.6 - 1.7] µM, and the Hill coefficient is 1.6 ± 0.2. The

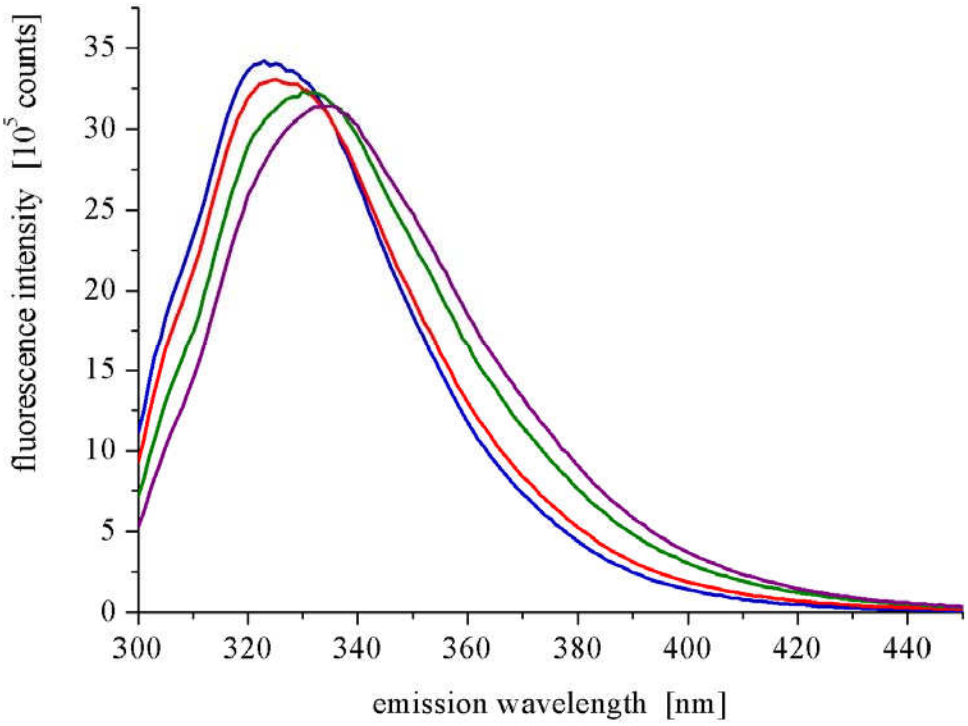

Fig. 2.37 Four selected tryptophan fluorescence spectra of Recoverin E85Q. 2µM solutions of Recoverin E85Q in calcium buffers of different free Ca^{2+} concentration were excited at 280 nm. Free Ca^{2+} concentrations were 65 nM (blue), 2.8 µM (red), 14 µM (green) and 440 µM (purple). The fluorescence emission maximum shifted to the red with increasing Ca^{2+} concentration and the fluorescence intensity decreased.

purple line shows a fit with the Hill coefficient kept fixed at value 1. Here, the estimated K_D is 11 [9.3 - 13] µM. The fit quality is not as good as for the fit with a freely varying Hill coefficient. This indicates some cooperativity in the conformational changes.

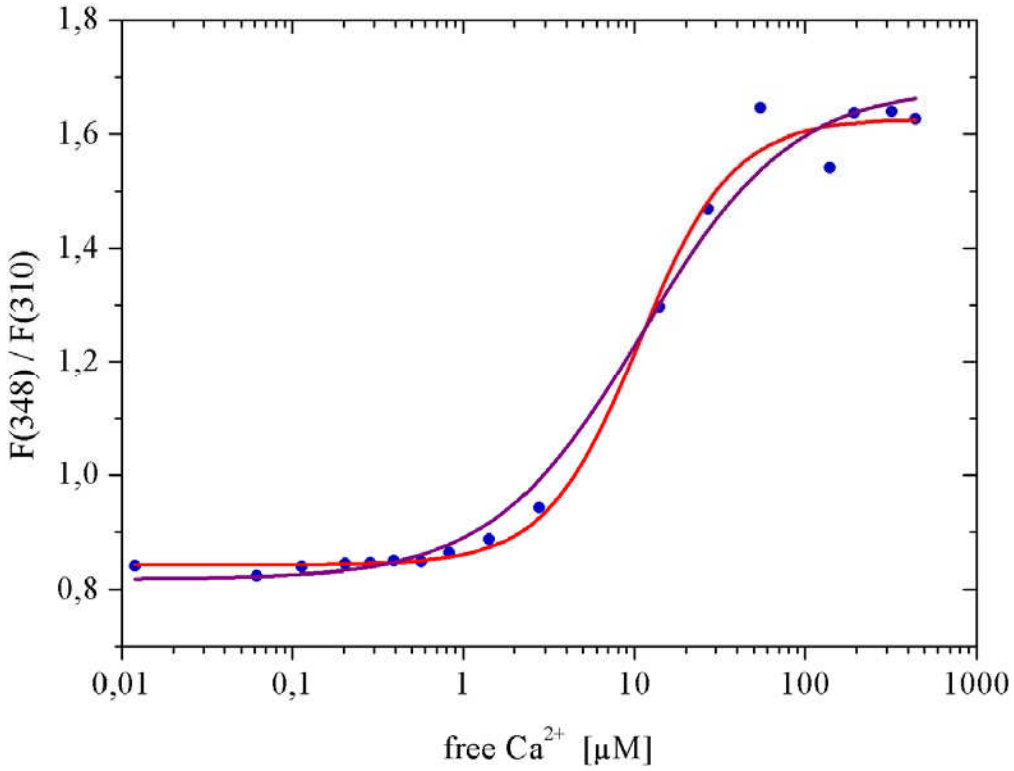

Fig. 2.38 Quotient of tryptophan fluorescence emission of Recoverin E85Q at 348 nm and 310 nm dependent on the free Ca^{2+} concentration. Only one Ca^{2+} ion is bound to Recoverin E85Q so there should be no cooperativity. The red line shows the best fit according to Eq. 2.2 with the Hill coefficient as a free fitting parameter. The estimated K_D is 10.6 [9.6 - 11.7] µM and the Hill coefficient is 1.6 ± 0.2. The purple line in contrast shows the best fit with a Hill coefficient fixed at 1. The estimated K_D is here 11 [9.3 - 13] µM. The fit quality is not as good as for the free Hill coefficient.

2.4.5 Shift in tryptophan fluorescence in the presence of lipid

The myristoyl residue of Recoverin functions as a membrane anchor. Extruding the hydrophobic myristoyl residue into water is energetically disfavored. But insertion of the myristoyl residue into a lipid membrane stabilizes the conformation of Recoverin where the myristoyl residue extends outside the protein. This suggests that access to a lipid membrane should increase the calcium affinity of Recoverin and would shift the calcium concentration necessary for maximal binding into the physiological range of calcium concentrations (50 nm - 1 µM; Korenbrot and Miller 1989, Lagnado *et al.* 1992, Gray-Keller and Detwiler 1994, Woodruff *et al.* 2002, Nakatani *et al.* 2002). This is discussed in more detail in chapter 2.5.1.

A suspension of 20 mg/ml (2%) small vesicles made of DOPC was used together with a set of 18 calcium buffers with different free Ca^{2+} concentrations to measure the binding affinity of unlabeled Recoverin to lipid membranes at

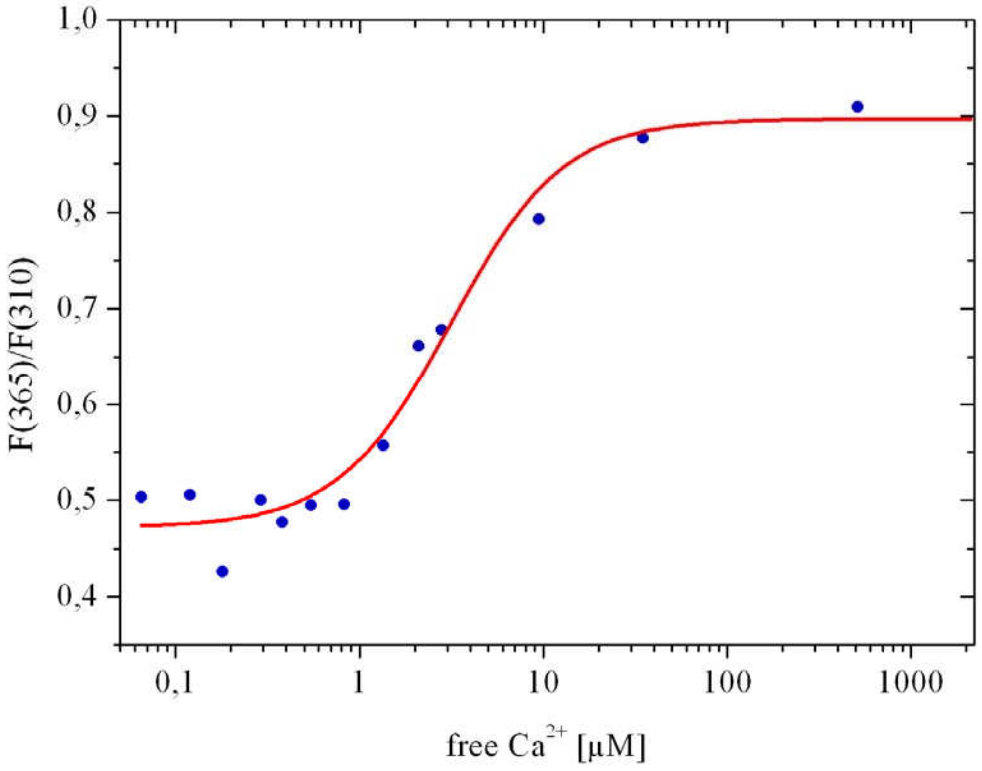

Fig. 2.39 Quotient of tryptophan fluorescence emission at 365 nm and 310 nm dependent on the free Ca^{2+} concentration of wild type Recoverin. The red line shows the best fit according to Eq. 2.2. The estimated K_D is 3.1 [2.6 – 3.7] µM and the Hill coefficient is 1.4 ± 0.4.

varying calcium concentration. Due to binding of Ca^{2+} to phospholipids, I used calcium buffers with higher buffer capacity than those used for the measurements without lipid. Similarly to the tryptophan fluorescence measurements without lipid, protein concentration was equal to 2 µM.

Due to the high vesicle concentration, the samples showed a high scattered light intensity, making the measured data more noisy than in the measurements without lipid.

The ratio of tryptophan fluorescence intensity at 365 nm and 310 nm for wild type Recoverin as a function of the free Ca^{2+} concentration is shown in Fig. 2.39.

The estimated K_D is 3.1 [2.6 – 3.7] µM, compared to K_D = 12.3 [11.8 - 12.8] µM for wild type Recoverin without lipid. The Hill coefficient is 1.4 ± 0.4, which is similar to the measurement without lipid.

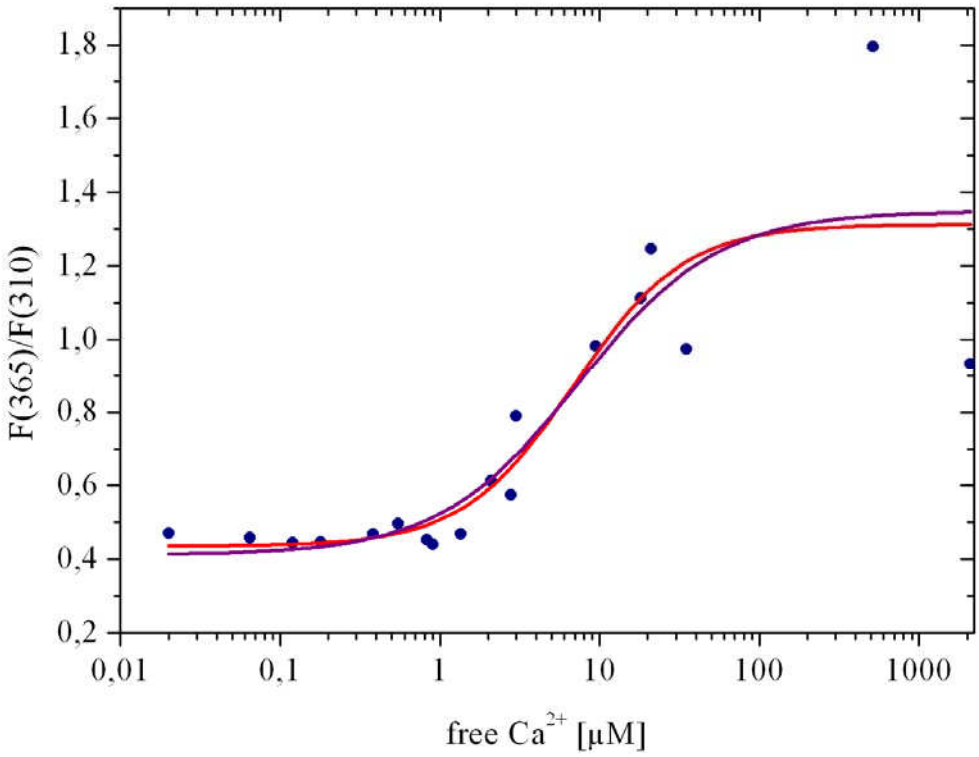

Fig. 2.40 Quotient of tryptophan fluorescence emission at 365 nm and 310 nm dependent on the free Ca^{2+} concentration of Recoverin E85Q in the presence of lipid. The red line shows the best fit according to Eq. 2.2. The estimated K_D is 6.9 [4.5 - 10.5] µM and the Hill coefficient is 1.2 ± 0.6. The purple line shows the best fit with the Hill coefficient fixed at 1, the K_D is here 7.4 [4.7 – 11.6] µM.

2.4.6 Discussion of tryptophan fluorescence experiments

The spectral shift in tryptophan fluorescence monitors the environmental change around the tryptophan residues in Recoverin. *A priori*, it is not known whether this shift reflects the binding of the first or the second calcium ion, or the extrusion of the myristoyl residue, or a global conformational change of the protein. W104 is adjacent to the EF-3 binding loop and might respond to the presence of the first bound calcium ion. W31 and W104 interact with the myristoyl residue in the calcium free conformation of the protein and might therefore respond to the extrusion of the myristoyl residue.

I measured the spectral shift as a function of calcium concentration to compare the results of this label free method with the results of my 2fFCS measurements where Recoverin needs to be fluorescently labeled. With 2fFCS, I measured the global conformational change upon calcium binding and extrusion of the myristoyl residue, which changed the diffusion of the protein. I found lower K_D values than previously reported with other methods, which I explained by the interaction of the fluorescent dye with the myristoyl residue, leading to a higher calcium affinity of the protein.

Upon calcium binding, the tryptophan fluorescence emission maximum of wild type Recoverin shifted towards the red, and the fluorescence intensity decreased. This effect was already observed by Dizhoor *et al.* (1991). Ray *et al.* (1992) reproduced this effect and found a decrease in fluorescence intensity and a shift of the emission maximum from 333 nm at 70 nM free Ca^{2+} to 339 nm at 10 µM free Ca^{2+}. Ray *et al.* (1992) also found that the tryptophan fluorescence emission maximum of non-myristoylated Recoverin is independent on the free Ca^{2+} concentration and is similar to the spectrum of calcium-bound myristoylated Recoverin. This supports the idea that the relaxed state of the N-terminal domain, which is taken in the wild type protein only after binding of the second calcium ion, together with the missing interaction of W31 and W104 with the myristoyl residue in the calcium-bound state, are the reasons for the spectral shift in tryptophan emission.

Ames *et al.* (1995) measured calcium dependent tryptophan fluorescence emission spectra of wild type Recoverin and found a red-shift of the emission maximum by 7 nm when Ca^{2+} is bound. A K_D value of 15 µM and a Hill coefficient of 1.8 were estimated. In agreement to this study a red-shift of the emission maximum by 9 nm, a value of K_D, 12.3 ± 0.5 µM, and the Hill coefficient of 1.4 ± 0.1 were found in the present study. The K_D value of 12.3 ± 0.5 µM as estimated from the spectral shift in tryptophan fluorescence is much higher than the K_D value of 4 µM as found with 2fFCS.

For a direct comparison of the calcium affinity of unlabeled and labeled Recoverin, I measured also the calcium dependent tryptophan fluorescence of Recoverin-Alexa647. The K_D value estimated from these measurements was 4.2 µM, which is much lower than the K_D of 12.3 µM as estimated from the

measurements on unlabeled Recoverin. This result clearly confirms the influence of the fluorescent dye Alexa647 on the calcium affinity of Recoverin.

Permyakov *et al*. (2000) monitored the calcium dependent spectral shift of tryptophan fluorescence for wild type Recoverin and the Recoverin mutant E85Q. They found a red-shift of 7 nm and a small increase of fluorescence intensity with increasing calcium concentration for wild type protein, and a smaller shift of 3.5 nm and no change in fluorescence intensity for the mutant. In contrast to the results of Permyakov et al. (2000), I did not find a difference in the red-shift between wild type protein and mutant. For both proteins, the emission maximum shifted by 9 nm from 324 nm at low calcium concentration to 333 nm at high calcium concentration.

Ames et al. (2002) also found a difference in red-shift between wild type Recoverin (10 nm) and mutant E85Q (6 nm). The emission intensity increased by 20% for the wild type protein, and decreased by 15% for the mutant E85Q (both towards calcium-bound state).

Matsuda et al. (1998) investigated the tryptophan fluorescence of S-modulin and S-modulin mutants. S-modulin is the frog homolog of Recoverin. The EF-hands 2 and 3 were disabled by exchange of the bidentate glutamic acid ligands to methionine. Tryptophan fluorescence of the wild type protein and the mutants E85M and E121M were almost the same at low calcium concentration. The emission spectrum of E121M was not affected by increasing calcium concentration. The wild type protein showed a red-shift and an intensity decrease at high calcium concentration, whereas the mutant E85M showed a smaller red-shift and also an intensity decrease.

The binding of Recoverin to lipid membranes and the calcium affinity of the protein in the presence of lipid is discussed in more detail in chapter 2.5.4.

2.5 Binding of Recoverin to small lipid vesicles

2.5.1 Interaction of Recoverin and lipids

Dizhoor *et al*. (1991) tried to resolve the amino acid sequence of Recoverin via Edman-Degradation. They found that the N-terminus of Recoverin is blocked. Later, the same group could show that the N-terminus of Recoverin is indeed modified by myristoleate and related small fatty acids (Dizhoor *et al*., 1992). The heterogeneous N-terminal acylation modulates the interaction of Recoverin with the membrane and therefore the inhibition of Rhodopsin Kinase at saturating calcium concentration (Sanada *et al*., 1995). For S-modulin, the frog homolog of Recoverin with an approximately 80% identical amino acid sequence, Kawamura *et al*. (1991 and 1992) found that the protein binds to ROS membranes at high calcium concentration and becomes soluble at low calcium concentration. Zozulya and Stryer (1992) investigated the function of the posttranslational modification of Recoverin and came up with the calcium-myristoyl switch model: they suggested that the myristoyl residue is extruded into solution upon binding of calcium and allows Recoverin to insert into a lipid bilayer membrane. They could show that myristoylated Recoverin binds to ROS membranes as well as to DOPC liposomes in dependence on the calcium concentration. This means that the myristoyl residue interacts with the lipid bilayer and not, as was also suggested, with a protein in the ROS membrane. Non-myristoylated Recoverin did not bind to ROS membranes or liposomes. The fraction of bound Recoverin was proportional to the lipid concentration. By using fluorescence and NMR spectroscopy Hughes *et al*. (1995) could show that the myristoyl residue is indeed translocated into solution upon binding of Ca^{2+}, and the NMR-structures of calcium-free and calcium-bound Recoverin left no doubt that the N-terminal myristoyl residue is buried inside the protein within a hydrophobic pocket in the calcium-free conformation and extruded to solution in the calcium-bound sate (Tanaka *et al*., 1995; Ames *et al*., 1997).

Recoverin has a relatively low affinity for lipids because it has no cluster of basic residues such as v-Src, the product of the v-src gene of the Rous sarcoma virus. Electrostatic interactions of this cluster with acidic phospholipids contribute significantly to the membrane binding affinity of v-Src (Buser *et al*., 1994; Sigal *et al*., 1994). But unlike Src, Recoverin has to bind reversible to the membrane to fulfill its physiological function. The impulse of withdrawing the myristoyl residue from the lipid membrane has to be large enough to leave the membrane, so the membrane affinity of Recoverin has to be low and should depend exclusive on the myristoyl residue. It was also shown by AFM measurements that the forces necessary to extract Recoverin from a supported bilayer are consistent with forces measured for extraction of lipids from a membrane (Desmeules *et al*., 2002). Matsuda *et al*. (1999) studied the contribution of positive charged amino acids at the C-terminus of S-modulin to membrane binding. In contrast to this study, Valentine *et al*. (2003) could show with solid state NMR-spectroscopy that the

C-terminus of Recoverin does not interact with the lipid bilayer. Recoverin binds to the membrane with a single fixed orientation and shows little structural rearrangement when compared to the structure in solution (Ames *et al*., 1997). The N-terminus points towards the membrane and the myristoyl residue is positioned deeply inside the hydrophobic area of the lipid bilayer. The long molecular axis of Recoverin is oriented approximately 45° with respect to the membrane normal. The basic residues K5, K11, K37, K43 and K84 are solvent-exposed and make close contact (< 6 Å) with the negatively charged phospholipid headgroups. This electrostatic interaction may contribute to membrane binding (Valentine *et al*., 2003). Senin *et a*l. (2004) showed that cholesterol promoted binding of Recoverin to lipid bilayers.

Since Ca^{2+}-binding promotes the binding of Recoverin to lipid membranes, the presence of lipid membranes in return should promote the binding of Ca^{2+} to Recoverin. This means that Recoverin has to recognize the presence of lipid. There are three different possibilities: Firstly, there is an interaction of Recoverin with lipid also in the calcium-free conformation of Recoverin which thermodynamically stabilizes the calcium-bound conformation of the protein. Secondly, Recoverin binds calcium also at low calcium concentrations and the myristoyl residue is exposed, but this calcium-Recoverin complex has a very short lifetime. The lifetime of such a calcium-Recoverin complex might be prolonged when calcium-Recoverin meets a lipid membrane that stabilizes the calcium-bound conformation via interaction of the myristoyl residue with the lipid membrane. And thirdly, it could be possible that the conformation of Recoverin might dynamically switch between the calcium-bound and calcium-free conformation which means that the myristoyl residue is extruded even without calcium binding. The interaction of the myristoyl residue with lipid would then stabilize its position outside of the protein and would promote calcium binding. The first possibility is unreasonable because a calcium-myristoyl switch would be unnecessary if Recoverin can interact with lipids anyway. The third possibility is unreasonable as well because binding of calcium would be unnecessary for Recoverin membrane interaction.

Thus, most probably, Recoverin binds calcium also at low calcium concentration but with low probability (due to the small collision rate of calcium ions), and the lifetime of such a complex is short. In the presence of lipid, the calcium-Recoverin complex is stabilized due to the interaction of the myristoyl residue with the lipid membrane. This would mean that the calcium binding constant of Recoverin is a function of lipid concentration.

As a result, I expected to find a lower K_D value for calcium binding in the presence of lipid vesicles than that measured by 2fFCS experiments in aqueous solution without lipid. I expected also to find a dependence of this K_D value on lipid concentration.

2.5.2 Binding to DOPC vesicles

The idea of the experiments in the present section is to use small unlabeled lipid vesicles and fluorescently labeled Recoverin to investigate the binding of Recoverin to lipid vesicles by 2fFCS. In such a measurement, one expects to detect two differently diffusing species: free Recoverin in solution, and slower diffusing vesicles with bound Recoverin. If the brightness of the attached fluorescent label does not change upon binding Recoverin to a vesicle, the correlation amplitude of the two components will be proportional to the fractions of bound and free Recoverin. This experiment provides in contrast to preparations of disk membranes a perfectly homogeneous and defined lipid phase. The binding process of Recoverin to the lipid membrane is in equilibrium during the measurement in contrast to experiments where the fraction of bound protein is determined by centrifuging membrane fragments together with bound protein to discriminate it from the unbound fraction.

Recoverin has a relatively low affinity for lipids and, so one needs a high lipid concentration to detect binding of Recoverin to vesicles at the necessary low Recoverin concentration that one has to use for 2fFCS. Moreover, the number of vesicles had to be at least a hundred times higher than the number of Recoverin molecules to exclude binding of two Recoverin molecules to the same vesicle. This is important because a quantitative evaluation of the 2fFCS measurements is only possible if one vesicle binds at maximum only one Recoverin. Varying the lipid concentration revealed that a concentration of 20 mg/ml DOPC was optimal to detect binding of Recoverin. Assuming a cross-section area per lipid molecule of 0.5 nm^2 in a lipid bilayer, vesicles with 100 nm in diameter and a lipid concentration of 20 mg/ml (2%) correspond to a vesicle concentration of roughly 200 nM which is more than two hundred times higher than the Recoverin concentration as used for 2fFCS. A concentration of 200 nM means that the average distance between vesicles is 285 nm, which is a quite close packing, but the disk packing in photoreceptors is even denser: the distance between two disk membranes is roughly 20 nm.

To investigate the binding of Recoverin to vesicles as a function of lipid concentration, I used beside 20 mg/ml DOPC also 10 mg/ml and 5 mg/ml DOPC. In case of 5 mg/ml DOPC, there are approximately 50 times more vesicles than Recoverin molecules. The probability to find two Recoverin molecules bound to the same vesicle is then 1/50 (100% of Recoverin is bound to vesicles). In case of a large fraction of bound Recoverin molecules, this fraction might be underestimated.

The crucial point of these experiments was to prepare monodisperse small vesicles. Polydisperse vesicles would result in a broad distribution of diffusion coefficients, making a quantitative evaluation of FCS measurements difficult. I used the extrusion technique for preparation of monodisperse vesicle solutions.

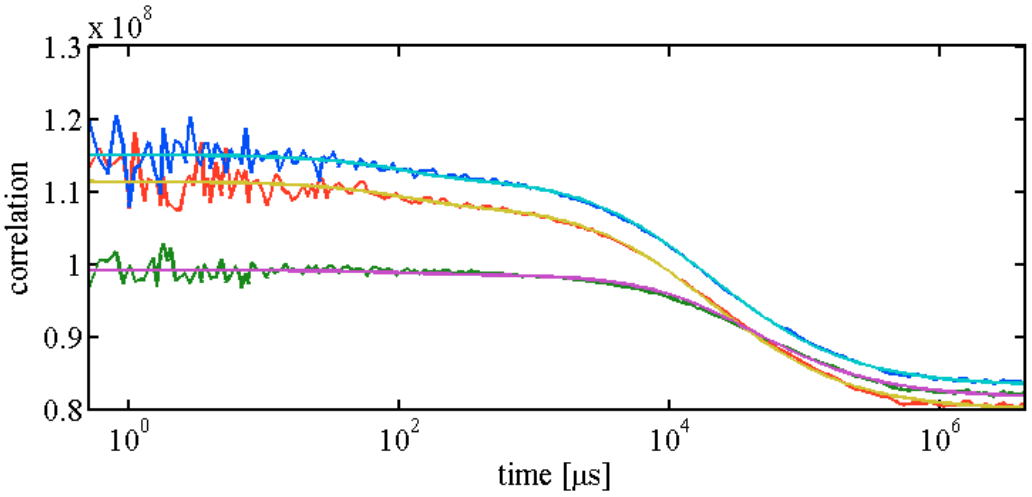

Fig. 2.41 2fFCS measurement of vesicle diffusion. Monodisperse vesicles were prepared via extrusion. A small amount of fluorescent lipids (DOPE-Atto655) were used to label the vesicles. The two autocorrelations (red and blue) and the cross-correlation (green) were fitted (cyan, yellow and purple lines) with a one component diffusion model.

Fig. 2.41 shows fitted 2fFCS data of the diffusion of extruded small vesicles. The model assuming only one diffusing component with one diffusion coefficient fits the data fairly well, so that one can assume that vesicles size distribution is rather monodisperse. With vesicles of this quality I started to investigate the binding of wild type Recoverin-Alexa647 to DOPC vesicles.

A suspension of high concentrated lipid vesicles scatters light strongly. Although this scattering does not contribute to the lag-time dependent part of the correlation function, the sample had to be measured under perfectly dark conditions to avoid any further data noising.

Measurements at lipid concentrations as high as 20 mg/ml made it challenging to adjust and buffer the free calcium concentration. The phosphate groups of phospholipids bind calcium ions, leading to an additional calcium buffering. The buffer capacity of the used calcium buffers for samples with high lipid content has to be large enough to overcome the calcium binding by the phosphate groups for keeping the calcium concentration constant. I used calcium buffers with 30 mM EGTA or NTA.

After adding labeled Recoverin at sub-nanomolar concentration to the vesicle suspension, 2fFCS was measured for at least 30 min with a total excitation power of 5–7 µW per laser. The fit quality of the data was fair. The diffusion coefficient of Recoverin in solution was fixed to the value measured before without vesicles, and the diffusion coefficient found for the slow component was similar to the diffusion coefficient found for vesicles measured before with labeled vesicles.

The results of the measurements with 20 mg/ml DOPC are shown in Fig. 2.42. The data were fitted with the Hill curve as given by Eq. 2.2 and already used to fit the 2fFCS measurement results without lipid (chapter 2.3.2). The results of binding to 10 mg/ml DOPC and 5 mg/ml DOPC are shown in Fig. 2.43 and Fig. 2.44, respectively.

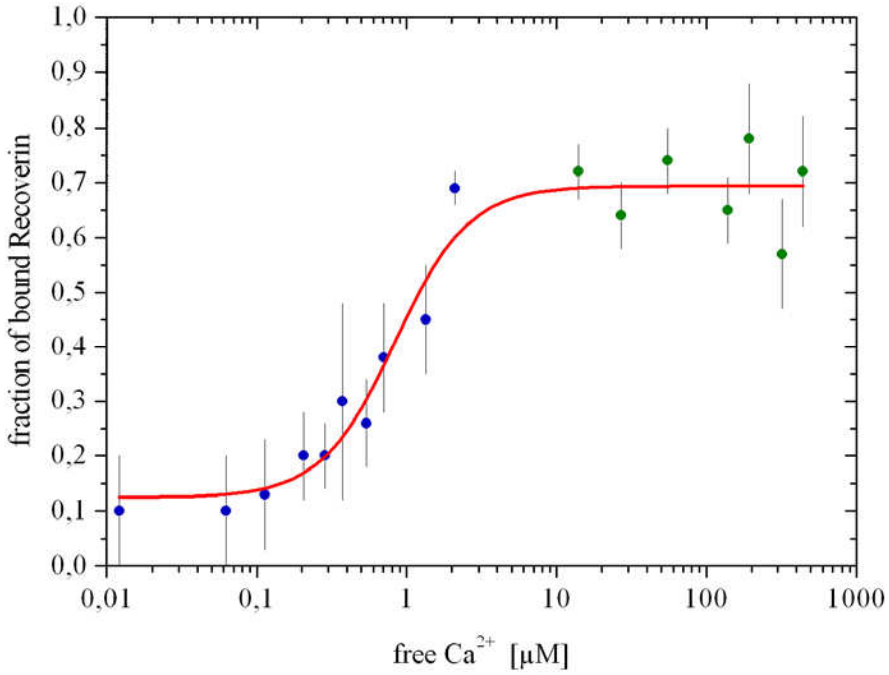

Fig. 2.42 Binding of wild type Recoverin-Alexa647 to 20 mg/ml DOPC vesicles. Data from measurements with EGTA-buffer are shown in blue and measurements in NTA-buffers are indicated with green. Binding is half maximal at 0.8 ± 0.2 µM free Ca^{2+}. The Hill coefficient is 1.8 ± 0.5.

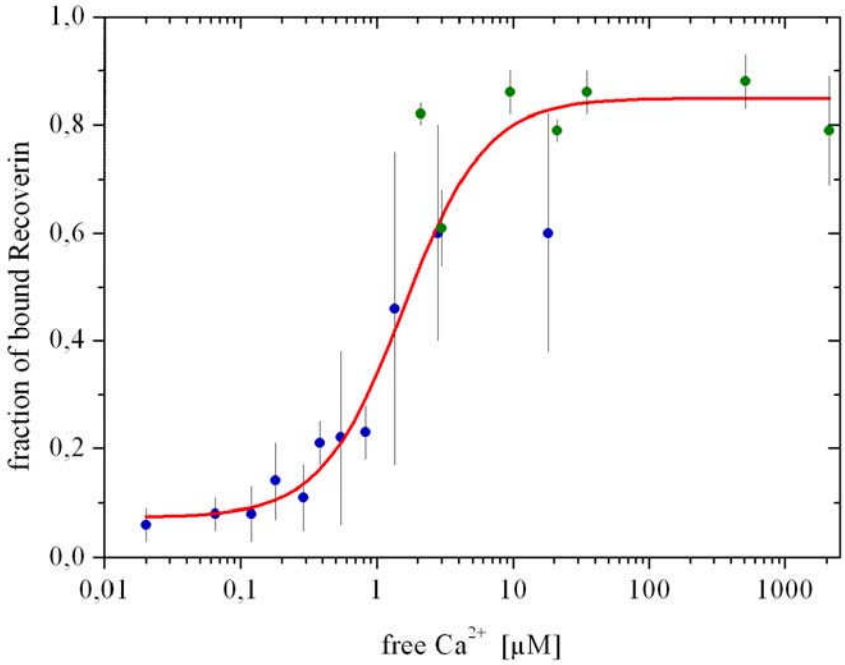

Fig. 2.43 Binding of wild type Recoverin-Alexa647 to 10 mg/ml DOPC vesicles. Data from measurements with EGTA-buffer are shown in blue and measurements in NTA-buffers are indicated with green. Binding is half maximal at 1.6 ± 0.2 µM free Ca^{2+}. The Hill coefficient is 1.5 ± 0.2.

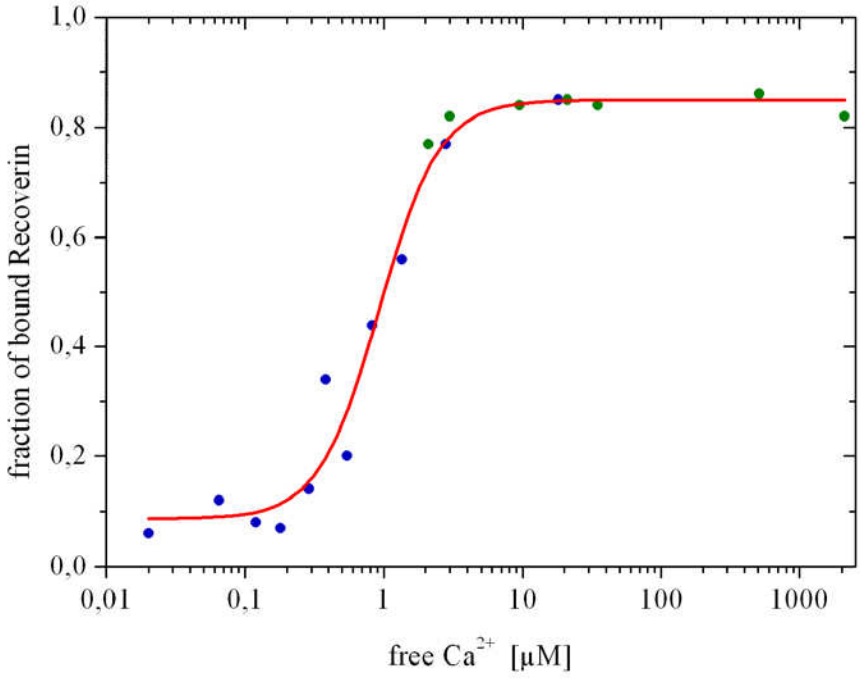

Fig. 2.44 Binding of wild type Recoverin-Alexa647 to 5 mg/ml DOPC vesicles. Data from measurements with EGTA-buffer are shown in blue and measurements in NTA-buffers are indicated with green. Binding is half maximal at 0.9 ± 0.02 µM free Ca^{2+}. The Hill coefficient is 2.0 ± 0.3.

The fit quality was fair. Fitting was unstable for very low calcium concentrations. The determined slow diffusion coefficient was used to estimate the reliability of the fit. Data quality was heavily dependent on the vesicle preparation. Lower lipid concentrations resulted in vesicle suspensions of better quality.

At low free Ca^{2+} concentration, 5 - 15% of Recoverin molecules bind to the DOPC vesicles. This fraction increases, as expected, with increasing free Ca^{2+} concentration to 70 – 85%. In contrast to the expected tendency neither the fraction of bound Recoverin nor the calcium affinity of Recoverin increases with increasing lipid concentration.

Table 2.5 Binding of Recoverin to lipid vesicles as a function of calcium concentration

DOPC conc.	Bound fraction at low Ca^{2+}	Bound fraction at high Ca^{2+}	K_D [µM]	Hill coeff.
20 mg/ml	0.12	0.69	0.84	1.8
10 mg/ml	0.07	0.85	1.6	1.5
5 mg/ml	0.09	0.85	0.9	2.0

I investigated also the interaction of the mutants E85Q and E121Q with 20 mg/ml DOPC vesicles. The results of these experiments are shown in Fig. 2.45 and Fig. 2.46, respectively.

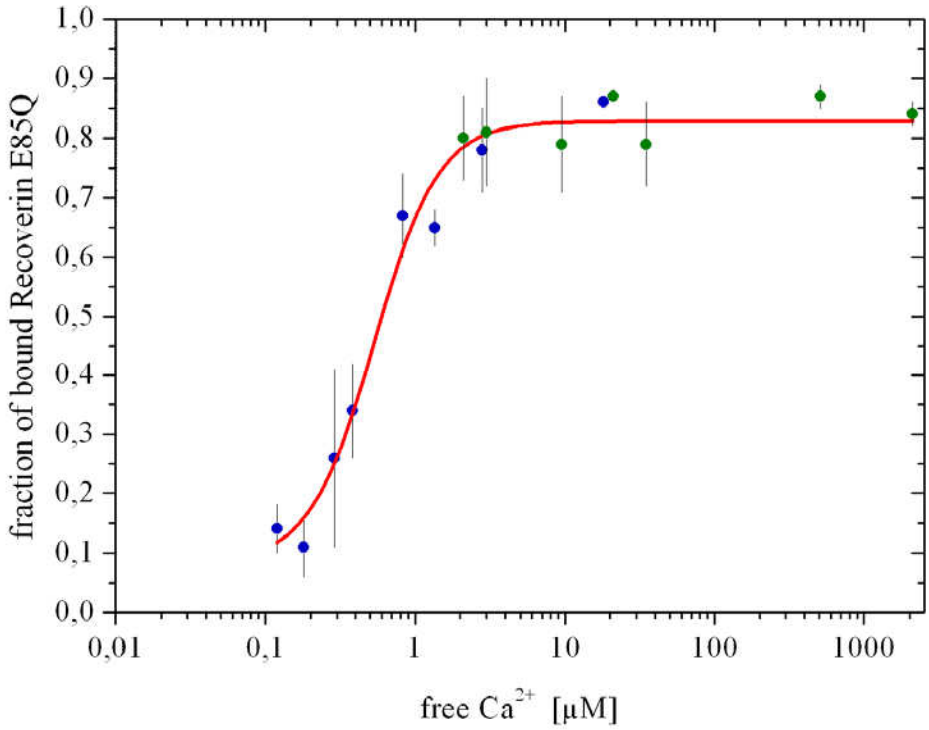

Fig. 2.45 Binding of Recoverin-Alexa647 E85Q to small DOPC vesicles (20 mg/ml). Data from measurements with EGTA-buffer are shown in blue and measurements in NTA-buffers are indicated with green. The red line shows the best fit corresponding to Eq. 2.2. Measurement temperature was 25° C. Binding is half maximal at 0.5 ± 0.1 µM free Ca^{2+} and the Hill coefficient was determined as 2.0 ± 0.4.

E85Q showed a strong binding to DOPC vesicles, although this mutant can bind only one calcium ion. Roughly 15% of E85Q interacts with the vesicles at low free Ca^{2+} concentration. This fraction increases up to 85% at high free Ca^{2+} concentration. Binding of E85Q to DOPC vesicles is half maximal at 0.5 ± 0.1 µM free Ca^{2+}. The Hill coefficient is 2.0 ± 0.4 which means that binding of E85Q to lipid vesicles is also a cooperative process. The maximal fraction of bound E85Q is larger than that of the wild type protein. Moreover, half maximal binding occurs at lower free Ca^{2+} concentrations than for the wild type protein.

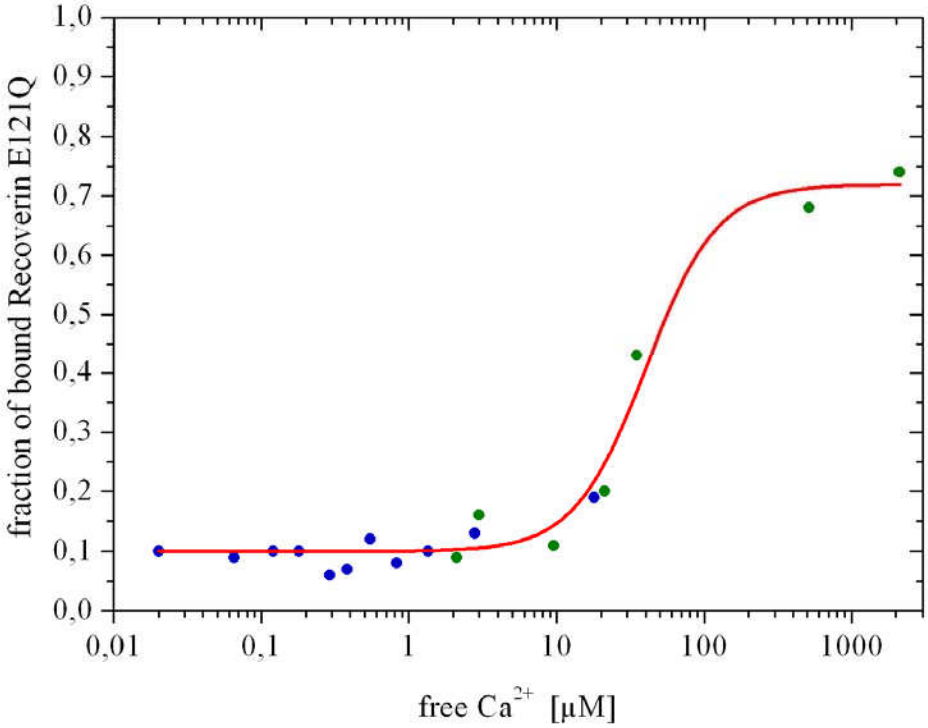

Fig. 2.46 Binding of Recoverin-Alexa647 E121Q to 20 mg/ml DOPC vesicles. The red line shows the best fit corresponding to Eq. 2.2. Data from measurements with EGTA-buffer are shown in blue and measurements in NTA-buffers are indicated with green. Binding to vesicles is half maximal at 40 ± 3.5 µM free Ca^{2+}. The Hill coefficient is 1.8 ± 0.5.

Although E121Q should not bind Ca^{2+} and the myristoyl residue should stay buried inside the protein, there is a fraction of 70% bound to the DOPC vesicles at high free Ca^{2+} concentration. At low free Ca^{2+} concentration, about 10% of the protein is bound to the vesicles. Binding is half maximal at 40 ± 3.5 µM free Ca^{2+}.

2.5.3 Binding to vesicles made from an artificial ROS-lipid mixture

To investigate the influence of different (charged) head groups and cholesterol on the binding of Recoverin to lipid vesicles, I prepared an artificial ROS lipid mixture which mimics the lipid composition of the photoreceptor disk membranes. This mixture consists of 40% DOPC (no net charge), 38% DOPE (also no net charge), 15% DOPS (negatively charged) and 7% cholesterol (Anderson and Maude, 1970).

At low free Ca^{2+} concentration, 10-15% of wtRecoverin-Alexa647 molecules do bind to the artificial ROS lipid vesicles. This fraction increases to 60% at high free Ca^{2+} concentration. The data were fitted again with a Hill curve. Binding of wtRecoverin-Alexa647 vesicles is half maximal at 2.0 ± 0.5 µM free Ca^{2+}. The Hill coefficient is equal to one, which means that binding of wtRecoverin-Alexa647 to artificial ROS lipid vesicles is not, in contrast to DOPC

vesicles, a cooperative process. Fig. 2.47 displays the fraction of bound Recoverin as a function of calcium concentration.

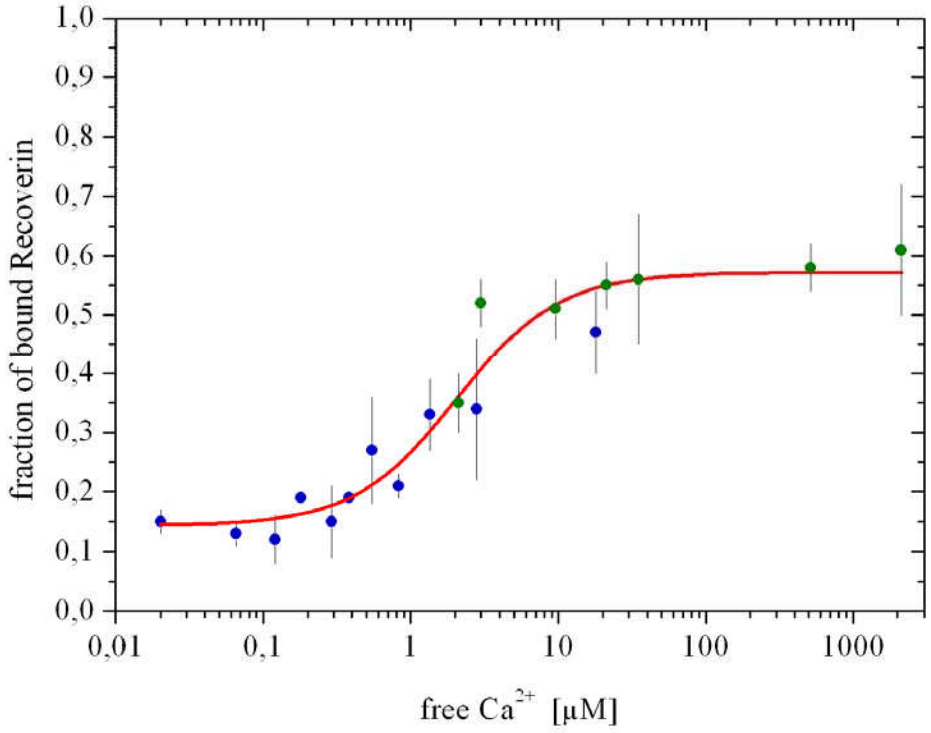

Fig. 2.47 Binding of wtRecoverin-Alexa647 to small vesicles made from an artificial ROS lipid mixture (20 mg/ml). Data from measurements with EGTA-buffer are shown in blue and measurements in NTA-buffers are indicated with green. The red line shows the best fit corresponding to Eq. 2.2. Binding is half maximal at 2.0 ± 0.5 µM free Ca^{2+}. The Hill coefficient is 1 which means that binding of wtRecoverin-Alexa647 to ROS lipid vesicles shows in contrast to binding to DOPC vesicles no cooperativity.

2.5.4 Discussion of Recoverin binding to small lipid vesicles

Data of these measurements were analyzed by fitting two diffusion coefficients and one term for the triplet state dynamics of the label to the measured correlation curves. Fitting was unstable or not reliable for measurements at very low and very high calcium concentration. A small fraction of Recoverin bound to vesicles could not be fitted reproducible. At high calcium concentrations a small fraction of Recoverin in solution could not be fitted reliable, the amplitude of the fast diffusion component mixed up with the amplitude caused by the microsecond photophysics of Alexa647.

In chapter 2.3.8, I discussed the influence of the fluorescent dye Alexa647 linked to C38 of Recoverin on the calcium affinity of the protein. I measured calcium binding of Recoverin and its mutants with 2fFCS in solution in the absence of lipid and found that Alexa647 promotes calcium binding to Recoverin due to the stabilization of the calcium-bound conformation. The hydrophobic dye interacts with the myristoyl residue and stabilizes its extension into solution. The fluorescent hydrophobic dye is at a position close to the myristoyl residue where it can also interact with the membrane. Thus, the question arises: does the hydrophobic dye, besides influencing the calcium affinity of Recoverin, act as an additional membrane anchor? I could not find any interaction of pure Alexa647 with DOPC vesicles, and I could also not measure binding of non-myristoylated Recoverin-Alexa647 to DOPC vesicles. Thus, Alexa647 itself shows no binding to lipid vesicles and does not act as additional membrane anchor of Recoverin.

In the literature, one finds several measurements of the calcium dependent binding of Recoverin to ROS membranes and to pure phospholipid membranes, but for all these measurements the lipid concentration and the structure of the lipid phase are not well defined. ROS preparations can have different lipid concentrations, even if the Rhodopsin concentration is the same. Furthermore, the properties of ROS disk membranes can be different due to more or less vigorous preparation techniques. Despite the different reported values of the binding constants, all measurements have in common that binding of Recoverin to membranes happens at lower free calcium concentrations than calcium binding to Recoverin in the absence of lipid. Thus, the presence of lipid promotes calcium binding of Recoverin, followed by the extrusion of the myristoyl residue. I found also half maximal binding of Recoverin to DOPC vesicles (20mg/ml) at 0.84 ± 0.2 µM free calcium, in contrast to half maximal calcium binding in the absence of lipid at 4 [1.3 – 12] µM free calcium. Comparing this values with the results of the tryptophan fluorescence measurements as a function of calcium concentration (see chapter 2.4) reveal the influence of the fluorescent label of Recoverin on the binding to lipid membranes. In the absence of lipid calcium binding of Recoverin was half-maximal at 12.3 [11.8 – 12.8] µM free calcium. This value decreased in the presence of 20 mg/ml DOPC vesicles to 3.1 [2.6 - 3.7] µM free calcium. This shows that the dye, although it does not

interact with the membrane itself, promotes membrane binding of Recoverin due to increasing the calcium affinity of the protein. Thus, the fluorescent dye has the same effect on Recoverin as the presence of lipid. This might be one reason for the independence of the fraction of bound Recoverin on the used lipid concentration. The influence of different lipid concentrations on Recoverin can not overcome the effect of the fluorescent label on the protein.

Zozulya and Stryer (1992) showed that the fraction of bound Recoverin depends on the membrane concentration, but they found different dissociation constants of Recoverin for different ROS membrane preparations. This shows that different ROS preparations are not comparable, and that the lipid concentration is not well defined by Rhodopsin concentration. Lange and Koch (1997) investigated the binding of Recoverin to lipid membranes by surface plasmon resonance (SPR) spectroscopy. In these measurements, either the protein or the lipid is immobilized on a surface, and the analyte (either lipid or protein respectively) is flushed over the surface. Binding is measured by monitoring changes in reflectivity that are caused by refractive index changes close to the surface. Half maximal binding of Recoverin to phospholipid vesicles was found at 4.0 ± 0.5 µM free calcium when Recoverin was the analyte, and at 7.7 ± 0.6 µM when lipid vesicles were flushed over the surface where Recoverin was immobilized. These differing binding constants reflect the different relative concentrations of Recoverin and lipid immobilized or in solution. The lipid phase in the experiments presented in this study is well defined. The concentration as well as the composition of lipid vesicles is known and adjustable. But nevertheless, the vesicles used in the experiments are also a source of data scattering. An inhomogeneous vesicle preparation easily spoiled measurements. Vesicle suspensions with low lipid concentration could be prepared in a higher quality than high concentrated suspensions. Large amounts of lipid had a negative impact on the quality of the polymer membrane used in the extruder.

What can be said about the membrane binding of the Recoverin mutants E85Q and E121Q? Matsuda *et al*. (1998) studied the binding of the S-modulin mutants E85M and E121M to ROS membranes. They did not find any difference in membrane association between wild type S-modulin and E85M. Binding was half maximal below 1 µM free calcium. The mutant E121M showed a low affinity to ROS membranes above 100 µM free calcium. Senin et al. (2002) investigated the similar Recoverin mutants E85Q and E121Q and found, in contrast to Matsuda *et al*. (1998) for the S-modulin mutants a difference in ROS membrane association of wild type Recoverin and E85Q. Binding of wtRecoverin was half maximal at 4.7 µM free calcium. For the mutant, a two step binding curve was found: the first step was half maximal at 9 µM, and the second at 2.6 mM. Qualitatively, the same behavior was found by SPR spectroscopy. There, the association of wtRecoverin to phospholipid vesicles was half maximal at 2.2 µM, and the association of Recoverin E85Q showed also a two step binding curve with the first step half maximal at 2.2 µM with an amplitude of 25% of total binding,

and the second at 681 µM with 75% amplitude of the total signal, respectively. The mutant E121Q showed a low affinity above 3 mM free calcium to ROS membranes. I found a one step binding curve for Recoverin E85Q with half maximal binding at 0.52 ± 0.08 µM free calcium and a Hill coefficient of 1.8 ± 0.4. The maximal fraction of bound Recoverin-Alexa647 E85Q was with 85% even higher than for wild type Recoverin. Thus, the combined effects of Alexa647 and lipid overcome the effect of the mutated low affinity binding site EF-2. Calcium binding and extrusion of the myristoyl residue seems to function in the mutant E85Q similar to the wild type protein. The dye linked to C38 of Recoverin seems to have the same influence on the protein as an exchange of the glutamic acid for the hydrophobic amino acid methionine in S-modulin E85Q (Matsuda *et al*. 1998), assuming that one can directly compare these two homologous proteins.

Additionally to the pure phospholipid DOPC, a lipid mixture imitating the composition of the ROS disk membrane was used. This mixture contained 15% of negatively charged DOPS and 7% cholesterol. Lipid vesicles formed from this artificial ROS mixture had a higher quality. The suspensions were not as turbid as the ones made from DOPC. Senin et al. (2004) showed that the binding of Recoverin to membranes strongly depends on the cholesterol content. The fraction of bound Recoverin increases with cholesterol concentration. In contrast to this finding was the fraction of bound Recoverin to the artificial ROS mixture lower in this study compared to binding to DOPC. One explanation is again the influence of the fluorescent dye linked to Recoverin. Alexa647 is most probably negatively charged. Sulfonic acid esters are often used to increase the solubility of red fluorescent dyes. Thus, the negatively charged dye avoids interaction with the negatively charged lipid vesicles.

The data analysis of these experiments has one sore spot: most likely, the assumption that the fluorescence brightness does not change upon binding of the protein to the membrane is not valid. This means that one cannot use the correlation amplitudes to correctly estimate the fractions of bound and free Recoverin. The binding curves are stretched due to overestimating either the fraction of Recoverin in solution or the fraction bound to the membrane. I realized that, for example, the calcium chelator EGTA enhances fluorescence of the dye whereas the EGTA-Calcium-complex quenches it. This means that even the fluorescence brightness of the dye in solution is not constant across various calcium buffers. Binding of Recoverin to the membrane might prohibit the interaction of chelator and fluorescent dye and thus might change the brightness of the dye again. To account for this problem, a modified data analysis was set up which is presented in the next section.

2.5.5 3-Photon correlation – an outlook

Standard FCS evaluates the two-photon correlation (or autocorrelation) function, $g_2(\tau)$, which is proportional to the probability to detect two photons a time τ apart from each other. When detecting two photons a time τ apart, they can originate either from the same molecule, or from two different molecules (neglecting any background for a moment). If they originate from two different molecules, and if there are no intermolecular interactions between these molecules, the probability to see such a photon pair is completely independent on time τ and simply proportional to the square of the average fluorescence intensity, $\langle i_1 \rangle$, of one molecule times the square of the concentration c of fluorescent molecules. However, if the two photons come from one and the same molecule, the probability to see them a time τ apart will be dependent on τ, due to photophysical changes within the molecule and its diffusion out of the detection volume. This probability scales linearly with the concentration of fluorescing molecules. Thus, in a very general sense, one has for the full second-order correlation function

$$g_2(\tau) = c\varepsilon^2 \tilde{g}_2(\tau) + c^2 \langle i_1 \rangle^2 ,$$

where we call $\tilde{g}_2(\tau)$ the irreducible one-molecule second-order correlation function describing how the two-photon correlation depends on time distance τ for a photon from a single molecule, and ε is a factor proportional to the intrinsic fluorescence brightness of a single molecule. If there is additional background signal with average signal strength b present in the measurement, it will affect only the τ-independent part, and $g_2(\tau)$ has a similar form as above, only with $\langle i_1 \rangle$ replaced by $\langle i_1 \rangle + b$.

If one has more than a single fluorescing molecular species, say n species, in the sample, the expression for $g_2(\tau)$ is generalized in a straightforward way to

$$g_2(\tau) = \sum_{\alpha=1}^{n} c_\alpha \varepsilon_\alpha^2 \tilde{g}_{2,\alpha}(\tau) + \left(b + \sum_{\alpha=1}^{n} c_\alpha \langle i_{1,\alpha} \rangle \right)^2 .$$

If the individual one-molecule correlation functions $\tilde{g}_{2,\alpha}(\tau)$ are sufficiently different, for example due to sufficiently different diffusion coefficients of the species, on can extract from a fit of an experimentally measured curve the individual prefactors $c_\alpha \varepsilon_\alpha^2$ of each function $\tilde{g}_{2,\alpha}(\tau)$. If, incidentally, the intrinsic fluorescence brightness values ε_α of each species have the same value, then the ratio of the prefactors is equal to the ratio of species concentrations. This is behind using an autocorrelation analysis for measuring a binding curve of fluorescently tagged molecules to some target molecules with different diffusion coefficient. However, this will work correctly only if the fluorescence brightness of the tagged molecules does not change upon binding to the target, an assumption that will often be not true.

To improve on that situation, on may try to use the next order correlation function, namely the three-photon correlation function. In general, the third-order or three-photon correlation function is proportional to the probability for detecting three photons with time intervals of τ_1 and τ_2 between succeeding photons. Thus, a third order correlation function will, in general, be dependent on two time values, τ_1 and τ_2. In what follows, we will consider only the special case of $\tau_1 = \tau_2 \equiv \tau$. When considering the temporal correlation of three photons, one has now to consider three principally different possibilities: (i) all three photons are emitted by one and the same molecule, (ii) two of the photons come from the same and the remaining photon from a different molecule, and (iii) all three photons are emitted by different molecules. After some tedious algebra, one then finds the following general expression for the three-photon correlation function $g_3(\tau)$:

$$g_3(\tau) = c\varepsilon^3 \tilde{g}_3(\tau) + c^2\varepsilon^2\left[2\tilde{g}_2(\tau) + \tilde{g}_2(2\tau)\right]\langle i_1\rangle + c^3\langle i_1\rangle^3$$

where $\tilde{g}_3(\tau)$ is now the irreducible one-molecule third-order correlation function giving the probability to detect, from one and the same molecule, three photons in a row with time distance τ between consecutive photons. For a sample with several molecular species and with background, this expression is generalized to

$$g_3(\tau) = \sum_{\alpha=1}^{n} c_\alpha \varepsilon_\alpha^3 \tilde{g}_{3,\alpha}(\tau) + \\ + \left\{\sum_{\alpha=1}^{n} c_\alpha^2 \varepsilon_\alpha^2 \left[2\tilde{g}_{2,\alpha}(\tau) + \tilde{g}_{2,\alpha}(2\tau)\right]\right\}\left[b + \sum_{\alpha=1}^{n} c_\alpha \langle i_{1,\alpha}\rangle\right] + \left[b + \sum_{\alpha=1}^{n} c_\alpha \langle i_{1,\alpha}\rangle\right]^3 .$$

Thus, fitting a measured third-order correlation function will allow for extracting, among others, the prefactors $c_\alpha\varepsilon_\alpha^3$. Together with the prefactors $c_\alpha\varepsilon_\alpha^2$ extracted from fitting the second-order correlation function, one can now estimate the concentration of species α by the obvious relation

$$c_\alpha = \frac{\left(c_\alpha\varepsilon_\alpha^2\right)^3}{\left(c_\alpha\varepsilon_\alpha^3\right)^2}$$

giving an expression that is independent on the brightness value of the species.

It remains to find a suitable expression for the irreducible one-molecule third-order correlation function, which will be needed for fitting experimental data. For simplicity reasons, we will derive that function under the simplified assumption that the molecule detection function can be described by a three-dimensional Gaussian distribution,

$$U(\mathbf{r}) \propto \exp\left[-\frac{2\left(x^2+y^2\right)}{a^2}-\frac{2z^2}{b^2}\right],$$

where a and b are the characteristic half axes of the Gaussian distribution. Then, $\tilde{g}_3(\tau)$ can be found by the multiple integral

$$\tilde{g}_3(\tau) \propto \int d\mathbf{r}_1 \int d\mathbf{r}_2 \int d\mathbf{r}_3 \frac{U(\mathbf{r}_3)U(\mathbf{r}_2)U(\mathbf{r}_1)}{(4\pi D\tau)^3} \exp\left[-\frac{(\mathbf{r}_2-\mathbf{r}_1)^2+(\mathbf{r}_3-\mathbf{r}_2)^2}{4D\tau}\right]$$

leading to the analytical expression

$$\tilde{g}_3(\tau) \propto \frac{1}{\left(64\tau^2+32a^2\tau+3a^4\right)\sqrt{64\tau^2+32b^2\tau+3b^4}}.$$

Although it is well known that a three-dimensional Gaussian distribution is a rather poor description of the MDF, the derived expression for the three-photon correlation function will be sufficient for extracting the correct prefactors $c_\alpha \varepsilon_\alpha^3$ from the experimentally measured correlation function.

In practice, data fitting proceeds in two steps: firstly, using 2fFCS, one determines the diffusion coefficients of the different species present in the sample. Secondly, by fitting the two-and three-photon correlation functions with fixed value for the diffusion coefficients, as found by 2fFCS, one extracts the prefacer values $c_\alpha \varepsilon_\alpha^2$ and $c_\alpha \varepsilon_\alpha^3$, thus finding finally the value of c_α.

This extended analysis was applied to two sets of measurements: binding of Recoverin to 5 mg/ml DOPC and 10 mg/ml DOPC vesicles as a function of calcium concentration. The resulting binding curves are displayed in Fig. 2.48 and Fig. 2.49, respectively. Recoverin binding to 5 mg/ml vesicles was determined to be half-maximal at 2.0 µM free calcium, in contrast to half-maximal binding at 0.9 µM free calcium, as determined with two-photon correlation. This tendency to a higher binding constant for lower lipid concentration is what one would expect. The determined fraction of bound Recoverin does not differ from the fraction determined by two-photon correlation. Thus, the fluorescence brightness of the label close to the membrane does not change dramatically compared to its brightness in solution, but nevertheless this small difference had an impact on the determined binding constant.

The calcium dependent binding curve of Recoverin to 10 mg/ml DOPC vesicles is noisy and cannot be used to reliably determine a binding constant. This is the challenge when using three-photon correlation: data quality has to be excellent, because any inhomogeneity in e.g. vesicles size has a much larger impact on the quality of the three-photon correlation function than it has on the quality of two-photon correlation function.

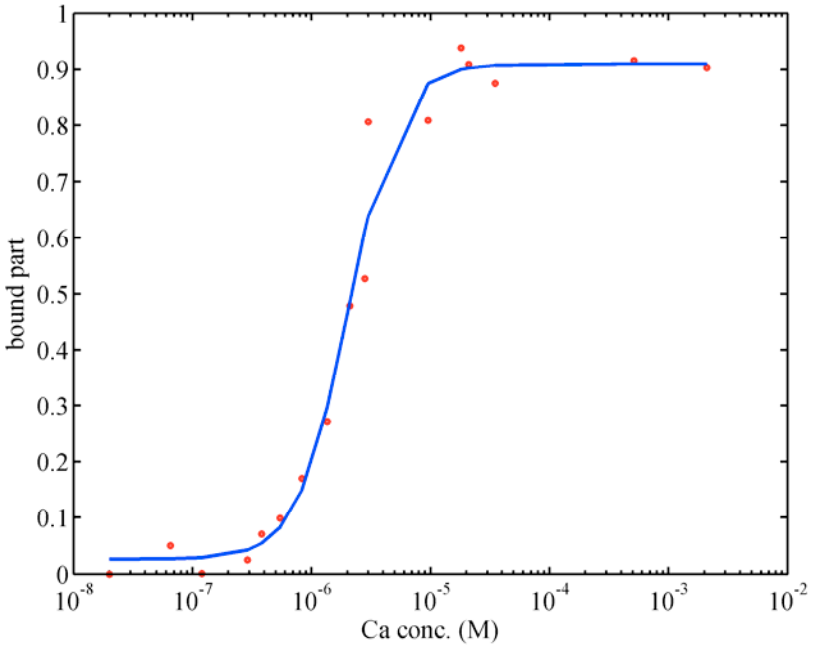

Fig. 2.48 Binding of Recoverin to 5 mg/ml DOPC vesicles as a function of free calcium concentration analysed by fitting the 2- and 3-photon correlation functions to account for changes in fluorescence brightness of the dye upon Recoverin binding to the membrane. Half-maximal binding was achieved at 2.0 µM free Ca^{2+}. The Hill coefficient was determined to be 2.1.

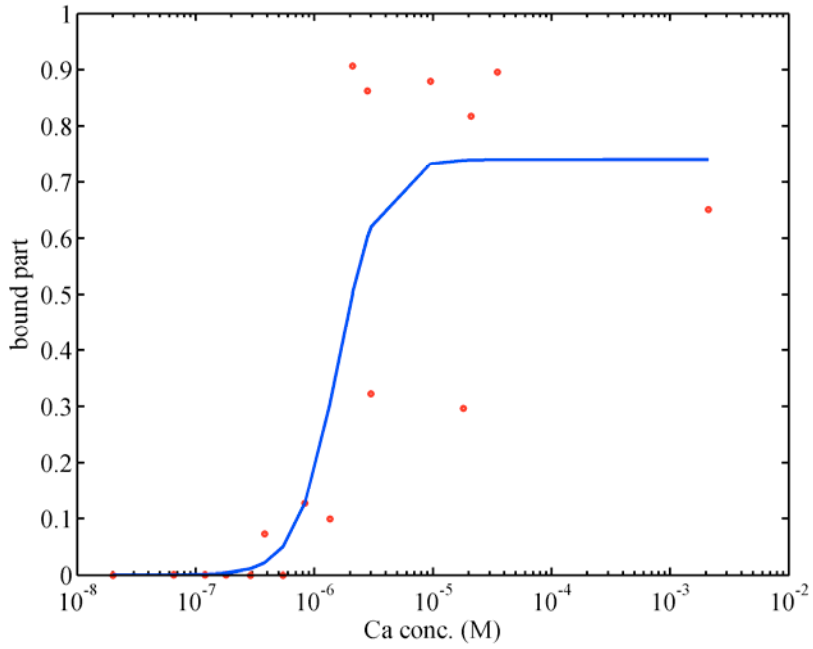

Fig. 2.49 Recoverin binding to lipid vesicles (10 mg/ml DOPC) as a function of free calcium concentration. Data were analysed by fitting the 2- and 3-photon correlation functions to account for changes in fluorescence brightness of the dye upon Recoverin binding to the membrane. Binding to the membrane was half-maximal binding at 1.6 µM free Ca^{2+}. The Hill coefficient was determined to be 2.5.

3 Summary

Recoverin is a neuronal calcium sensor protein (NCS protein) from the mammalian photoreceptors. It plays an important role in adaptation of the photoreceptor cell to different light intensities. It displays a calcium myristoyl switch and functions as model protein for the whole NCS protein family. The aim of this study was to quantify the properties of Recoverin with a new single molecule measurement method. The dynamics of the calcium dependent interaction between Recoverin and a lipid membrane was investigated with the focus on the influence of lipid type or membrane composition, and the density of lipid membranes, on Recoverin's the calcium affinity. The complexity of the biological system had to be reduced to make a physical description of the system possible. Therefore, an appropriate model membrane system was chosen to investigate the calcium dependent binding of Recoverin with lipid bilayers.

3.1 Model membrane systems

The first step for investigating the interaction of Recoverin with lipid bilayers was to find an adequate model membrane system that allowed for investigating of the binding of Recoverin to membranes. This system should allow control of all parameters like lipid composition and it should be suitable for use with dual-focus fluorescence correlation spectroscopy (2fFCS).

I prepared fluid and continuous supported phospholipid bilayers (SPBs) from various phospholipids and mixtures of phospholipids with cholesterol on glass cover slides. However, these SPBs contained defects, as was revealed by single molecule imaging. These SPBs did not prevent the interaction of Recoverin with the glass support underneath. Thus, Recoverin did not bind to the lipid bilayer but adsorbed irreversible to the glass cover slide. The Brownian motion of fluorescently labeled lipids within such a lipid bilayer was observed with single molecule imaging and measured with 2fFCS.

I specifically addressed the problem of surface adsorption/desorption of molecules diffusing in a glass-supported phospholipid bilayer (Dertinger *et al.*, 2006). A theoretical model describing this issue was developed and successfully applied to 2fFCS and also to the z-scan FCS technique (Benda *et al.*, 2003). For both methods, equal diffusion coefficients (3.3 µm²/s) were determined, and equal adsorption ($1/k_{on}$ [s] = 0.086) and desorption rates ($1/k_{off}$ [s] = 2.7) of molecules to and from the glass support.

In the next step, I prepared free standing phospholipid bilayers of giant unilamellar vesicles (GUVs). Compared to supported bilayers (3.3 µm²/s), a more than twice as large diffusion coefficient was observed for lipid diffusion in the free standing GUV lipid bilayers (8.0 ± 0.2 µm²/s). Furthermore, I measured the influence of different sugar solutions and salt buffers on the diffusion coefficient of labeled lipids diffusing within the bilayers. It was found that aqueous solutions of glucose (7.5 ± 0.4 µm²/s) as well as sucrose (6.8 ± 0.2 µm²/s) surrounding the

GUV bilayer lead to slower diffusion coefficients, probably due to clustering of lipid molecules induced by hydrogen bonds between phospholipids and sugar molecules, whereas salt-containing buffers did compensate this effect. Diffusion coefficients of 9.0 ± 0.4 µm²/s and 7.3 ± 0.4 µm²/s with glucose or sucrose solutions inside the vesicle and [100 mM KCl; 30 mM Hepes pH 7.2; 10 mM K_2CaEGTA] outside the vesicle were found.

3.2 Conformational changes of Recoverin investigated with 2fFCS

Recoverin is a very well characterized protein and was therefore an ideal system for testing the recently developed method of dual-focus fluorescence correlation spectroscopy (2fFCS). The method was used for measuring the hydrodynamic radius of Recoverin as a function of free calcium. I observed minute changes (on the order of one Ångström) of the hydrodynamic radius due to calcium-dependent conformational changes of Recoverin. This has never been achieved with conventional FCS.

The measurements of the hydrodynamic radius of Recoverin and its mutants E85Q, E121Q as well as non-myristoylated Recoverin resulted in calcium binding curves. The hydrodynamic radius of wild type Recoverin (25.3 ± 0.3 Å to 24.1 ± 0.3 Å) and its mutant E85Q (25.2 ± 0.2 Å to 24.6 ± 0.2 Å) decreased with increasing calcium concentration, whereas the hydrodynamic radius of non-myristoylated Recoverin (23.3 ± 0.2 Å to 24.0 ± 0.2 Å) increased with increasing calcium concentration. The hydrodynamic radius of the mutant E121Q (26 ± 0.1 Å) was independent on calcium concentration. The calcium binding curves were fitted with a standard Hill model. A calcium binding constant of $K_D = 4$ [1.3 - 12] µM and a Hill coefficient of 1 was found for wild type Recoverin. The estimated K_D value for Recoverin E85Q was $K_D = 1.4$ [0.58 - 3.4] µM and the Hill coefficient was also equal to 1. For non-myristoylated Recoverin, a higher calcium binding constant of 10 [3.7 - 27] µM was found. The found low values of the binding constant, which are smaller as those reported in the literature, were attributed to the interaction of the myristoyl residue with the fluorescent label Alexa647 which was linked to Recoverin at position C38. The calcium dependent shift in triplet state lifetime of the fluorescent label as well as measurements of the tryptophan fluorescence of fluorescently labeled and unlabeled Recoverin confirmed the influence of the dye on the proteins calcium affinity.

3.3 Interaction of Recoverin with small lipid vesicles

The calcium dependent interaction of Recoverin with lipid membranes was measured in solutions of small unilamellar vesicles (SUVs, 100 nm in diameter) of different lipid composition. Monodisperse vesicles were prepared with the extrusion technique. Diffusion measurements were used to determine the fraction of free and lipid-bound Recoverin using the strongly different diffusion

coefficients of both fractions. The presence of lipid enlarged the calcium affinity of Recoverin. Binding to DOPC vesicles (20 mg/ml) was half-maximal at 0.84 ± 0.2 µM free calcium compared to the found calcium binding constant of 4 [1.3 - 12] µM without lipid. At low calcium concentration a fraction of approximately 0.12 Recoverin was bound to vesicles increasing to 0.7 at high calcium concentration. In contrast to the expected lower fraction of bound Recoverin and a higher binding constant with decreasing lipid concentration, half-maximal binding at 1.6 ± 0.2 µM free calcium to 10 mg/ml DOPC and 0.9 ± 0.1 µM free calcium to 5 mg/ml DOPC was found. The fraction of bound Recoverin increased from 0.07 - 0.09 at low calcium concentration to 0.85 at high calcium concentration. Inhomogeneity of the vesicle suspension causing data noising might be the reason for these unexpected findings. The Recoverin mutant E85Q, binding only one Ca^{2+} with high affinity, showed half-maximal binding to DOPC vesicles (20 mg/ml) at 0.5 ± 0.1 µM free calcium. For membrane binding of the mutant E121Q (no high affinity calcium binding) a K_D value of 40 ± 3.5 µM free calcium was determined. Although it was expected to find a higher, compared to pure DOPC, affinity of Recoverin to an artificial ROS lipid mixture (40% DOPC, 38% DOPE, 15% DOPS, and 7% cholesterol), the determined binding constant was higher, namely K_D = 2.0 ± 0.5 µM free calcium.

Data analysis had one sore spot: the assumption, that the fluorescence brightness of the fluorescent label free in solution and close to the membrane is the same, is most probably untrue. To account for the fluorescence brightness difference of the dye label, a new three-photon correlation analysis was developed and tested.

4 Materials and Methods

4.1 Glass

Borosilicate cover slides were purchased from Menzel GmbH & Co KG, Braunschweig, Germany. Measurement chambers Lab-Tek II with a cover slide at their base were purchased from Nalge Nunc International Corp., Naperville, IL, USA.

4.1.1 Cleaning with Piranha-etch

Piranha-etch is a mixture of aqueous hydrogenperoxide solution (30%) and concentrated sulfuric acid with a volume ratio of roughly 1:2. It is also named Caro's acid. Hydrogenperoxide and sulfuric acid form peroxomonosulfuric acid and water. Piranha-etch oxidizes organic materials to carbon and further to carbondioxide. Peroxomonosulfuric acid is instable, so Piranha-etch has to be prepared freshly before use.

Some coverslides for cleaning were placed in a glass beaker and doused with hydrogenperoxide solution (30%, KMF Laborchemie Handels-GmbH, Lohmar, Germany) and sulfuric acid (96%, Fluka, Sigma-Aldrich Laborchemiekalien GmbH, Seelze, Germany) in a volume ratio of 1:2. The solution cools down during 15 - 20 min. The cover slides were taken from the beaker and washed intensively with distilled water. They were dried in a stream of nitrogen shortly before use.

It should be possible to wet the cover slides completely with water otherwise the cleaning procedure should be repeated. One can store the cover slides covered with water for a couple of hours.

4.1.2 Blocking glass for unspecific binding of proteins by Bovine Serum Albumin

Almost every kind of protein sticks to glass surfaces. This matters when proteins are used in low concentrations for FCS measurements. Then the sample concentration decreases and background from the surface increases because of the fluorescence tags of the sample protein. To prevent adsorption of the sample protein to the glass cover slide the surface is blocked with a non-expensive and non-fluorescent protein (e.g. Bovine Serum Albumin) before getting in contact with the sample protein.

The cover slides were blocked over night in a aqueous solution of 3% Bovine Serum Albumin (BSA, Fraction V, Sigma-Aldrich Chemie GmbH, Steinheim, Germany) at room temperature. 0.1% sodium azide (AppliChem GmbH, Darmstadt, Germany) is added to the BSA solution to prevent growth of microorganisms. The cover slides were rinsed with distilled water before use.

4.2 Lipids

For this study unsaturated synthetic phospholipids, extracts of natural phospholipids and cholesterol were used to mimic the composition of the bovine photoreceptor membranes. Lipids were stored at -20 °C under a nitrogen atmosphere ether as lyophilized powder or dissolved in chloroform. Chloroform solutions of lipids were handled in glassware only and any seal in a tube cap or other polymer parts having contact with the chloroform solution were made of PTFE.

1,2-Dioleyl-sn-glycero-phosphocholine (DOPC) and 1,2-dioleyl-sn-glycero-phosphoserine (DOPS) were purchased from Avanti Polar Lipids (Alabaster, AL, USA). 1,2-Dioleyl-sn-glycero-phosphoethanolamine (DOPE) was purchased from Sigma-Aldrich Chemie GmbH (Steinheim, Germany). Cholesterol and L-α-Lecithin from soybean were bought at Sigma Chemical Company (St. Louis, MO, USA).

Artificial rod outer segment (ROS) lipid mixture was composed of 40% DOPC, 38% DOPE, 15% DOPS and 7% cholesterol corresponding to the lipid composition in bovine ROS membranes (Anderson and Maude, 1970).

Oregon Green® 488 1,2-dihexadecanoyl-sn-glycero-3-phospoethanol-amine (DHPE) a less photostable dye linked to a phospholipid for FRAP experiments in supported bilayers was purchased from Invitrogen GmbH (Karlsruhe, Germany).

4.3 Small vesicles

Phospholipids and cholesterol were dissolved in chloroform. Labeled lipids were dissolved in methanol. Mixtures of fluorescently labeled and unlabeled lipids were prepared with a labeling ratio of 1:400,000 for FCS measurements. After evaporating the solvent with a stream of nitrogen and the formation of a thin lipid film at the tube wall, the sample was kept in vacuum for additional 45 min to remove remaining solvent. The lipids were hydrated with bidistilled water or buffer solutions depending on the experiment needs. After addition of the hydrating medium, vortexing for five minutes formed a lipid suspension. The temperature during hydration (usually room temperature) was kept above the gel/liquid-crystal phase transition temperature of the used lipids. The resulting suspensions of large multilamellar vesicles (LMVs) were sized down either by sonification or extrusion to form suspensions of small unilamellar vesicles (SUVs).

4.3.1 Preparation by sonification

Two different sonicators were used to prepare small vesicles from the lipid suspensions, a small bath sonicator (Sonifier B-12, Branson, Danbury, CT, USA), and a tip-sonicator (Sonifier Cell Disrupter B12, Branson, Danbury, CT, USA). It is not suitable to use glassware in the bath sonicator because the ultrasound cannot pass glass properly, therefore the sample was transferred to a

polymer tube for sonification in the bath sonicator. During sonification the solution was cooled with an ice-bath to prevent degradation of the lipids. Nevertheless, the temperature had to be kept above the gel/liquid-crystal phase transition temperature of the lipids. The tip-sonicator delivered a higher energy to the sample and was also more appropriate for use with bigger amounts of lipid suspensions but had the drawback of releasing small metal particles from the tip which had to be removed by centrifugation. Sonification to clarity which usually took 15 min in the bath sonicator and 5 min with the tip sonicator, yielded solutions of small unilamellar but polydisperse vesicles with a diameter between 80 nm and 100 nm. Vesicle size was determined by dynamic light scattering (DynaPro-E-20-660, Proterion Corp. Ltd., High Wycombe, England).

4.3.2 Preparation via extrusion

Extrusion of lipid suspensions is a powerful method to prepare monodisperse SUVs from almost all kinds of lipids. LMVs produced via hydration of the lipid film are downsized by shearing forces while pressing the suspension several times through a polycarbonate membrane with a well-defined pore size.

For preparation, a LiposoFast-Basic extruder purchased from Avestin Europe GmbH (Mannheim, Germany) was used. The polycarbonate membrane, which was also purchased from Avestin Europe GmbH, had a pore diameter of 100nm and was placed without any crease or kink between the two O-rings of the PTFE membrane support. The membrane sandwich was locked in the stainless-steel housing of the extruder. The plungers of the gas-tight syringes were wetted before inserting them into the syringe barrel to make the syringe moving smoothly and to increase the lifetime of the plunger. The syringes were connected to the membrane support unit, and the whole system was washed three times with 500 µl buffer, before one syringe was filled with the LMV suspension. The suspension was pressed by hand for at least 20 times from one syringe to another across the membrane until the suspension became transparent. The suspension was removed from the originally empty syringe to avoid having any larger unextruded vesicles in the resulting SUV suspension.

It is not recommended to use any fluorescently labeled lipids or dyes in the extruder, because it is impossible to clean the PTFE parts of the extruder properly.

4.4 Building a supported bilayer

Phospholipid vesicles fuse spontaneously to form supported bilayers (Brian and McConnell, 1984) on glass surfaces that have been cleaned carefully in an argon plasma or with Piranha-etch.

Borosilicate glass cover slides were cleaned with freshly prepared Piranha-etch, washed extensively with water, and stored under water until use. Cleaning the glass slide with Piranha-etch has to be done not more than two hours

before forming the membrane, otherwise the properties of the glass surface such as protonation or oxidation resulting from the Piranha-etch change in a way that prevents vesicle fusion. The glass slide was dried in a stream of nitrogen, and the vesicle suspension was deposited (500 µM) on the glass slide. The sample was incubated for at least 3 min at room temperature to allow the vesicles to adsorb at the glass surface and to form a supported bilayer via fusion. The resulting bilayer was intensely but carefully rinsed to remove redundant vesicles. It is not recommended to expose the resulting bilayer to air. The formation of a continuous supported bilayer under these conditions was verified by fluorescence microscopy imaging and FRAP measurements.

4.5 Giant unilamellar vesicles (GUVs)

Giant unilamellar vesicles were prepared using the electroformation method introduced by Angelova and Dimitrov in 1986.

A chloroform solution of fluorescently labeled and unlabeled lipids (labeling ratio 1:400,000 for FCS measurements) with a concentration of 1 mg/ml was prepared. The solution contained also 0.1mol% biotinylated lipids (DOPE-Biotin, Avanti Polar Lipids, Alabaster, AL, USA) for immobilization of the GUVs later on. 15 µl of this solution were distributed evenly on one ITO-coated glass slide (22 x 22 mm, 15 - 30 Ω/cm, SPI Supplies, West Chester, PA, USA) by sliding a glass capillary flat over the surface during solvent evaporation. The lipid-coated ITO-slide was kept in vacuum for additional 45 min to remove remaining solvent. 5 µg/cm² lipid corresponding to 25 lipid bilayers remained on the glass slide. A second ITO-coated glass slide was incubated with a neutravidin (Pierce Biotechnology Inc., Rockford, IL, USA; 0.1mg/ml) solution for 15 minutes to build a self-assembled protein layer (Bohlinger *et al*., 2004).

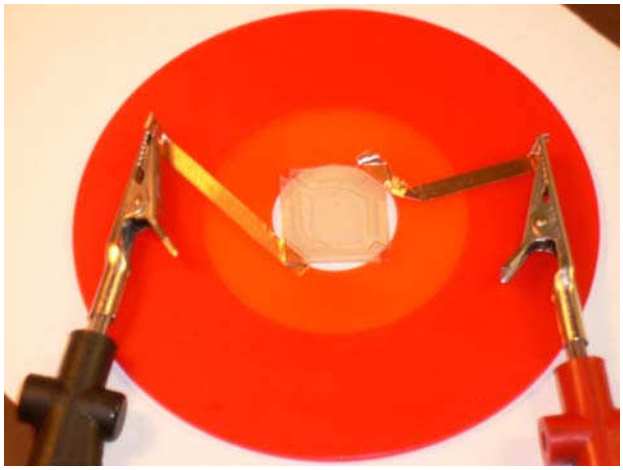

Fig. 4.1 The GUV electroformation cell: two ITO-coated cover slides contacted with self-adhesive copper foil and a silicone seal in-between. The copper foil is also used to fix the position of the cell on the red polymer microscope holder

The electroformation cell was assembled by placing a tailored 1 mm thick soft silicone seal (versilic, Saint-Gobain Performance Plastics Verneret, Charny, France) between the two cover slides. Dry silicone sticks easily to glass, so it is not necessary to press the fragile cover slides firmly together for sealing. Two small channels were left open for filling the chamber with glucose solution (247 mM). It is impossible to use ion containing solution for electroformation under these

conditions. Even the presence of only 0.01% of sodium azid, usually used to avoid the growth of micro organisms in the glucose solution, prevents the building of GUVs. The glass slides were contacted with self-adhesive copper foil coated with an electrically conducting paste (Laird Technologies, Rosenheim, Germany) and connected to a pulse generator (Exact Electronics Inc., model 5043, Hillsboro, OR, USA). An oscillating electric voltage with an amplitude of 1.5 V and 15 Hz was applied for at least two hours. The temperature during formation of the vesicles was kept above the gel-liquid crystal phase transition temperature of the lipids.

After formation, there was a dense layer of GUVs sliding and rolling over the surface and bumping into each other so that it was necessary to separate and immobilize the vesicles to avoid their motion, e.g. out of the FCS focus during measurements. Therefore, the glucose solution in the formation cell was exchanged by an isotonic sucrose solution (238 mM). This sucrose solution had a higher density compared to the glucose solution inside the vesicles. As a result, the vesicles floated towards the upper neutravidin coated glass slide. There they were immobilized by binding of the biotinylated lipids to neutravidin. For FCS measurements on the immobilized vesicles, the electroformation chamber was turned headfirst.

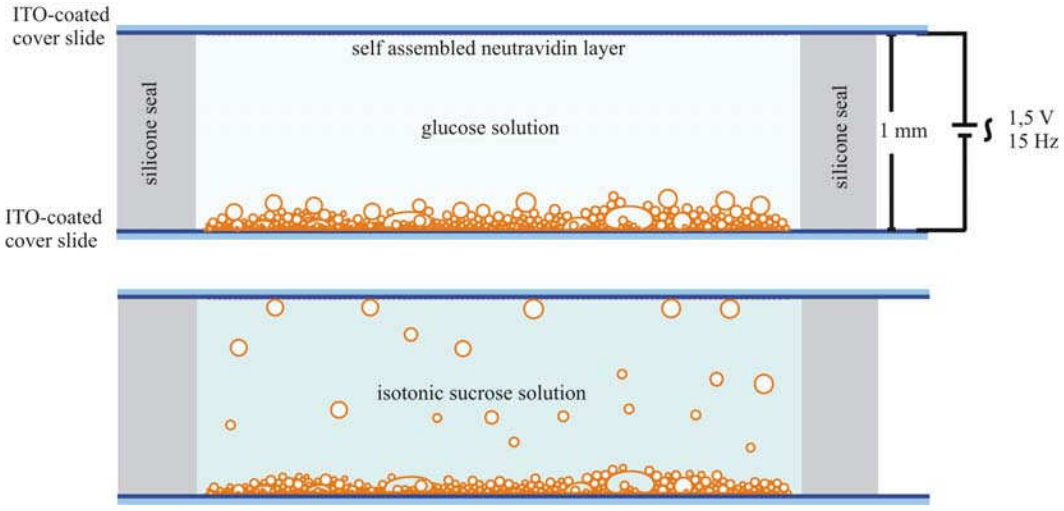

Fig. 4.2 Schematic of the immobilization procedure of GUVs. During the electroformation process GUVs grew on the lower ITO-coated cover slide. GUVs were filled with glucose solution. After electroformation the glucose solution was exchanged for an isotonic sucrose solution with higher density than the glucose solution inside the vesicles. The vesicles ascended like helium filled balloons towards the upper ITO-coated cover slide and were immobilized there by binding of the biotinylated lipids to neutravidin.

After immobilization, the GUVs can be immersed in any buffer that is isotonic to the inside glucose solution. It is, of course, also possible to form GUVs in sucrose solution and exchange the outer medium by any isotonic solution with lower density to allow the GUVs to settle down on a neutravidin coated cover slide for immobilization. Proteins and fluorescent dye molecules cannot pass the GUV membrane.

Sometimes it is a problem to detach the GUVs from the ITO-coated glass slide. Exchanging the outer solution with an ionic solution helps to detach the GUVs. A possible reason for this observation is the small osmotic stress one produces when exchanging the solution. Also, ion-lipid interactions reduce intrinsic lipid-lipid interactions and also lipid interactions with the ITO-coated glass slide.

4.6 Recoverin and its mutants

Recombinant wild-type bovine Recoverin and the Recoverin mutants Rec^{E85Q} and Rec^{E121Q} with non-functional EF-hands 2 or 3 as well as the non-myristoylated wild-type Recoverin were a kindly provided by K. Koch and K. Komolov (University of Oldenburg, Germany)

Mutagenesis of Recoverin was described by Alekseev *et al.*(1998). Bovine wild-type Recoverin and Recoverin mutants Rec^{E85Q} and Rec^{E121Q} were heterologously expressed in *E. coli* and purified by column chromatography as described by Senin *et al.* (2002) and Senin *et al.* (2003). Myristoylated forms were obtained by co-expression of the plasmid pBB-131 containing the N-myristoyltransferase 1 (NMT1) from *Saccharomyces cerevisae* (kindly provided by J.I. Gordon, Washington University School of Medicine, St. Louis, USA) as described also previously by Senin *et al.* (2002) and Senin *et al.* (2003). The degree of myristoylation was determined by reversed-phase high performance liquid chromatography (HPLC) analysis as described by Hwang and Koch (2002) using a Vydac 238TP C18 reverse-phase column (4.6 x 250 mm²) or a Phenomenex Luna reverse-phase column (5 µm;18; 4.6 x 250 mm²).

4.7 Labeling with fluorescent dyes

Samples for 2fFCS have to be fluorescent. Proteins are built from twenty different amino acids and only three of them, the aromatic amino acids tryptophan, tyrosine and phenylalanine, show fluorescence emission in the UV. But these amino acids are neither sufficiently bright nor photostable as being suitable for 2fFCS experiments. Thus, one has to label proteins with fluorescent dyes for 2fFCS measurements. This is usually done in a site-specific manner by labeling cysteine residues with maleimid-functionalized dyes, or in a less specific manner labeling lysine residues with succinimid ester-functionalized dyes. The labeling at cysteine residues is more specific than at lysines because proteins usually contain only very few cysteines in their amino acid sequence. To label a protein with an organic fluorescent dye is a much smaller intervention than e.g. generating GFP-fusion-proteins, or labeling with fluorescent quantum dots. Nevertheless, one should keep in mind that labeling is an intervention like the mutation of a protein and might influence its properties. Thus, how to label and where to label a certain protein is a very important question, and control experiments for checking the properties of the protein are important and necessary. Furthermore, one should keep in mind that one detects the fluorescence

emission of the dye linked to the protein in whatever environment. A changing environment of the fluorescent dye may change its fluorescence properties which might influence the outcome of an 2fFCS experiment. This is especially important when performing measurements in complex systems or living cells, where one does not know all possible interactions between proteins, fluorescent dye and other biomolecules.

4.7.1 Fluorescent Dyes

Recoverin and its mutants were labeled with maleimid conjugates of Alexa647 (Invitrogen GmbH, Karlsruhe, Germany) and Tetramethylrhodamine (TMR; Sigma-Aldrich Chemie GmbH, Steinheim, Germany) whereas DOPE was labeled with N-succinimidyl esters (NHS esters) of Atto655 (Atto-Tec GmbH, Siegen, Germany) or TMR (Sigma-Aldrich Chemie GmbH, Steinheim, Germany).

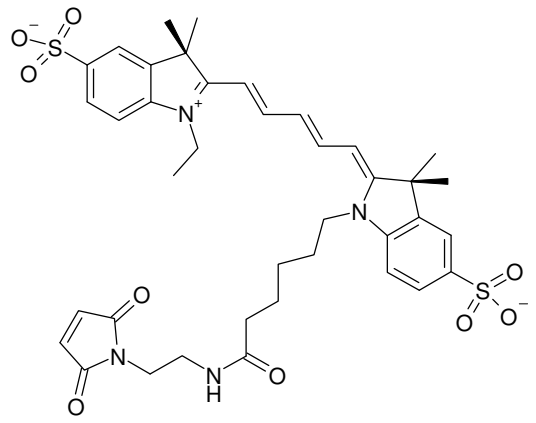

Fig. 4.3 Molecular structure of Cy5 maleimid. Cy5 is a cyanine dye like Alexa647

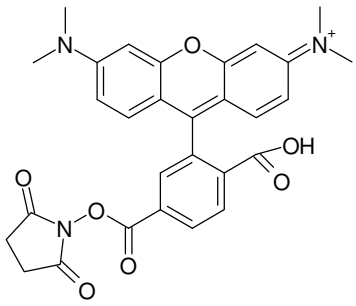

Fig. 4.4 Molecular structure of 6-carboxy-TMR NHS ester. This dye was used for labelling DOPE

The exact structure of Alexa647 is not available due to intellectual property reasons. Alexa647 is a cyanine dye similar to Cy5 and shows a very similar spectrum. Alexa647 has its absorption maximum at 650 nm and shows an emission peak at 668 nm. The molecular weight of Alexa 647 is approximately 1250 g/mol, it has a fluorescence lifetime of 1 ns and a quantum yield of 0.33.

Like all cyanine dyes, Alexa647 exhibits cis-trans photoisomerization in the polymethine bridge (Widengren and Schwille 2000; Heilemann *et al*. 2005). This shows up as fast exponential decay terms in the measured fluorescence correlation functions.

Tetramethylrhodamine-5-maleimid (TMR-maleimid) has a molecular weight of 481.5 g/mol, a quantum yield of ~0.50 in water which might decrease after protein conjugation. TMR has a fluorescence lifetime of ~2.3 ns.

The molecular structure of Atto655 is also not available. It is known that Atto655 is an oxazine derivative similar to the dye MR121 (Neuweiler et. al., 2002).

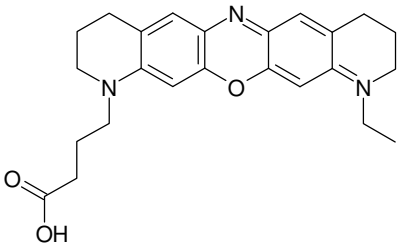

Fig. 4.5 Molecular structure of MR121 free acid. MR121 is an oxazine derivative like Atto655

Atto655 has the rare property not to show any triplet state photophysics. A second special property is its ability to form stacks with the amino acid tryptophan. The fluorescence of the dye in such a stack is quenched due to photoinduced electron transfer. This may cause some difficulties when using Atto655 for protein labeling. However, it can also be used to detect conformational changes in proteins that are accompanied with changes of the distance between Atto655 and a tryptophan residue.

4.7.2 Labeling Recoverin and its mutants with Alexa647maleimid or TMRmaleimid

Wild type Recoverin contains a single cystein in the first EF-Hand at position 39 in the amino acid sequence. This cystein was used to specifically label Recoverin with maleimide-functionalized fluorescent dyes. Maleimids react with thiol groups to form stable thio-ether bonds. This reaction requires a pH around 7.0 - 7.5. At this pH-value, the thiol groups are sufficiently nucleophilic, and protein amino groups are not reactive to maleimids due to their high protonation degree. It is not recommended to use Atto655-maleimid to label Recoverin because the tryptophan residue at position 31 in the amino acid sequence quenches its fluorescence.

1 mg Alexa647-maleimide or 1 mg TMR-maleimide was solved in 200 µl anhydrous DMSO and stored at -20°C up to one year. 2ml of a 1.25 - 2µM Recoverin (2.5 - 4nmol) solution in 100mM KCl and 30mM Hepes at pH 7.2 were prepared, and a 1.5 - 3 fold molar excess of reactive dye was added. The solutions were mixed thoroughly and incubated for at least three hours at room temperature. A higher molar excess of dye to accelerate the reaction or shift the reaction equilibrium towards the labeled protein is not recommended because it is difficult to remove remaining free dye after labeling. Free dye and labeled protein were separated via gel filtration. A PD-10 sephadex column (GE Healthcare Bio-Sciences AB, Uppsala, Sweden) was equilibrated with 25ml of 100mM KCL and 30mM Hepes at pH 7.2. The sample was added and eluted with the same buffer. In case of TMR used for labeling, the excluded fractions containing the protein were well separated from the slower moving dye-containing fractions. Alexa647 is more than twice as big as TMR and moves quite fast on the column. In that case, the last protein containing fraction contains also free dye, so one has to repeat gel filtration with this fraction.

It is not recommended to freeze solutions of labeled Recoverin because it tends to aggregate after thawing.

4.7.3 Labeling DOPE with Atto655-NHS-ester or TMR-NHS-ester

DOPE was purchased from Sigma Chemical Company (St. Louis, MO, USA). Atto655-NHS-ester was purchased from Atto-Tec GmbH (Siegen, Germany). TMR-NHS-ester was bought from Sigma-Aldrich Chemie GmbH (Steinheim, Germany).

1.14 µmol DOPE, 1.14 µmol triethylamine, and 1.6 µmol Atto655-NHS-ester or 1.6 µmol TMR-NHS-ester were dissolved in 60 µl anhydrous methanol and incubated for 90 min at room temperature. Reaction progress was followed by thin layer chromatography using silica gel 60-F_{254} plates (Merck, Darmstadt, Germany). The plates were developed with a 60:25:4 (v/v) mixture of chloroform:methanol:water.

Atto655-DOPE or TMR-DOPE was purified by chromatography on a silica gel column (eluent: chloroform:methanol:water 60:25:4 (v/v)). The presence of Atto655-DOPE or TMR-DOPE in each fraction was monitored by thin layer chromatography. The solvent was removed and Atto655-DOPE or TMR-DOPE was solved in anhydrous methanol and stored at -20°C in a nitrogen atmosphere until use.

4.7.4 SDS polyacrylamide gel electrophoresis (SDS-PAGE)

The labeling ratio of Recoverin with Alexa647-maleimid was analyzed by denaturing, discontinuous SDS polyacrylamide gel electrophoresis described by U.K. Laemmli (1970).

Introduction of Alexa647 to Recoverin increased the molecular mass by 1.3 kDa and therefore decreased the electrophoretic mobility.

A 10% separating gel with a 5.1% collecting gel on top was poured between two glass slides. One microgramm of labeled and unlabeled Recoverin was added together with a mixture of protein standards to the gel and analyzed by electrophoresis (15 mA inside the collecting gel and 20 mA inside the separating gel; electrophoresis chamber: Minigel Twin G42, Biometra; power supply: EPS 500/400, Pharmacia).

The gel was colored for one hour in 0.2% Coomassie solution, excess stain was washed out with destaining solution. The destained gel was scanned with the Image Station 440 CF (Kodak Digital Science).

Table4.1 Composition of acrylamide gels

	separating gel	collecting gel
	10% acrylamide	5,1% acrylamide
1.5 M Tris / HCl pH 8,8	1,5 ml	-
0.5 M Tris / HCl pH 6,8	-	0.5 ml
10% SDS (w/v)	60 µl	20 µl
30% Acrylamide	2 ml	0.34 ml
10% Ammonium peroxydisulfate (w/v)	40 µl	40 µl
Tetramethylethylendiamine (TEMED)	3 µl	2 µl
ddH_2O	2.4 ml	1.1 ml

sample buffer:	50 mM Tris/HCl pH 7,2	
	12.5 % glycerol (v/v)	
	1 % β-mercaptoethanol (w/v)	
	1.6 % SDS (w/v)	
	0.13 % bromophenol blue (w/v)	
protein standards:	Low Molecular Weight Calibration Kit	
	(LMW; Amersham)	
	Phosphorylase b	94 kDa
	Bovine Serum Albumin	67 kDa
	Ovalbumin	43 kDa
	Carboanhydrase	30 kDa
	Trypsin-Inhibitor	20.1 kDa
	α-Lactalbumin	14.4 kDa
electrophoresis buffer:	25 mM Tris	
	192 mM glycine	
	0.1 % SDS (w/v)	
Coomassie dying solution:	25 % ethanol	
	5 % acetic acid	
	0.2 % Coomassie-Brilliant Blue R250 (Serva Blue R)	
destaining solution:	25 % ethanol	
	5 % acetic acid	

4.8 Calcium buffer

4.8.1 Buffer preparation

The calcium chelator ethylene glycol bis(2-aminoethyl)ether N,N,N',N'-tetraacetic acid (EGTA) was used to prepare a set of buffers with free calcium concentrations in the nanomolar range. EGTA shows a more than 10^5 fold selectivity of Ca^{2+} compared to Mg^{2+}. The dissociation constant of a chelator varies with ionic strength, temperature and, in particular for EGTA, with pH. Thus, the straightforward approach of mixing concentrated solutions of EGTA

and $CaCl_2$ is not advisable. The reaction of EGTA with Ca^{2+} releases two protons, leading to an acidification of the solution. Furthermore, small errors in the titer of Ca^{2+} or EGTA cause large errors in the final free Ca^{2+} concentration, especially when the amount of $CaCl_2$ approaches that of EGTA. Therefore, the calcium buffers were prepared using a different method described by Tsien and Pozzan (1989). This pH-metric approach uses the acidification of the EGTA solution after addition of calcium as long as EGTA is in excess over calcium to make a concentrated solution of the calcium-EGTA complex. In this solution the concentrations of calcium and EGTA are verified to be within 0.5% of each other.

For 10 ml of 1 M K_2CaEGTA stock solution, 3.84 g EGTA free acid (1% over the theoretical weight of 10 mmol to consider the typical purity of 99%) and 19 mmol KOH (1.2 g of 85% pellets) were mixed in 6 ml water. Afterwards, 0.95 g (9.5 mmol) $CaCO_3$ was added in small portions. The mixture was slowly heated to 90 – 100°C until CO_2 evolution ceases, and the solution was allowed to cool down to room temperature. 10 µl aliquots of concentrated aqueous KOH solution were added to reach a pH of 7 – 8 and to dissolve all the solids. 1 M $CaCl_2$ solution was added in aliquots of 10 µl, and the pH was measured. The pH was restored with KOH solution to 7 – 8 when it dropped below 6.5. $CaCl_2$ addition was stopped when $\Delta pH / \Delta Ca$ sank below one-half of its initial value. The mixture was transferred to a volumetric flask and filled with water to 10 ml.

By cross-diluting the 1 M K_2CaEGTA and a 1 M K_2H_2EGTA solution at different ratios solutions with any desired free calcium concentrations (in between zero free Ca^{2+} and 40 µM free Ca^{2+}) were obtained.

EGTA was used to buffer the free calcium concentration in the nanomolar range. Due to its low K_D, buffering with EGTA is not feasible in the micromolar range. Thus, nitrilotriacetic acid (NTA) with a higher K_D for Ca^{2+} was used to adjust the free calcium concentration in the micromolar range.

The viscosity of the calcium buffers was measured to be 1.8% higher than the viscosity of water at 20° C, as determined with an Ostwald micro-viscosimeter (Schott-Geräte GmbH, Hofheim am Taunus, Germany). The viscosity of all calcium buffers was checked also by measuring the diffusion coefficient of Atto655.

All calcium buffers (except the stock solutions) contained besides different amounts of EGTA and CaEGTA or NTA and $CaCl_2$ 100 mM KCl and 30 mM Hepes/KOH pH 7.2. For measurements with lipid vesicles, calcium buffers with a higher buffer capacity were used. These buffers contained 30 mM of calcium chelator instead of 10 mM as used for measurements without lipids.

4.8.2 Measuring the concentration of free calcium with Fura-2 and bis-Fura

The calcium chelating fluorescent dyes fura-2 and bis-fura (both from invitrogen GmbH, Karlsruhe, Germany) can be used for ratiometric measurements: The ratio of the fluorescence emission when excited at 340 nm and

at 380 nm changes with calcium concentration but is independent on dye concentration or photobleaching. Fura-2 and bis-fura exhibit also sufficiently high fluorescence intensity to permit measurements at dye concentrations that are unlikely to cause Ca^{2+}-buffering.

The custom-made EGTA-calcium buffers had the same composition as a set of calibration buffers purchased from Invitrogen GmbH (Karlsruhe, Germany). Therefore, the response of these buffers was directly comparable to the custom-made buffers. The "calcium calibration kit with magnesium #2" was used to record a calibration curve. The response of the custom-made buffers was checked under identical conditions, and the calcium concentration was estimated using the recorded calibration curve.

Due to the low K_D of fura-2 or bis-fura, checking the calcium concentration of the NTA buffers was impossible with these dyes.

4.8.3 Measuring the free calcium concentration with a calcium sensitive electrode

To check the concentration of both sets of custom-made calcium buffers, a calcium-sensitive electrode (World Precision Instruments, Inc., Sarasota, FL, USA) was used together with a reference electrode also purchased from World Precision Instruments. The electrode was calibrated with the calibration buffers of Invitrogen GmbH that were used for the fura-2 and bis-fura measurements, providing EGTA-calcium buffers in the range of zero to 39 µM free calcium, and with a second set of calibration buffers providing 1 µM to 1 mM free calcium. With these two sets of calibration buffers, the full range of the free calcium concentrations of the custom-made buffers was covered. The response of the custom-made buffers was measured under identical conditions, and the free calcium concentration was estimated using the recorded calibration curve.

4.9 Tryptophan fluorescence measurements

Measurements were performed with a commercial fluorescence spectrometer (QM-4, Photon Technology International, NJ, USA) operating in right angle configuration and equipped with a xenon-arc lamp as excitation source, two monochromators in the excitation and emission pathway, and a photomultiplier for detection.

Excitation was done at 280 nm and fluorescence emission was collected between 300 nm and 450 nm in steps of 1 nm. Background spectra of calcium buffers were subtracted. Concentrations of Recoverin and its mutant Rec^{E85Q} were 2 µM. Concentration of DOPC was 20 mg/ml.

4.10 Extraction of ROS-lipids

4.10.1 Preparation of retinae

The sclerae of freshly excised bovine eyes were sliced around the cornea and the vitreous body and lens were removed by reverting the eyeground. The retinae were stripped carefully from the pigmented epithelium. In doing so, the visual nerve was cut in two. The retinae were suspended in 1 ml per retina dense sucrose buffer (1.5 M sucrose; 115 mM NaCl; 2.5 mM KCl; 1 mM $MgCl_2$; 10 mM Hepes/KOH pH 7.4; 1 mM DTT), quick-frozen in liquid nitrogen and stored at -80° C.

4.10.2 Preparation of rod outer segments (ROS)

About 200 retinae were suspended in 200 ml dense sucrose buffer (1.5 M sucrose; 115 mM NaCl; 2.5 mM KCl; 1 mM $MgCl_2$; 10 mM Hepes/KOH pH 7.4; 1 mM DTT) and shaken vigorously to shear off the ROS. The suspension was centrifuged for 7 min with 3500 g at 4° C to sediment the retinae but not the ROS. The supernatant was passed through a gauze net in a 500 ml graduated cylinder and diluted with the same volume of sucrose-free buffer (115 mM NaCl; 2.5 mM KCl; 1 mM $MgCl_2$; 10 mM Hepes/KOH pH 7.4; 1 mM DTT). After mixing carefully, the suspension was centrifuged for 10 min with 4700 g at 4° C. The lower medium density now allowed for ROS sedimentation. The supernatant was transferred to new centrifuge tubes and again centrifuged. All pellets were suspended in 36 ml lightweight sucrose buffer (800 mM sucrose; 115 mM NaCl; 2.5 mM KCl; 1 mM $MgCl_2$; 10 mM Hepes/KOH pH 7.4; 1 mM DTT). For further ROS purification a continuous gradient of light to dense sucrose buffer was covered with ROS suspension and centrifuged for 90 min with 70,000 g at 4° C. The red rhodopsin-containing layer was collected and diluted with the same volume sucrose free buffer (115 mM NaCl; 2.5 mM KCl; 1 mM $MgCl_2$; 10 mM Hepes/KOH pH 7.4; 1 mM DTT) and centrifuged for 10 min at 12.400 g at 4° C to sediment and concentrate the purified ROS. The pellets were re-suspended in 25 ml of 10 mM Hepes/KOH pH 7.4; 1 mM DTT and 0.1 mM PMSF. The suspension was covered with argon, quick-frozen in liquid nitrogen, and stored at -80° C.

4.10.3 Extraction of lipids from ROS

Lipid extraction was done as described by Thomas R. Appel (IMB Jena e.V.). The protocol is based on the method described by Bligh and Dyer (1959). Firstly, “synthetic phases” which consist of pure solvents without sample were prepared. 2.5 ml chloroform, 2.5 ml methanol, 1 ml water and 1.25 ml 1 M aqueous KCl solution were mixed by vortexing, and the solution centrifuged in a glass tube (Schott, Duran, 16 x 100 mm, 12 ml, DIN 58970) for 2 min with 4000 g in a swing-out rotor (the glass tubes break in a rotor with a fixed angle) for phase separation. The resulting synthetic upper phase and synthetic lower phase were transferred to different glass flasks which were sealed tightly.

For extraction of ROS lipids, 1 ml ROS suspension was mixed with 1.25 ml chloroform and 2.5 ml methanol. The mixture was homogenized by vortexing. Then, 1.25 ml chloroform was added, and the solution mixed again. After adding 1.25 ml 1 M aqueous KCl solution and mixing, the suspension was centrifuged in glass tubes for 5 min with 4000 g for phase separation. The lower lipid-containing chloroform phase was transferred to a new glass flask. The remaining upper phase was mixed with 750 µl synthetic lower phase and centrifuged for 5 min with 4000 g for phase separation. The lower phase was combined with the lower phase of the first extraction. The washing step was repeated. To wash the combined lower phases, they were mixed with 2.5 ml synthetic upper phase and centrifuged to separate the phases again. The solvent of the washed lipid containing lower phase was evaporated with a stream of nitrogen and kept in vacuum for additional 45 min to remove remaining solvent. 12 - 13 mg crude lipid could be extracted from 1 ml ROS suspension.

Unfortunately, the lipid extract contained also retinal, the chromophor of rhodopsin. It was impossible to form GUVs with this extract. Removing the retinal by extraction with acetone failed, as well as preparative chromatography on a silica gel column.

4.11 Two-focus fluorescence correlation spectroscopy (2fFCS)

Diffusion due to Brownian motion is a fundamental molecular process. The parameter which describes the diffusion of a molecule in solution is its diffusion coefficient. Two-focus Fluorescence Correlation Spectroscopy (2fFCS) is a recently developed variant (Dertinger, 2007) of Fluorescence Correlation Spectroscopy (FCS), which occurred to be a powerful method to determine diffusion coefficients precisely and absolutely at picomolar concentrations. It offers a wide range of potential applications in the investigation of protein properties. Any change in the hydrodynamic radius of a protein due to a conformational change, as a result of ion binding, or interaction with a ligand or another biomolecule, directly alters the diffusion behavior of the protein. Thus, one can use the diffusion coefficient to monitor e.g. binding processes of proteins. For monitoring small changes in the hydrodynamic radius associated with most conformational changes in proteins, it is necessary to measure the diffusion coefficient with an error smaller than a few percent. Methods that achieve this accuracy are dynamic light scattering (Berne and Pecora, 2000), pulsed-field gradient NMR (Callaghan, 1991), analytical ultracentrifugation (Cole and Hansen, 1999) or size-exclusion electrophoresis (Harvey, 2000). All these methods operate, in contrast to single-molecule sensitive 2fFCS, at high sample concentration far away from the limit of infinite dilution. Often it is problematic to obtain a sufficiently large amount of biological material as necessary for these methods, and many proteins are prone to aggregation at high concentrations.

In what follows, I will briefly describe the possibilities and possible problems of FCS (for an extensive discussion see (Dertinger 2007)). What exactly

is FCS? It was invented more than 30 years ago (Magde *et al.*, 1972), but it took nearly two decades until the development of stable lasers with high beam quality, low noise single photon detectors, and high quality microscope objectives with high numerical aperture, before this technique became widely used (for a review see: Schwille, 2001; Rigler and Elson, 2001; Hess *et al.*, 2002; Widengren and Mets, 2002). The core idea of FCS is to analyze fluctuations of the fluorescence signal resulting from the entering and leaving of individual fluorescing molecules into or out of a certain small detection volume. The measurement system is characterized by this volume, which is defined by locations in the sample where efficient fluorescence excitation and detection takes place. When the concentration of fluorescent molecules in solution is sufficiently small so that only one or very few molecules are present within the detection volume at any time, the resulting measured fluorescence signal is strongly fluctuating due to the diffusion of molecules into and out of the detection volume. The detected fluorescence intensity is multiplied with a time-shifted replica of itself for different values of time shift (lag-time). The result is the autocorrelation function (ACF):

$$g(\tau) = \left\langle I(t)I(t+\tau)\right\rangle_t \qquad \textbf{Eq. 4.1}$$

$I(t)$ is the fluorescence intensity at time t and $I(t+\tau)$ is the intensity at time t + τ. The triangular brackets denote averaging over all time values t. The physical meaning of the autocorrelation function is that it is directly proportional to the probability to detect a photon at time τ when there was a photon detection event at time zero. This probability is composed of two basically different terms: The two photons detected at time zero and at time τ can originate from uncorrelated background or from different fluorescing molecules thus having no physical correlation (provided there is no interaction of the different fluorescing molecules). These events will contribute to a constant offset of $g(\tau)$ that is completely independent on τ (the probability to detect two physically uncorrelated photons is completely independent on the time distance between their detection). Alternatively, the two photons can originate from one and the same molecule and are then physically correlated. Suppose now a fluorescing molecule is close to the centre of the detection volume. There will be a high probability to detect a large number of consecutive fluorescence photons from this molecule (the fluorescence signal will be highly correlated in time) until the molecule, due to diffusion, starts to exit the detection volume. Then, the probability to see further fluorescence photons will decrease leading to a continual decrease of the correlation until the molecule will have left the detection volume altogether. The characteristic decay time of $g(\tau)$ with increasing lag time τ is proportional to the diffusion speed of the molecule – the larger the diffusion coefficient the faster the correlation decays. The time where the fluorescence decay is half-maximal is called the average diffusion time and the normalised amplitude of the ACF is proportional to the

reciprocal number of particles in the detection volume. Fig. 3.6 shows a typical AFC for a fluorescent dye in aqueous solution.

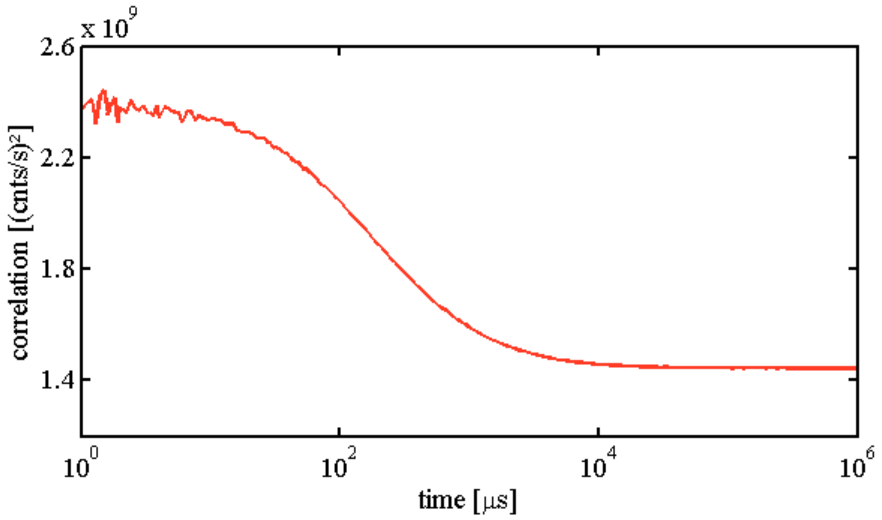

Fig. 4.3 A typical autocorrelation curve of the fluorescent dye Atto655 in aqueous solution. There is a prominent decay in the correlation on the millisecond time scale due to diffusion of the molecules out of the detection volume. The long-time constant offset is due to physically uncorrelated photon pairs from background light or from different fluorescent molecules.

For a quantitative evaluation of an FCS measurement, one has to know exactly the size and shape of the detection volume, which is described by the so-called molecule detection function (MDF) giving the probability to detect a fluorescence photon from a molecule at a given position in sample space. The MDF sensibly depends on manifold parameters of the optical setup, such as the peculiarities of laser focusing or fluorescence light collection, which are difficult or impossible to control exactly, making an exact, quantitative evaluation of FCS measurements rather difficult (Hess and Webb, 2002; Nagy *et al.*, 2005a; Perroud *et al.*, 2005). Furthermore, properties of the sample like refractive index or cover slide thickness, or laser beam astigmatism (Enderlein *et al.*, 2004; Enderlein *et al.*, 2005; Gregor and Enderlein, 2005) all influence the outcome of an FCS experiment. One of the most disturbing observations was the dependence of the MDF on excitation intensity due to optical saturation of fluorescence even at very low total excitation power (Berland and Shen, 2003; Nishimura and Kinjo, 2004; Gregor *et al.*, 2005; Nagy *et al.*, 2005b). All these potential error sources are linked to a fundamental problem of FCS – the absence of an intrinsic length scale in the measurement. The fluorescence correlation decay of the ACF depends on diffusion speed and the spatial extend and shape of the MDF, but the former is to be measured and the latter is not well known. 2fFCS is a robust modification of FCS that introduces an *external ruler* into the measurement by generating two identical overlapping foci and corresponding detection regions with a fixed sub-micron distance in such a way that the corresponding MDFs are sufficiently well described by a simple two parameter model. This allows for reproducible, quantitative and absolute measurements of diffusion coefficients.

4.11.1 2fFCS setup and measurement conditions

The 2fFCS setup was built and characterized by T. Dertinger (T. Dertinger, 2007). The 2fFCS setup is shown schematically in Fig. 3.7.
It is based on a conventional confocal epi-fluorescence microscope (IX 71, Olympus Europa, Hamburg, Germany). Briefly, excitation was done by two identical interleaved pulsed lasers (50 ps pulse duration, 40 MHz repetition rate, PDL 808 "Sepia", PicoQuant, Berlin, Germany) of the same wavelength (640 nm, LDH-P-635, PicoQuant, Berlin, Germany). The polarization of the lasers was linear and orthogonal to each other. The light was combined by a polarizing beam splitter (Narrow Band Polarizing Beamsplitter Cube 633, Ealing Catalogue, St. Aspah, UK) and coupled into a polarisation-maintaining single-mode optical fiber. At the output of the fiber, the light is again collimated resulting in a train of

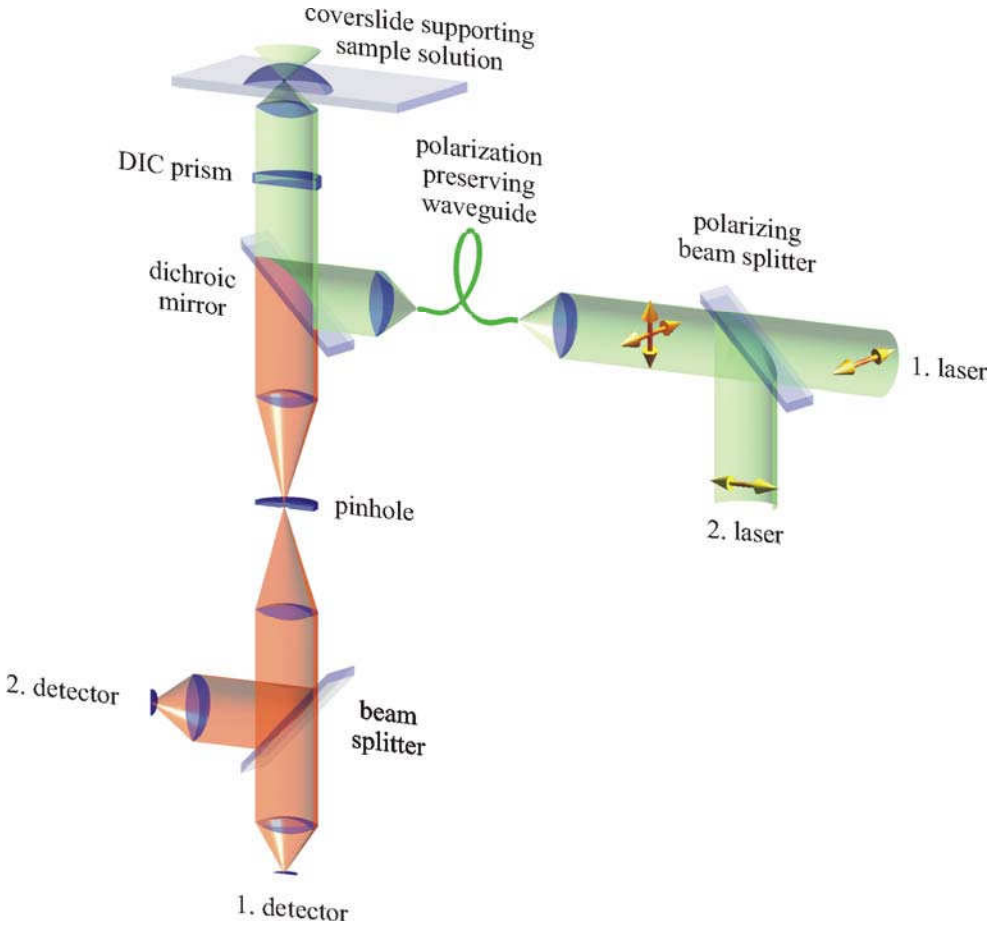

Fig. 4.4 Schematic of the 2fFCS setup. For description see text. Figure is taken from (Dertinger, 2007)

laser pulses with alternating orthogonal polarization. The beam is then reflected with a dichroic beam splitter (Q 660 LP, Chroma Technology, Rockingham, VT, USA), through a differential interference contrast (DIC) prism (U-DICTHC, Olympus Europa, Hamburg, Germany) also called Nomarski prism. The principal axes of the prism were aligned with the orthogonal polarizations of the laser pulses, so that the DIC prism deflects the pulses into two different directions

corresponding to their polarization. After passing the DIC prism, a microscope objective (UPLAPO 60x W, 1.2 N.A., Olympus Europa, Hamburg, Germany) focused the two beams into two laterally shifted and overlapping foci. The distance between the beams is uniquely defined by the chosen Nomarski prism and is independent on the sample's refractive index, cover slide thickness, or optical saturation, because all these effects introduce aberrations but will not change the distance (the external ruler of 2fFCS) between the focus centers. Fluorescence was collected by the same objective. The tube lens (175 mm focal length) focused the fluorescence light from both foci onto a single pinhole (200 µm) positioned symmetrically with respect to both focus positions. Subsequently, the fluorescence light was split by a 50/50 beam splitter (Linos Photonics GmbH & Co. KG, Göttingen, Germany) and detected by two single-photon avalanche diodes (SPADs) (SPCM-AQR-14, Perkin Elmer, Wellesley, MA, USA). A dedicated single-photon counting electronics (TimeHarp 200, PicoQuant, Berlin, Germany) was used to record the detected photons from both SPADs with picosecond temporal resolution. However, there is not yet any information on the spatial origin of the detected photons. However, the picosecond temporal resolution can now be used to decide which laser has excited which fluorescence photon. This is done by determining the detection time of each photon with respect to the time of the last preceding laser pulse (so-called time correlated photon counting or TCSPC). Knowing which photon was generated in which detection volume, the ACFs for each detection volume as well as the cross correlation function (CCF) between the two detection volumes can be calculated. The CCF is calculated in a similar way as the ACF but by cross-correlating photons from the two different detection volumes. The resulting CCF is directly proportional to the probability to detect a photon caused by the second laser at time τ when there was a photon detection event from the first laser at time zero or *vice versa*. If the distance between the foci is known, a global fitting of both ACFs and the CCF will yield an absolute value of the diffusion coefficient because the time delay of the CCF relative to the ACF scales with the square of the distance between the foci divided by the diffusion coefficient. Moreover, the relation between CCF to ACF amplitude will be a direct measure of the focus overlap. This poses a very restrictive and stabilizing fit-criterion (Dertinger, 2007).

During measurements of lipid diffusion in supported bilayers or GUV membranes, the objective was moved vertically with a piezo actuator (PIFOC, P-721-20, Physik Instrumente, Göttingen, Germany) for positioning the foci on the membrane.

4.11.2 Temperature control

The sample temperature was controlled using a custom-build copper sample holder that was kept at constant temperature by circulating water through channels within the holder. A brass ring which enclosed the objective was also

connected to this water flow to keep the objective at the same temperature as the sample. The water temperature was controlled with a thermostat (F12 + MB, JULABO Labortechnik GmbH, Seelbach, Germany). If not stated otherwise, sample temperature was kept at 25° C throughout all 2fFCS experiments.

4.12 Imaging setup

Excitation was done with either an argon ion gas laser (innova 70C, Coherent Inc., Santa Clara, CA, USA) or a dye laser (Radiant Dyes Laser & Accessories GmbH, Wermelskirchen, Germany). The light was coupled into a quartz multimode optical fiber and lead to a single-port epi-fluorescence condenser (TILL Photonics GmbH, Gräfelfing, Germany) at the back port of the inverted microscope (IX 71, Olympus America Inc., PA, USA). The light was reflected by a dichroic beam splitter into the objective (100 x, 1.3 NA, Olympus). Fluorescence was collected with the same objective and detected with an EM-CCD camera (iXon DV885, 1004x1002 pixel, 8 µm pixel size, Andor Technology, Belfast, Northern Ireland). Dichroic beam splitter and fluorescence filter were purchased from Omega Optical Inc. (Brattleboro, VT, USA).

5 Acknowledgement

The present work would have never come to this stage and would have even not been possible without the help and support of many people. I am glad to have done my PhD thesis in the INB-1 of the research centre Jülich. I enjoyed the interdisciplinary and international working atmosphere, it was really inspiring und prosperous. The well organized infrastructure of the centre was a huge support during my work.
Especially I would like to thank:

Jörg Enderlein
Jörg, thank you very much for the confidence you always had in me and my skills, for supporting me were ever possible, for answering patiently all my questions during long discussions, and sharing all your ideas, knowledge and experience with me. I really appreciate your way to guide me but also give me the freedom to find my way. Thank you for being a sympathetic teacher.

Ingo Gregor
Ingo, thank you very much for sharing all your knowledge and experience with me, for your great patience in helping me to answer all my questions and to solve all my problems in the lab, with my computer in general and especially with data analysis. I hope you did not always heave a sign when you heard “Ingo,…” in this very special tone.

Thomas Dertinger
Your infectious enthusiasm with which you were doing your work was always motivating for me. Thank you for the patience in explaining to me how to use this gorgeous two-focus setup and letting me measure with it running the risk that I might seriously misadjust it in the beginning. Thank you for sharing car with me although I was always late in the morning. I am sorry for the weird smells of the piranha-etch solution I used to clean the cover slides ☺

Jana Kriegsmann
Thank you for the right words in the really frustrating moments and for giving me the feeling not to be alone with all kinds of problems. I enjoyed discussing with you all the biophysical and lipid vesicle problems and of course all the gossip.

I also would like to thank the people spending like me a lot of time down in the cellar of the institute in the fluorescence labs: **Jan Sykora, Anastasiya Loman, Aleš Benda, Luru Dai and Luis Alvarez**. Thank you for your support, the motivating working atmosphere and all the short intermissive chats. I liked to work downstairs with you in the dark, seeing the sun only during lunch breaks.

Special thanks go to Anastasiya for having the right touch in adjusting the 2fFCS setup.

Daniel Portz
I would like to thank you Daniel for building every curious component guided by my unprofessional drawings and finding a solution for all problems.

Doris Höppner-Heitmann
Thank you for organizing the biochemical lab and assisting me with your huge experience in all problems and questions I had.

Anita Eckert
Thank you very much Anita for your great patience with these unorganized and undisciplined single molecule group and help with all administrative challenges.

Rudi Esser
Danke, für all die kleinen, wichtigen Dinge die Du tust. Wenn du Urlaub hattest war es immer ganz ungewöhnlich ruhig im Institut.

I also would like to thank **Prof. U. Benjamin Kaupp**, the institute's director, for giving me the opportunity to do this work in his institute.

Prof. Karl-Wilhelm Koch and **Konstantin Komolov** at the University of Oldenburg
Thank you for creating the Recoverin project together with Jörg and providing me with enough protein for all my experiments. I also appreciate the spontaneous and fruitful discussions via telephone and the short but very motivating visits in Oldenburg. Sorry, Kostya that Recoverin did not become the movie star it should during my PhD thesis.

Meinen Eltern **Irmgard und Fritz von der Hocht** und meiner Schwester **Eva**
Danke für Eure tatkräftige und finanzielle Unterstützung in jeder Hinsicht, die Möglichkeit zu studieren und am Forschungszentrum zu promovieren, danke, dass es immer was Leckeres zu essen gab, wenn ich nach Hause gekommen bin
Eva, ich finde es sehr schade, dass der Kaktus die Fahrten nach Jülich nicht verkraftet hat und Du jetzt mit Autos in langweiligen Farben fahren musst.

Thomas
Thank you for being there and awaiting me when I came home late from Jülich and just giving me a hug that made all troubles forget.

6 Abbreviations

ACF	autocorrelation function
BSA	bovine serum albumin
CCF	cross-correlation function
cGMP	guanosine 3',5'-cyclic monophosphate
DOPC	1,2-dioleoyl-sn-glycero-phosphocholine
DOPE	1,2-dioleoyl-sn-glycero-phosphoethanolamine
DOPS	1,2-dioleoyl-sn-glycero-phosphoserine
E85M	protein mutant of Recoverin were glutamic acid in position 85 of the amino acid sequence was exchanged for methionine
E121M	protein mutant of Recoverin were glutamic acid in position 121 of the amino acid sequence was exchanged for methionine
E85Q	protein mutant were glutamic acid in position 85 of the amino acid sequence was exchanged for glutamine
E121Q	protein mutant were glutamic acid in position 121 of the amino acid sequence was exchanged for glutamine
EGTA acid	ethylene glycol-bis(beta-aminoethyl ether)-N,N,N',N'-tetraacetic
FCS	fluorescence correlation spectroscopy
2fFCS	two focus fluorescence correlation spectroscopy
FRAP	fluorescence recovery after photobleaching
GUVs	giant unilamellar vesicles
Hepes	2-(4-(2-Hydroxyethyl)-1-piperazinyl)-ethanesulfonic acid
ITO	indium tin oxide
LUVs	large unilamellar vesicles
MDF	molecule detection function
NHS	N-hydroxysuccinimid
NMR	nuclear magnetic resonance
NTA	nitrilo triacetic acid
OS	outer segment of photoreceptors
PEG	poly (ethylene glycol)
PTFE	poly-tetra-fluor-ethylene or teflon®
RK	Rhodopsin Kinase

ROS	rod outer segment
SPB	supported lipid bilayer
SMVs	small multilamellar vesicles
SUVs	small unilamellar vesicles
TMR	tetramethylrhodamine
wt	wild type of a protein

Symbols for amino acids

A	Ala	alanine
B	Asx	asparagine or aspartic acid
C	Cys	cysteine
D	Asp	aspartic acid
E	Glu	glutamic acid
F	Phe	phenylalanine
G	Gly	glycine
H	His	histidine
I	Ile	isoleucine
K	Lys	lysine
L	Leu	leucine
M	Met	methionine
N	Asn	asparagine
P	Pro	proline
Q	Gln	glutamine
R	Arg	arginine
S	Ser	serine
T	Thr	threonine
V	Val	valine
W	Trp	tryptophan
Y	Tyr	tyrosine
Z	Glx	glutamine or glutamic acid

7 References

Alekseev,A.M., Shulga-Morskoy,S.V., Zinchenko,D.V., Shulga-Morskaya,S.A. Suchov,D.V., Vaganova,S.A., Senin,I.I., Zagarov,A.A., Lipkin,V.M., Akhtar,M. and Philippov,P.P. (1998) Obtaining and characterisation of EF-hand mutants of recoverin. *FEBS letters*, **440**, 116-118.

Ames,J.B., Tanaka,T., Stryer,L. and Ikura,M. (1994) Secondary Structure of Myristoylated Recoverin Determined by Three-Dimensional Heteronuclear NMR: Implications for the Calcium-Myristoyl Switch. *Biochemistry*, **33**, 10743-10753.

Ames,J.B., Porumb,T., Tanaka,T., Ikura,M. and Stryer,L. (1995) Amino-terminal Myristoylation Induces Cooperative Calcium Binding to Recoverin. *J. Biol. Chem.*, **270**, 4526-4533.

Ames,J.B., Ishima,R., Tanaka,T., Gordon,J.I., Stryer,L. and Ikura,M. (1997) Molecular mechanics of calcium-myristoyl switches. *Nature*, **389**, 198-202.

Ames,J.B., Hamasaki,N. and Molchanova,T. (2002) Structure and Calcium-Binding Studies of a Recoverin Mutant (E85Q) in an Allosteric Intermediate State. *Biochemistry*, **41**, 5776-5787.

Ames,J.B., Levay,K., Wingard,J.N., Lusin,J.D. and Slepak,V.Z. (2006) Structural Basis for Calcium-induced Inhibition of Rhodopsin Kinase by Recoverin. *J.Biol.Chem.*, **281**, 37237-37245.

Anderson,R.E. and Maude,M.B. (1970) Lipids of ocular tissues. 6. Phospholipids of rod outer segments. *Biochemistry*, **9** (18), 3624-3628.

Angelova,M.I. and Dimitrov,D.S. (1986) Liposome electroformation. *Faraday Discuss. Chem. Soc.*, **81**, 303-308.

Angelova,M.I. and Dimitrov,D.S. (1988) A mechanism of liposome electroformation. *Progr.Colloid&PolymerSci.*, **76**, 59-67.

Angelova,M.I., Soleau,S., Meleard,P., Faucon,J.F. and Bothorel,P. (1992) Preparation of giant vesicles by external AC electric fields. Kinetics and applications. *Progr.Colloid&PolymerSci.*, **89**, 127-131.

Baldwin,A.N. and Ames,J.B. (1998) Core Mutations That Promote the Calcium-Induced Allosteric Transition of Bovine Recoverin. *Biochemistry*, **37**, 17408-17419.

Bassereau,P. and Pincet,F. (1997) Quantitative Analysis of Holes in Supported Bilayers Providing the Adsorption Energy of Surfactants on Solid Substrate. *Langmuir*, **13**, 7003-7007.

Benda,A., Beneš,M., Mareček,V., Lhotskỳ,A., Hermens,W.T. and Hof,M. (2003) How To Determine Diffusion Coefficients in Planar Phospholipid Systems by Confocal Fluorescence Correlation Spectroscopy. *Langmuir*, **19**, 4120-4126.

Berland,K. and Shen,G. (2003) Excitation saturation in two-photon fluorescence correlation spectroscopy. *Appl.Opt.*, **42**, 5566-5576.

Berne,B.J. and Pecora,R. (2000) Dynamic Light Scattering with Applications to Chemistry, Biology, and Physics. Dover, New York.

Bligh,E.G. and Dyer,W.J. (1959) A Rapid Method of Total Lipid Extraction and Purification. *Can. J. Biochem. Physiol.*, **37**, 911-917.

Bolinger,P.-Y., Stamou,D. and Vogel,H. (2004) Integrated Nanoreactor systems: Triggering the Release and Mixing of Compounds Inside Single Vesicles. *JACS*, **126**, 8594-8595.

Braunewell,K.-H. and Gundelfinger,E.D. (1999) Intracellular neuronal calcium sensor proteins: a family of EF-hand calcium-binding proteins in search of a function. *Cell Tissue Res.*, **295**, 1-12

Brian,A.A., and McConnell,H.M: (1984) Allogenic stimulation of cytotoxic T cells by supported planar membranes. *PNAS*, **81**, 6159-6163.

Burgoyne,R.D., O'Callaghan,D.W., Hasdemir,B., Haynes,L.P. and Tepikin,A.V. (2004) Neuronal Ca^{2+}-sensor proteins: multitalented regulators of neuronal function. *Trends Neurosci.*, **27**, 203-209.

Burns,M.E. and Baylor,D.A. (2001) Activation, Deactivation, and Adaptation in Vertebrate Photoreceptor Cells. *Annu.Rev.Neurosci.*, **24**, 779-805.

Buser,C.A., Sigal,C.T., Resh,M.D. and McLaughlin,S. (1994) Membrane Binding of Myristylated Peptides Corresponding to the NH_2 Terminus of Src. *Biochemistry*, **33**, 13093-13101.

Callaghan,P.T. (1991) Principles of Nuclear Magnetic Resonance Microscopy. Clarendon Press, Oxford.

Calvert,P.D., Klenchin,V.A. and Bownds,M.D. (1995) Rhodopsin Kinase Inhibition by Recoverin. *J.Biol.Chem.*, **270**, 24127-24129.

Chen,C.-K., Inglese,J., Lefkowitz,R.J. and Hurley,J.B. (1995) Ca^{2+}-dependent Interaction of Recoverin with Rhodopsin Kinase. *J.Biol.Chem.*, **270**, 18060-18066.

Cole,J.L. and Hansen,J.C. (1999) Analytical Ultracentrifugation as a Contemporary Biomolecular Research Tool. *J.Biomol.Tech.*, **10**, 163-176.

Dertinger,T., von der Hocht,I., Benda,A., Hof,M. and Enderlein,J. (2006) Surface Sticking and Lateral Diffusion of Lipids in Supported Bilayers. *Langmuir*, **22**, 9339-9344.

Dertinger,T. (2007) Two-Focus Fluorescence Correlation Spectroscopy. *Dissertation*, Universität zu Köln, published online.

Desmeules,P., Grandbois,M., Bondarenko,V.A., Yamazaki,A. and Salesse,C. (2002) Measurement of Membrane Binding between Recoverin, a Calcium-Myristoyl Switch Protein, and Lipid Bilayers by AFM-Based Force Spectroscopy. *Biophys. J.*, **82**, 3343-3350.

Dimitrov,D.S. and Angelova,M.I. (1986) Swelling and electroswelling of lipids: Theory and experiment. *studia biophysica*, **113**, 15-20

Dimitrov,D.S. and Angelova,M.I. (1987) Lipid swelling and liposome formation on solid surfaces in external electric fields. *Progr.Colloid&PolymerSci.*, **73**, 48-56.

Dimitrov,D.S. and Angelova,M.I. (1987a) Electric field mediated lipid swelling and liposome formation. *studia biophysica*, **119**, 61-65.

Dimitrov,D.S. and Angelova,M.I. (1988) Lipid swelling and liposome formation mediated by electric fields. *Bioelectron.Bioenerg.*, **19**, 323-336.

Dizhoor,A.M., Ray,S., Kumar,S., Niemi,G., Spencer,M., Brolley,D., Walsh,K.A., Philipov,P.P., Hurley,J.B. and Stryer,L. (1991) Recoverin: A Calcium Sensitive Activator of Retinal Rod Guanylate Cyclase. *Science*, **251**, 915-918.

Dizhoor,A.M., Ericsson,L.H., Johnson,R.S., Kumar,S., Olshevskaya,E., Zozulya,S., Neubert,T.A., Stryer,L., Hurley,J.B. and Walsh,K.A. (1992) The NH_2 Terminus of Retinal Recoverin Is Acylated by a Small Family of Fatty Acids. *J. Biol. Chem.*, **267**, 16033-16036.

Dizhoor,A.M., Chen,C.-K., Olshevskaya,E., Sinelnikova,V.V., Phillipov,P. and Hurley,J.B. (1993) Role of the Acylated Amino Terminus of Recoverin in Ca^{2+}-Dependent Membrane Interaction. *Science*, **259**, 829-832.

Dizhoor,A.M., Olshevskaya,E.V., Henzel,W.J., Wong,S.C., Stults,J.T., Ankoudinova,I. and Hurley,J.B. (1995) Cloning, Sequencing, and Expression of a 24-kDa Ca^{2+}-binding Protein Activating Photoreceptor Guanylyl Cyclase. *J.Biol.Chem.*, **270**, 25200-25206.

Dizhur (Dizhoor),A.M., Nekrasova,E.N. and Filippov (Philippov),P.P. (1991) A Novel Photoreceptor Cell-Specific Protein with Molecular Weight 26 kD Capable of Binding to Immobilized Delipidated Rhodopsin. *Biokhimiya*, **56**, 225-229 (english translation)

Doeven,M.K., Folgering,J.H.A., Krasnikov,V., Geertsma,E.R., van den Bogaart,G. and Poolman,B. (2005) Distribution, Lateral Mobility and Function of Membrane Proteins Incorporated into Giant Unilamellar Vesicles. *Biophys.J.*, **88**, 1134-1142.

Enderlein,J., Gregor,I., Patra,D. and Fitter,J. (2004) Art and artefacts of fluorescence correlation spectroscopy. *Curr.Pharm.Biotechnol.*, **5**, 155-161.

Enderlein,J., Gregor,I., Patra,D., Dertinger,T. and Kaupp,U.B. (2005) Performance of fluorescence correlation spectroscopy for measuring diffusion and concentration. *Chemphyschem.*, **6**, 2324-2336.

Erickson,M.A., Lagnado,L., Zozulya,S., Neubert,T.A., Stryer,L. and Baylor,D.A. (1998) The effect of recombinant Recoverin on the photoresponse of truncated rod photoreceptors. *PNAS*, **95**, 6474-6479.

Flaherty,K.M., Zozulya,S., Stryer,L. and McKay,D.B. (1993) Three-Dimensional Structure of Recoverin, a Calcium Sensor in Vision. *Cell*, **75**, 709-716.

Fradin,C., Abu-Arish,A., Granek,R. and Elbaum,M. (2003) Fluorescence Correlation Spectroscopy Close to a Fluctuating Membrane. *Biophys.J.*, **84**, 2005-2020.

Frins,S., Bönigk,W., Müller,F., Kellner,R. and Koch,K.-W. (1996) Functional Characterization of a Guanylyl Cyclase-activating Protein from Vertebrate Rods. *J.Biol.Chem.*, **271**, 8022-8027.

Gensch,T., Komolov,K.E., Senin,I.I., Philippov,P.P. and Koch,K.W. (2007) Ca^{2+}-Dependent Conformational Changes in the Neuronal Ca^{2+}-Sensor Recoverin Probed by the Fluorescent Dye Alexa647. *Proteins*, **66**, 492-499.

Gorczyca,W.A., Gray-Keller,M.P., Detwiler,P.B. and Palczewski,K. (1994) Purification and physiological evaluation of a guanylat cyclase activating protein from retinal rods. *PNAS*, **91**, 4014-4018.

Gorodovikova,E.N. and Philippov,P.P. (1993) The presence of a calcium-sensitive p26-containing complex in bovine retina rod cells. *FEBS Lett.*, **335**, 277-279.

Gorodovikova,E.N., Gimelbrant,A.A., Senin,I.I. and Philippov,P.P. (1994a) Recoverin mediates the calcium effect upon rhodopsin phosphorylation and cGMP hydrolysis in bovine retina rod cells. *FEBS Lett.*, **349**, 187-190.

Gorodovikova,E.N., Senin,I.I. and Philippov,P.P. (1994b) Calcium-sensitive control of rhodopsin phosphorylation in the reconstituted system of photoreceptor membranes, rhodopsin kinase and recoverin. *FEBS Lett.*, **353**, 171-172.

Gray-Keller,M.P., Polans,A.S., Palczewski,K. and Detwiler,P.B. (1993) The Effect of Recoverin-like Calcium-Binding Proteins on the Photoresponse of Retinal Rods. *Neuron*, **10**, 523-531.

Gray-Keller,M.P. and Detwiler,P.B. (1994) The calcium feedback signal in the phototransduction cascade of vertebrate rods. *Neuron*, **13**, 849-861.

Gregor,I. and Enderlein,J. (2005) Focusing astigmatic Gaussian beams through optical system with a high numerical aperture. *Opt.Lett.*, **30**, 2527-2529.

Gregor,I., Patra,D. and Enderlein,J. (2005) Optical saturation in fluorescence correlation spectroscopy under continuous-wave and pulsed excitation. *Chemphyschem.*, **6**, 164-170.

Hargrave,P.A., Fong,S.-L., McDowell,J.H., Mas,M.T., Curtis,D.R., Wang,J.K., Juszczak,E. and Smith,D.P. (1980) The partial primary structure of bovine rhodopsin and its topography in the retinal rod cell disc membrane. *Neurochem. Int.*, **1**, 231-244.

Harvey,D. (2000) Modern Analytical Chemistry. McGraw Hill, Boston, 593-595.

Heilemann,M., Margeat,E., Kasper,R., Sauer,M. and Tinnefeld,P. (2005) Carbocyanine Dyes as Efficient Reversible Single-Molecule Optical Switch. *JACS*, **127**, 3801-3806.

Hess,S.T., Huang,S., Heikal,A.A. and Webb,W.W. (2002) Biological and chemical applications of fluorescence correlation spectroscopy: a review. *Biochemistry*, **41**, 697-705.

Hess,S.T. and Webb,W.W. (2002) Focal volume optics and experimental artefacts in confocal fluorescence correlation spectroscopy. *Biophys.J.*, **83**, 2300-2317.

Higgins,M.K., Oprian,D.D. and Schertler,G.X. (2006) Recoverin Binds Exclusively to an Amphiphatic Peptide at the N Terminus of Rhodopsin Kinase, Inhibiting Rhodopsin Phosphorylation without Affecting Catalytic Activity of the Kinase. *J.Biol.Chem.*, **281**, 19426-19432.

Hughes,R.E., Brzovic,P.S., Klevit,R.E. and Hurley,J.B. (1995) Calcium-Dependent Solvation of the Myristoyl Group of Recoverin. *Biochemistry*, **34**, 11410-11416.

Hurley,J.B., Dizhoor,A.M., Ray,S. and Stryer,L. (1993) Recoverin's Role: Conclusion Withdrawn. *Science*, **260**, 740.

Hwang,J.-Y. and Koch,K.-W. (2002) Calcium- and Myristoyl-Dependent Properties of Guanylate Cyclase-Activating Protein-1 and Protein-2. *Biochemistry*, **41**, 13021-13028.

Hwang,J.-Y., Lange,C., Helten,A., Höppner-Heitmann,D., Duda,T., Sharma,R.K. and Koch,K.-W. (2003) Regulatory modes of rod outer segment membrane guanylate cyclase differ in catalytic efficiency and Ca^{2+}-sensitivity. *Eur.J.Biochem.*, **270**, 3814-3821.

Inglese,J., Koch,W.J., Caron,M.G. and Lefkowitz,R.J. (1992) Isoprenylation in regulation of signal transduction by G-protein-coupled receptor kinases. *Nature*, **359**, 147-150.

Kawamura,S. and Murakami,M. (1991) Calcium-dependent regulation of cyclic GMP phosphodiesterase by a protein from frog retinal rods. *Nature*, **349**, 420-423.

Kawamura,S., Takamatsu,K. and Kitamura,K. (1992) Purification and characterization of S-modulin, a calcium-dependent regulator on cGMP Phosphodiesterase in frog rod photoreceptors. *Biochem. Biophys. Res. Commun.*, **186**, 411-417.

Kawamura,S. (1993) Rhodopsin phosphorylation as a mechanism of cyclic GMP phosphodiesterase regulation by S-modulin. *Nature*, **362**, 855-857.

Kawamura,S., Hisatomi,O., Kayada,S., Tokunaga,F. and Kuo,C.-H. (1993) Recoverin Has S-modulin Activity in Frog Rods. *J.Biol.Chem.*, **268**, 14579-14582.

Kawamura,S., Cox,J.A. and Nef,P. (1994) Inhibition of rhodopsin phosphorylation by non-myristoylated recombinant Recoverin. *Biochem.Biophys.Res.Commun.*, **203**, 121-127.

Keller,C.A., Glasmästar,K., Zhdanov,V.P. and Kasemo,B. (2000) Formation of Supported Membranes from Vesicles. *Phys.Rev.Lett.*, **84**, 5443-5446.

Klenchin,V.A., Calvert,P.D. and Bownds,M.D. (1995) Inhibition of Rhodopsin Kinase by Recoverin. *J.Biol.Chem.*, **270**, 16147-16152.

Koch,K.-W. and Stryer,L. (1988) Highly cooperative feedback control of retinal rod guanylate cyclase by calcium ions. *Nature*, **334**, 64-66.

Komolov,K.E., Zinchenko,D.V., Churumova,V.A., Vaganova,S.A., Weiergräber,O.H., Senin,I.I., Philippov,P.P. and Koch,K.-W. (2005) One of the Ca 2+ bining sites of recoverin exclusively controls interaction with rhodopsin kinase. *Biol.Chem.*, **386**, 285-289.

Korenbrot,J.I. and Miller,D.L. (1989) Cytoplasmic free calcium concentration in dark-adapted retinal rod outer segments. *Vision Research*, **29**, 939-948.

Kühn,H. and Dreyer,W.J. (1972) Light Dependent Phosphorylation of Rhodopsin by ATP. *FEBS Lett.*, **20**, 1-6.

Kutuzov,M.A., Shmukler,B.E., Suslov,O.N., Dergachev,A.E., Zargarov,A.A. and Abdulaev,N.G. (1991) P26 – calcium binding protein from bovine retinal photoreceptor cells. *FEBS Lett.*, **293**, 21-24.

Laemmli,U.K. (1970) Cleavage of structural proteins during the assembly of the head of bacteriophage T4. *Nature*, **227**, 680-685.

Lagnado,L., Cervetto,L. and McNaughton,P.A. (1992) Calcium homeostasis in the outer segments of retinal rods from the tiger salamander. *J. Physiol.*, **455**, 111-142.

Lambrecht,H.-G. and Koch,K.-W. (1991) A 26 kd calcium binding protein from bovine rod outer segments as modulator of photoreceptor guanylate cyclase. *EMBO J.*, **10**, 793-798.

Lambrecht,H.-G. and Koch,K.-W. (1992) Recoverin a novel calcium-binding protein from vertebrate photoreceptors. *Biochim.Biophys.Acta*, **1160**, 63-66.

Lange,C. and Koch,K.-W. (1997) Calcium-dependent binding of recoverin to membranes monitored by surface plasmon resonance spectroscopy in real time. *Biochemistry*, **36**, 12019-12026.

Levay,K., Satpaev,D.K., Pronin,A.N., Benovic,J.L. and Slepak,V.Z. (1998) Localization of the Sites for Ca^{2+}-Binding Proteins on G Protein-Coupled Receptor Kinases. *Biochemistry*, **37**, 13650-13659.

Magde,D., Elson,E. and Webb,W.W. (1972) Thermodynamic Fluctuations in a Reacting System – Measurement by Fluorescence Correlation Spectroscopy. *Phys.Rev.Lett.*, **29**, 705-708.

Makino,C.L., Dodd,R.L., Chen,J., Burns,M.E., Roca,A., Simon,M.I. and Baylor,D.A. (2004) Recoverin Regulates Light-dependent Phosphodiesterase Activity in Retinal Rods. *J.Gen.Physiol.*, **123**, 729-741.

Matsuda,S., Hisatomi,O., Ishino,T., Kobayashi,Y. and Tokunaga,F. (1998) The Role of Calcium-binding Sites in S-modulin Function. *J. Biol. Chem.*, **273**, 20223-20227.

Matsuda,S., Hisatomi,O. and Tokunaga,F. (1999) Role of Carboxyl-Terminal Charges on S-Modulin Membrane Affinity and Inhibition of Rhodopsin Phosphorylation. *Biochemistry*, **38**, 1310-1315.

McGinnis,J.F., Stepanik,P.L., Baehr,W., Subbaraya,I. and Lerious,V. (1992) Cloning and sequencing of the 23 kDa mouse photoreceptor cell-specific protein. *FEBS Lett.*, **302**, 172-176.

Merkel,R., Sackmann,E., Evans,E. (1989) Molecular friction and epitactic coupling between monolayers in supported bilayers. *J.Phys.(Paris)*, **50**, 1535-1555.

Montes,L.-R., Alonso,A., Goñi,F.M. and Bagatolli,L.A. (2007) Giant Unilamellar Vesicles Electroformed from Native Membranes and Organic Lipid Mixtures under Physiological Conditions. *Biophys.J.*, **93**, 3548-3554.

Müller,F. and Kaupp,U.B. (1998) Signaltransduktion in Sehzellen. *Naturwissenschaften*, **85**, 49-61.

Nagy,A., Wu,J. and Berland,K.M. (2005a) Observation volumes and γ-factors in two-photon fluorescence fluctuation spectroscopy. *Biophys.J.*, **89**, 2077-2090.

Nagy,A., Wu,J. and Berland,K.M. (2005b) Characterizing observation volumes and the role of excitation saturation in one-photon fluorescence fluctuation spectroscopy. *J.Biomed.Opt.*, **10**, 44015.

Nakatani,K., Chen,C., Yau,K.-W. and Koutalos,Y., (2002) Calcium and Phototransduction. *Adv. Exp. Med. Biol.*, **514**, 1-20.

Neuweiler,H., Schulz,A., Vaiana,A.C., Smith,J.C., Kaul,S., Wolfrum,J. and Sauer,M. (2002) Detection of Individual p53-Autoantibodies by Using Quenched Peptide-Based Molecular Probes. *Angew. Chem. Int. Ed.*, **41** (24), 4769-4773.

Nishimura,G. and Kinjo,M. (2004) Systematic error in fluorescence correlation measurements identified by a simple saturation model of fluorescence. *Anal.Chem.*, **76**, 1963-1970.

Osborn,T.D. and Yager,P. (1995) Modeling Success and Failure of Langmuir-Blodgett Transfer of Phospholipid Bilayers to Silicon Dioxide. *Biophys.J.*, **68**, 1364-1373.

Palczewski,K., Buczyłko,J., Lebioda,L., Crabb,J.W. and Polans,A.S. (1993) Identification of the N-terminal Region in Rhodopsin Kinase Involved in Its Interaction with Rhodopsin. *J.Biol.Chem.*, **268**, 6004-6013.

Palczewski,K., Subbaraya,I., Gorczyca,W.A., Helekar,B.S., Ruiz,C.C., Ohguro,H., Huang,J., Zhao,X., Crabb,J.W., Johnson,R.S., Walsh,K.A., Gray-Keller,M.P., Detwiler,P.B. and Baehr,W. (1994) Molecular cloning and characterization of retinal photoreceptor guanylyl cyclase-activating protein. *Neuron*, **13**, 395-404.

Permyakov,S.E., Cherskaya,A.M., Senin,I.I., Zargarov,A.A., Shulga-Morskoy,S.V., Alekseev,A.M., Zinchenko,D.V., Lipkin,V.M., Philippov,P.P., Uversky,V.N. and Permyakov,E.A. (2000) Effects of mutations in the calcium-binding sites of recoverin on its calcium affinity: evidence for successive filling of the calcium binding sites. *Protein Eng.*, **13**, 783-790.

Perroud,T.D., Huang,B. and Zare,R.N. (2005) Effect of bin time on the photon counting histogram for one-photon excitation. *Chemphyschem.*, **6**, 905-912.

Piehler,J., Brecht,A., Valiokas,R., Liedberg,B. and Gauglitz,G. (2000) A high-density poly(ethylene glycol) polymer brush for immobilization on glass-type surfaces. *Biosens.Bioelectron.*, **15**, 473-481.

Polans A.S., Buczylko,J., Crabb,J. and Palczewski,K. (1991) A Photoreceptor Calcium Binding Protein Is Recognized by Autoantibodies Obtained from Patients with Cancer-associated Retinopathy. *J.Cell.Biol.*, **112**, 981-989.

Polans,A.S., Witkowska,D., Haley,T.L., Amundson,D., Baizer,L. and Adamus,G. (1995) Recoverin, a photoreceptor-specific calcium-binding protein, is expressed by the tumor of a patient with cancer-associated retinopathy. *PNAS*, **92**, 9176-9180.

Przybylo,M., Sỳkora,J., Humpolíčková,J., Benda,A., Zan,A. and Hof,M. (2006) Lipid Diffusion in Giant Unilamellar Vesicles Is More than 2 Times Faster than in Supported Phospholipid Bilayers under Identical Conditions. *Langmuir*, **22**, 9096-9099.

Pugh,E.N. and Cobbs,W.H. (1986) Visual Transduction in Vertebrate Rods and Cones: A Tale of Two Transmitters, Calcium and Cyclic GMP. *Vision Res.*, **26**, 1613-1643.

Pugh,E.N., Nikonov,S. and Lamb,T.D. (1999) Molecular mechanisms of vertebrate photoreceptor light adaptation. *Curr.Opin.Neurobiol.*, **9**, 410-418.

Ray,S., Zozulya,S., Niemi,G.A., Flaherty,K.M., Brolley,D., Dizhoor,A.M., McKay,D.B., Hurley,J. and Stryer,L. (1992) Cloning, expression, and crystallization of recoverin, a calcium sensor in vision. *PNAS*, **89**, 5705-5709.

Rädler,J., Strey,H. and Sackmann,E. (1995) Phenomenology and Kinetics of Lipid Bilayer Spreading on Hydrophilic Surfaces. *Langmuir*, **11**, 4539-4548.

Reviakine,I. and Brisson,A. (2000) Formation of Supported Phospholipid Bilayers from Unilamellar Vesicles Investigated by Atomic Force Microscopy. *Langmuir*, **16**, 1806-1815.

Richter,R.P., Bérat,R. and Brisson,A.R. (2006) Formation of Solid-Supported Lipid Bilayers: An Integrated View. *Langmuir*, **22**, 3497-3505.

Rigler,R. and Elson,E.S. (2001) Fluorescence Correlation Spectroscopy. Springer,Berlin.

Sackmann,E. (1996) Supported Membranes: Scientific and Practical Applications. *Science*, **271**, 43-48.

Sampath,A.P., Strissel,K.J., Elias,R., Arshavsky,V.Y., McGinnis,J.F., Chen,J., Kawamura,S., Rieke,F. and Hurley,J.B. (2005) Recoverin Improves Rod-Mediated Vision by Enhancing Signal Transmission in the Mouse Retina. *Neuron*, **46**, 413-420.

Sanada,K., Kokame,K., Yoshizawa,T., Takao,T., Shimonishi,Y. and Fukada,Y. (1995) Role of Heterogenous N-terminal Acylation of Recoverin in Rhodopsin Phosphorylation. *J. Biol. Chem.*, **270**, 15459-15462.

Sanada,K., Shimizu,F., Kameyama,K., Haga,K., Haga,T. and Fukada,Y. (1996) Calcium-bound recoverin targets rhodopsin kinase to membranes to inhibit rhodopsin phosphorylation. *FEBS Lett.*, **384**, 227-230.

Satpaev,D.K., Chen,C.-K., Scotti,A., Simon,M.I., Hurley,J.B. and Slepak,V.Z. (1998) Autophosphorylation and ADP Regulate the Ca^{2+}-Dependent interaction of Recoverin with Rhodopsin Kinase. *Biochemistry*, **37**, 10256-10262.

Schwille,P. (2001) Fluorescence correlation spectroscopy and its potential for intracellular applications. *Cell.Biochem.Biophys.*, **34**, 383-408.

Senin,I.I., Zargarov,A.A., Alekseev,A.M., Gorodovikova,E.N., Lipkin,V.M. and Philippov,P.P. (1995) *N*-Myristoylation of recoverin enhances its efficiency as an inhibitor of rhodopsin kinase. *FEBS Lett.*, **376**, 87-90.

Senin,I.I., Fischer,T., Komolov,K.E., Zinchenko,D.V., Philippov,P.P. and Koch,K.W. (2002) Ca^{2+}-Myristoyl Switch in the Neuronal Calcium Sensor Recoverin Requires Different Functions of Ca^{2+}-binding Sites. *J. Biol. Chem.*, **277**, 50365-50372.

Senin,I.I., Koch,K.-W., Akhtar,M. and Philippov,P.P. (2002a) Ca^{2+}-dependent control of Rhodopsin phosphorylation: Recoverin and Rhodopsin Kinase. *Adv.Exp.Med.Biol.*, **514**, 69-99.

Senin,I.I., Vaganova,S.A., Weiergräber,O.H., Ergorov,N.S., Philipppov,P:P: and Koch,K.-W. (2003) Functional Restoration of the Ca^{2+}-myristoyl Switch in a Reoverin Mutant. *J. Mol. Bio.*, **330**, 409-418.

Senin,I.I., Höppner-Heitmann,D. Polkovnikova,O.O., Churumova,V.A., Tikhomirova,N.K., Philippov,P.P. and Koch,K.-W. (2004) Recoverin and Rhodopsin Kinase Activity in Detergent-resistant Membrane Rafts from Rod Outer Segments. *J. Biol. Chem.*, **279**, 48647-48653.

Sigal,C.T., Zhou,W., Buser,C.A. and McLaughlin,S. (1994) Amino-terminal basic residues of Src mediate membrane binding through electrostatic interaction with acidic phospholipids. *PNAS*, **91**, 12253-12257.

Strissel,K.J., Lishko,P.V., Trieu,L.H., Kennedy,M.J., Hurley,J.B. and Arshavsky,V.Y. (2005) Recoverin Undergoes Light-dependent Intracellular Translocation in Rod Photoreceptors. *J.Biol.Chem.*, **280**, 29250-29255.

Stryer,L. (1986) Cyclic GMP Cascade of Vision. *Ann. Rev. Neurosci.*, **9**, 87-119.

Stryer,L. (1996) Biochemie. Spektrum akademischer Verlag GmbH, Heidelberg · Berlin, 4. Auflage

Tanaka,T., Ames,J.B., Harvey,T.S., Stryer,L. and Ikura,M. (1995) Sequestration of the membrane-targeting myristoyl group of recoverin in the calcium free state. *Nature*, **376**, 444-447.

Thompson,P. and Findlay,J.B.C. (1984) Phosphorylation of ovine rhodopsin. *Biochem.J.*, **220**, 773-780.

Tsien,R. and Pozzan,T. (1989) Measurement of Cytosolic Free Ca^{2+} with Quin2. *Methods in Enzymology*, **172**, 230-262.

Weiergräber,O.H., Senin,I.I., Philipov,P.P., Granzin,J. and Koch,K.-W. (2003) Impact of N-terminal Myristoylation on the Ca^{2+}-dependent Conformational Transition in Recoverin. *J. Biol. Chem.*, **278**, 22972-22979.

Widengren,J. and Schwille,P. (2000) Characterization of Photoinduced Isomerization and Back-Isomerization of the Cyanine Dye Cy5 by Fluorescence Correlation Spectroscopy. *J. Phys. Chem. A*, **104**, 6416-6428.

Widengren,J. and Mets,Ü. (2002) Conceptual Basis of Fluorescence Correlation Spectroscopy and Related Techniques as Tools in Bioscience. Single–Molecule Detection in Solution – Methods and Applications; Eds: Zander,C., Enderlein,J. and Keller,R.A., Wiley-VCH, Berlin, 69-95.

Wilden,U. and Kühn,H. (1982) Light-Dependent Phosphorylation of Rhodopsin: Number of Phosphorylation Sites. *Biochemistry*, **21**, 3014-3022.

Woodruff,M.L., Sampath,A.P., Matthews,H.R., Krasnoperova,N.V., Lem,J. and Fain,G.L. (2002) Measurement of cytoplasmic calcium concentration in the rods of wild-type and transducin knock-out mice. *J. Physiol.*, **542**, 843-854.

Valentine,K.G., Mesleh,M.F., Opella,S.J., Ikura,M. and Ames,J.B. (2003) Structure, Topology, and Dynamics of Myristoylated Recoverin Bound to Phospholipid Bilayers. *Biochemistry*, **42**, 6333-6340.

Yamagata,K., Goto,K., Kuo,C.-H., Kondo,H. and Miki,N. (1990) Visinin: A Novel Calcium Binding Protein Expressed in Retinal Cone Cells. *Neuron*, **2**, 469-476.

Zhang,L. and Granick,S. (2005) Lipid diffusion compared in outer and inner leaflets of planar supported bilayers. *J.Chem.Phys.*, **123**, 211104.

Zozulya, S. and Stryer,L. (1992) Calcium-myristoyl protein switch. *PNAS*, **89**, 11569-11573.

Erklärung

Ich versichere, dass ich die von mir vorgelegte Dissertation selbständig angefertigt, die benutzten Quellen und Hilfsmittel vollständig angegeben und die Stellen der Arbeit - einschließlich Tabellen, Karten und Abbildungen -, die anderen Werken im Wortlaut oder dem Sinn nach entnommen sind, in jedem Einzelfall als Entlehnung kenntlich gemacht habe; dass diese Dissertation noch keiner anderen Fakultät oder Universität zur Prüfung vorgelegen hat; dass sie – abgesehen von unten angegebenen Teilpublikationen – noch nicht veröffentlicht worden ist, sowie, dass ich eine solche Veröffentlichung vor Abschluss des Promotionsverfahrens nicht vornehmen werde. Die Bestimmungen dieser Promotionsordnung sind mir bekannt. Die von mir vorgelegte Dissertation ist von Prof. Dr. Jörg Enderlein betreut worden.

Köln, den 14. Januar 2008

Teilpublikationen:

Dertinger,T., von der Hocht,I., Benda,A., Hof,M. and Enderlein,J. (2006) Surface Sticking and Lateral Diffusion of Lipids in Supported Bilayers. *Langmuir*, **22**, 9339-9344.

Dertinger,T., Pacheco,V., von der Hocht,I., Hartmann,R., Gregor,I. and Enderlein,J. (2007) Two-Focus Fluorescence Correlation Spectroscopy: A New Tool for Accurate and Absolute Diffusion Measurements. *ChemPhysChem*, **8**, 433-443.

von der Hocht,I. and Enderlein,J. (2007) Fluorescence Correlation Spectroscopy in cells: Confinement and excluded volume effects. *Exp. Mol. Pathol.*, **82**, 142-146.

Jül-4272
Mai 2008
ISSN 0944-2952